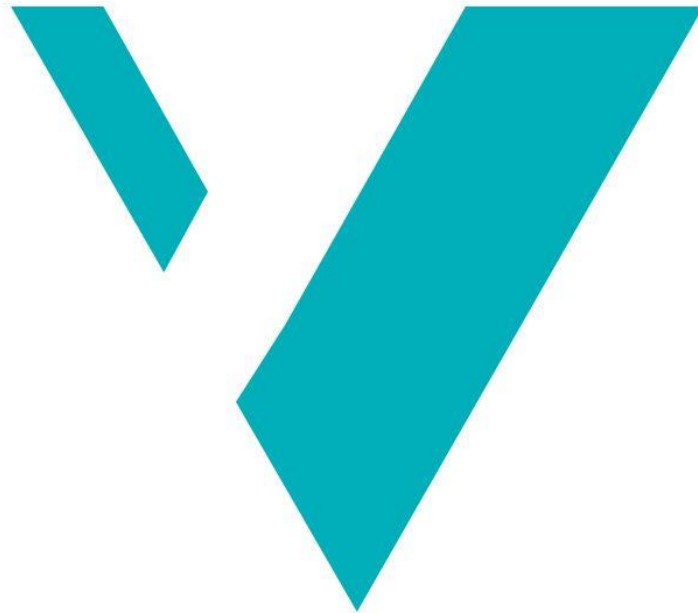


Glacial lake outburst floods of Harbardsbreen, Western Norway, and their relationship to long- term glacier mass balance and climate change



Samuel Eide

Master Thesis in Climate Change Management

Department of Environmental Sciences, Faculty of Engineering and Science

WESTERN NORWAY UNIVERSITY OF APPLIED SCIENCES

Sogndal, June 2021


I confirm that the work is self-prepared and that references/source references to all sources used in the work are provided, cf. Regulation relating to academic studies and examinations at the Western Norway University of Applied Sciences (HVL), § 10.



Western Norway
University of
Applied Sciences

Glacial-lake outburst floods of Harbardsbreen, Western Norway, and their relationship to long-term glacier mass balance and climate change

Master thesis in Climate Change Management

Author: Samuel Eide	Author sign. 
Thesis submitted: June 10 th 2021.	Open/confidential thesis: Open.
Main Supervisor: Thorben Dunse (HVL) Co-supervisor: Liss Marie Andreassen (NVE)	
Keywords: Harbardsbreen, glaciology, glacier, floods, geohazards, glacial lake outburst floods, GLOFs, climate change, satellite data, Sentinel-2, Landsat, Planet Labs.	Number of pages: 95 total Appendix: Place/Date/year: Sogndal, June 10 th 2021
This thesis is a part of the master's program in Climate Change Management (Planlegging for klimaendringar) at the Department of Environmental Sciences, Faculty of Engineering and Science at the Western Norway University of Applied Sciences. The author(s) is responsible for the methods used, the results that are presented and the conclusions in the thesis.	

Glacial lake outburst floods of Harbardsbreen, Western Norway, and their relationship to long- term glacier mass balance and climate change

**Master thesis by
SAMUEL EIDE**

Master graduate in Climate Change Management

Western Norway University of Applied Sciences/
Høgskulen på Vestlandet (HVL)

June 10th 2021
Sogndal, Norway

Sentinel (*noun*)

A soldier or guard whose job is to stand and keep watch.

Preface

This is the final master thesis in the master program Climate Change Management at Western Norway University of Applied Sciences (HVL), Sogndal. This thesis has given me the opportunity to study the long-term changes of the glacial lakes of Harbardsbreen, Western Norway, and how this is related to glacier mass balance and climate change, as well as studying the mechanisms of glacial lake outburst flood events at Harbardsbreen.

I would like to thank my supervisors Thorben Dunse (HVL) and Liss M. Andreassen (NVE) for all support, help, guidance, data and useful discussions. I hope you enjoyed it at least as much as I did. I would also like to thank Hallgeir Elvehøy (NVE) and Bjarne Kjølmoen (NVE) for useful data as well as field observations of Harbardsbreen, which has been most helpful.

The glacier lake mapping in this thesis is a contribution to Copernicus Bretjeneste/Copernicus Glacier Service: <https://www.nve.no/hydrology/glaciers/copernicus-glacier-service/>. After the submission of this thesis the polygon data of the mapped lakes will be made available through this service.

Sogndal, June 10th 2021



Samuel Eide

Abstract – English

In this study I have used various sources of satellite imagery to present long term changes of the two glacial lakes of Harbardsbreen, Luster municipality, Western Norway. I have made a time series which ranges from the first Landsat-1 satellite in 1972 to 2020. For the period 2010-2020 I have done a detailed study of the annual developments of the lakes to find evidence of glacial lake outburst floods (GLOFs). NVE's GLOF database shows registered and documented GLOF events at Harbardsbreen in 2010, 2012, 2015 and 2020. In this study, I additionally found evidence with high certainty of GLOF events in 2011, 2018 and in 2019, a probable GLOF event in 2014 and possible GLOF events in 2013 and 2017. In the period 2010-2020, 2016 was the only year in which neither of the two lakes at Harbardsbreen formed, likely due to the weather conditions this season.

Harbardsbreen has melted and thinned significantly in the period 2010-2020, with an average mass balance of -5.3 ± 0.6 meters water equivalents (m.w.e.), or -0.53 ± 0.06 m.w.e. per year. This is less negative than for the period 1996-2010 (-0.82 ± 0.05 m.w.e. a⁻¹) (Andreassen L. M., 2013), but more negative than the period 1966-1996 (-0.28 ± 0.07 m.w.e. a⁻¹) (Kjøllmoen B. , 1997). The lakes seem to be linked to this pattern, in the period 1996-2010 the average maximum known extent of the largest lake was 34% and 29% larger than in the periods 1966-1996 and 2010-2020 respectively.

I have proposed a possible early warning of GLOF events at Harbardsbreen. All the GLOF events in 2010, 2011, 2015 and 2020 shared the same characteristics in both lake development, size and weather data. However, it is evident that GLOFs also can occur at smaller lake extents/volumes (e.g. 2018 and 2019). Therefore, I have proposed a probable certainty of GLOF events for lake extents in the magnitude of 10^4 m², and high certainty of GLOF events for lake extents in the magnitude of 10^5 m². The risk will increase by the lake extent.

Samandrag – Norsk

I denne studien har eg nytta fleire kjelder til satellittbilete for å lage ein tidsserie av dei to bresjøane på Harbardsbreen i Luster kommune, Vestlandet. Denne tidsserien strekk seg frå oppstarten av satellitten Landsat-1 i 1972 til 2020. For perioden 2010-2020 har eg gjort ei detaljert undersøking av årlege endringar av bresjøane for å finne prov på jøkullaup/breflaumar (engelsk: glacial lake outburst floods (GLOFs)). NVE sin database over jøkullaup i Noreg syner dokumenterte hendingar ved Harbardsbreen i 2010, 2012, 2015 og 2020. I denne studien har eg i tillegg funne prov med høg sikkerheit at det var jøkullaup ved Harbardsbreen i 2011, 2018 og 2019, eit sannsynleg jøkullaup i 2014 og moglege jøkullaup i 2013 og 2017. I perioden 2010-2020 var det berre i 2016 kor ingen av bresjøane utvikla seg, truleg grunna vêrforholda denne sesongen.

Harbardsbreen har smelta mykje og blitt signifikant tynnare i perioden 2010-2020, med eit gjennomsnittleg tap av masse på -5.3 ± 0.6 meter vassekvivalentar (m.v.e.), eller -0.53 ± 0.06 m.v.e. per år. Dette er mindre negativt enn perioden 1996-2010 (-0.82 ± 0.05 m.v.e. per år) (Andreassen L. M., 2013), men meir negativt enn perioden 1966-1996 (-0.28 ± 0.07 m.v.e. per år) (Kjøllmoen B. , 1997). Tilsynelatande følgjer bresjøane dette mønsteret. I perioden 1996-2010 var det gjennomsnittlege største kjende arealet av den største bresjøen 34% og 29% større enn kva det var høvesvis i periodane 1966-1996 og 2010-2020.

Eg har føreslått ein mogleg tidleg åtvaring av jøkullaup på Harbardsbreen. Alle jøkullaupa i 2010, 2011, 2015 og 2020 viste dei same eigenskapar og karakterar i både utvikling og storleik av bresjøane og vêrdata. Samstundes vart jøkullaupa i blant anna 2018 og 2019 utløyst ved mykje mindre sjøareal/vassvolum enn i 2010, -11, -15 og -20. Difor har eg føreslått at det vil vere sannsynleg at eit jøkullaup vil finne stad når bresjøane oppnår eit areal i skalaen 10^4 m², og svært sikkert ved bresjøareal i skalaen 10^5 m². Sannsynet vil då auke med storleiken på bresjøane.

Contents

1	Introduction	1
1.1	Background.....	1
1.2	What is a glacial lake?	1
1.3	What is a glacial lake outburst flood (GLOF)?	2
1.4	Glaciers and temperature changes in Norway.....	4
1.5	Field location: Harbardsbreen.....	6
1.6	Registered GLOF events in Norway.....	10
1.7	Registered GLOF events at Harbardsbreen.....	11
1.8	Previous research	13
1.9	Research objectives.....	14
2	Data and methods	15
2.1	Satellite data.....	15
2.1.1	Planet Labs.....	16
2.1.2	Copernicus Open Access Hub.....	16
2.2	Glacier extent.....	18
2.3	Elevation change and mass balance	18
2.4	Weather data	19
2.4.1	Cumulative positive degree days (PDD).....	20
2.4.2	Precipitation	21
2.5	Software.....	21
2.6	Errors and uncertainties	21
2.6.1	Satellite data and cloud cover.....	21
2.6.2	Lake and glacier area	22
2.6.3	Weather data	22
2.6.4	Elevation data.....	23
3	Results.....	24
3.1	Maximum known lake extents	24
3.2	PDD values for drainage events.....	26
3.3	Temperature and precipitation	28
3.3.1	Temperature	28
3.3.2	Precipitation	29
3.4	Lake area and PDD	32

3.5	Detailed lake developments 2010-2020	33
3.5.1	Detailed graphs.....	33
3.6	Lake volume	47
3.7	“New” GLOFs and drainage events in the period 2010-2020.....	49
3.8	Harbardsbreen extent and area change.....	51
3.9	Elevation change.....	52
3.10	Geodetic mass balance 2010-2020	54
4	Discussion	56
4.1	Use of satellite photos	56
4.1.1	Availability and resolution of satellite images	56
4.1.2	Cloud cover	56
4.1.3	Preview of satellite imagery	57
4.1.4	Mapping of the lakes	57
4.1.5	Comparison of the different satellite data sources.....	58
4.2	Temperature and precipitation	59
4.3	Registered GLOF events in Norway	60
4.4	Defining GLOF events.....	61
4.5	Lake development in 2010 to 2020 and GLOFs	62
4.6	Lake volume and discharge volume.....	64
4.7	Mass balance.....	65
4.8	Proposed early warning of GLOF events at Harbardsbreen.....	66
4.9	Possibilities for future GLOF events at Harbardsbreen	67
4.10	Proposed future studies.....	68
5	Conclusions	69
5.1	Use of satellite data: Sentinel-2 and PlanetScope	69
5.2	Mass balance and climate change	69
5.3	Long term changes of the lakes at Harbardsbreen	70
5.4	GLOF events in 2010-2020.....	70
5.5	Proposed early warning of GLOF events.....	71
6	Data availability.....	72
7	References	73

List of figures

Figure 1: Detailed view of the glacial lakes of Harbardsbreen	2
Figure 2: Simplified illustration of how a glacier-dammed lake may cause a GLOF.....	3
Figure 3: Official summer temperature records by the Norwegian Meteorological Institute	5
Figure 4: Official winter temperature records by the Norwegian Meteorological Institute.....	5
Figure 5: Overview map of Harbardsbreen 1.....	7
Figure 6: Overview map of Harbardsbreen 2.....	8
Figure 7: Photo of the drained Western lake, captured from helicopter on 02.09.2020.....	9
Figure 8: The total number of registered GLOF events in Norway divided into 30-year periods.	10
Figure 9: The total number of registered GLOF events in Norway for the last 30-year period.....	11
Figure 10: Sentinel-2 satellite photo of the lakes as of August 24 th 2020.....	12
Figure 11: RapidEye satellite photo of the lakes as of August 21 st 2015.....	12
Figure 12: High resolution orthophoto of the lakes as of September 29 th 2010.....	13
Figure 13: Annual maximum known glacial lake extents of Harbardsbreen, 1972-2020	25
Figure 14: Cumulative PDD values for GLOFs and drainage events.	26
Figure 15: PDD values by date, 2010-2020	27
Figure 16: PDD values normalized by the first date of 20 PDD as a reference starting point.....	27
Figure 17: Annual cumulative positive degree days (PDD) from 1957 to 2020.....	28
Figure 18: 10-year averages of the annual number of days with temperatures above 0°C	29
Figure 19: Annual precipitation at the area of interest at Harbardsbreen.....	30
Figure 20: Annual precipitation at mean daily temperatures < 0.5°C, indicative as snow..	30
Figure 21: Annual precipitation at mean daily temperatures ≥ 0.5°C, indicative as rain.....	31
Figure 22: Detailed cumulative precipitation as rain from 2010-2020.	31
Figure 23: Development of the Western lake 2010-2020	32
Figure 24: Development of the Eastern lake 2010-2020.	33
Figure 25: Detailed lake development on Harbardsbreen in 2010.....	34
Figure 26: Detailed lake development on Harbardsbreen in 2011.....	35
Figure 27: Detailed lake development on Harbardsbreen in 2012.....	36
Figure 28: Detailed lake development on Harbardsbreen in 2013.....	37

Figure 29: Detailed lake development on Harbardsbreen in 2014.....	38
Figure 30: Detailed lake development on Harbardsbreen in 2015.....	39
Figure 31: Total cumulative PDD and cumulative precipitation as rain, 2016.....	40
Figure 32: Detailed lake development on Harbardsbreen in 2015.....	41
Figure 33: Detailed lake development on Harbardsbreen in 2018.....	42
Figure 34: Detailed lake development on Harbardsbreen in 2019.....	43
Figure 35: Detailed lake development on Harbardsbreen in 2020.....	44
Figure 36: Combined detailed development of the Western lake 2010-2020 by date.....	45
Figure 37: Combined detailed development of the Eastern lake 2010-2020 by date.....	45
Figure 38: Mosaic of Sentinel-2 (S-2) and 4-band PlanetScope (P-4) imagery from 2018.....	46
Figure 39: Western lake volume to lake area (from elevation model from 18.08.2020).....	47
Figure 40: Eastern lake volume to lake area (from elevation model from 18.08.2020).....	48
Figure 41: Estimated lake volume 2010-2020, based on the 2020 elevation model.....	48
Figure 42: The glacier extent of Harbardsbreen in 1966, 2010, 2019 and 2020.....	51
Figure 43: Elevation change in meters [m] of Harbardsbreen 29.09.2010-18.08.2020.....	53
Figure 44: Elevation change of Harbardsbreen 29.09.2010-18.08.2020, for the area of interest around the lakes.....	54
Figure 45: Geodetic mass balance measured in meters of water equivalents for the period 2010-2020.....	55
Figure 46: In-browser web preview of Sentinel-2.....	57
Figure 47: Example Sentinel-2 imagery (resolution: 10 by 10 meters per pixel) of the Eastern lake.....	58
Figure 48: A comparison of 3-band and 4-band PlanetScope, Sentinel-2 and Landsat 8.....	59
Figure 49: Results of radar survey in May 1999, from Kjølmoen & Engeset (2003).....	68

List of tables

Table 1: Documented GLOF events at Harbardsbreen.....	11
Table 2: Overview of satellites used in this study.....	17
Table 3: Estimated lake volume and probability of GLOF events.....	50
Table 4: Measured total area of Harbardsbreen in 2010, 2019 and 2020.	52
Table 5: Mass balance for the periods 1966-1996, 1996-2010 and 2010-2020	65

Dictionary

DEM	Digital Elevation Model.
Englacial	Within the glacier.
Firn	Snow that has survived at least one summer season.
GIS	Geographic Information System.
Glacial lake	A lake formed by glacial meltwater, either on, within, under, at the margin or in front of the glacier.
GLOF	Glacial Lake Outburst Flood.
HVL	Høgskulen på Vestlandet/Western Norway University of Applied Sciences.
LiDAR	Light Detection And Ranging, a pulse radar commonly used to create DEMs.
m.a.s.l.	Meters above sea level.
m.w.e.	Meters of water equivalents (melted snow and ice, measured vertically).
NDWI	Normalized Difference Water Index, a method to find water bodies using multispectral satellite imagery and GIS tools.
NIR	Near infra-red.
NVE	Noregs Vassdrags- og Energidirektorat/The Norwegian Water and Energy Directorate.
PDD	(Cumulative) Positive degree days.
Proglacial	In front of the glacier or at the glacier margin.
QGIS	“Quantum GIS”, my preferred GIS software.
Scene	A single satellite image.
Subglacial	Beneath the glacier.
Supraglacial	On top of the glacier.

1 Introduction

1.1 Background

Climate change has led to increased melting of mountain glaciers all over the world, including Norway (IPCC, 2019; Clarke L., 2014; Ruddiman, 2014), and the melting process has been shown to be accelerating the past couple of decades (Hugonett, et al., 2021). Consequently, the melting of mountain glaciers has caused an increase in glacial lakes, and both the number of lakes and the area of the glacial lakes are expected to further increase in the future (IPCC, 2019; Harrison, et al., 2018). Such lakes may drain completely in a matter of a few days or just a few hours once the water level reaches a critical limit (NVE, 2015). Sudden drainage events like this are called glacial lake outburst floods (GLOFs), or jökulhlaups.

GLOFs may potentially pose a significant risk to both people and infrastructure (Dubey & Goyal, 2020; Carrivick & Tweed, 2016). Norway has a long history of GLOFs which have caused significant damages to inhabited areas and even loss of lives (Liestøl, 1956; Jackson & Ragulina, 2014). There is, however, limited knowledge on the relations between climate change, glacial lakes and GLOFs, and how the frequencies and magnitudes of GLOFs may be affected by future climate changes. More knowledge on this topic will be beneficial for future studies in this field, and may contribute to early warnings of GLOFs.

1.2 What is a glacial lake?

A glacial lake is a lake formed by glacial meltwater which is located either on top of (supraglacial), within (englacial), beneath (subglacial) or at the margin of a glacier (proglacial). A glacial lake may be dammed by moraines, dead ice (a part of the glacier which has been disconnected from the main glacier due to melting), bedrock, avalanche or rockfall debris or by the glacier itself. Glacial lakes may often vary a lot in size through the melting season, and from year to year due to changes in the weather as well as glacial melt which changes the surface elevation of the glacier (Benn & Evans, 2010). A detailed orthophoto of the glacial lakes of Harbardsbreen, Western Norway, captured August 8th 2004, is shown in Figure 1.

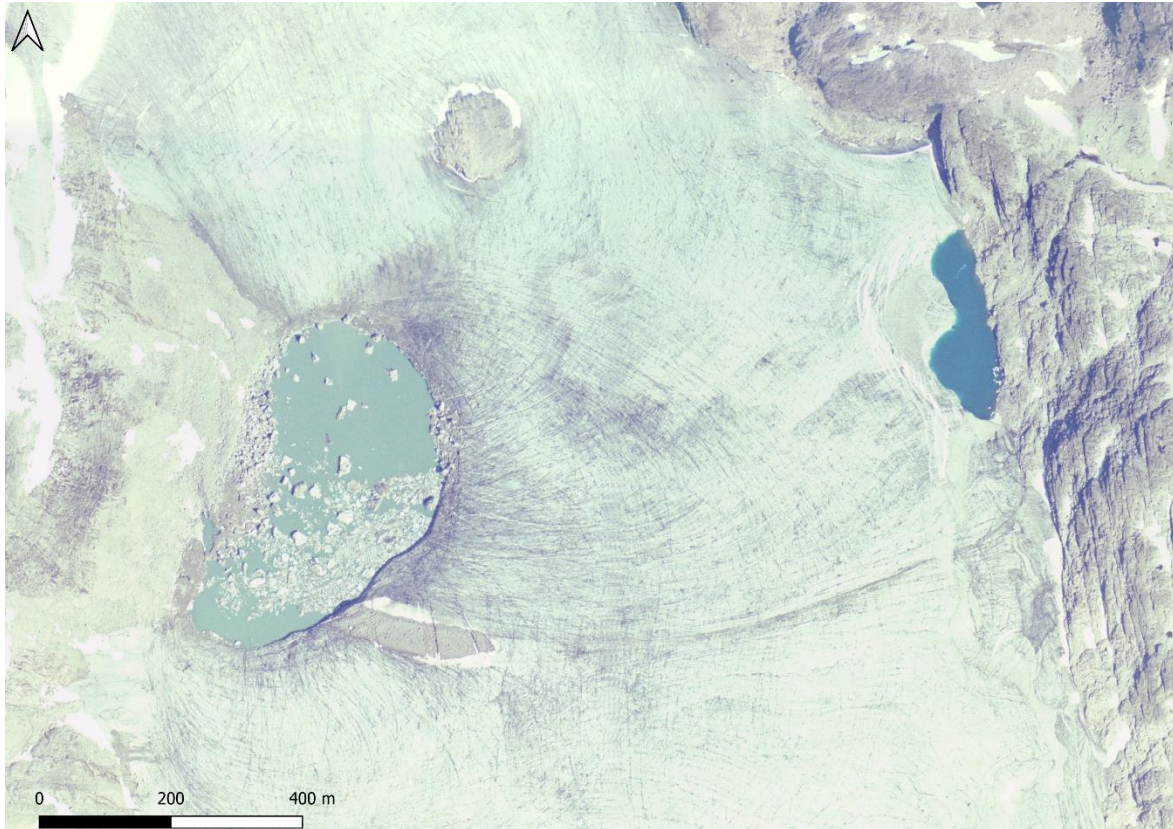


Figure 1: Detailed view of the glacial lakes of Harbardsbreen. Orthophoto captured on August 8th 2004. ©NorgeiBilder.

1.3 What is a glacial lake outburst flood (GLOF)?

Some glacial lakes may have a slow, yet steady outflow of water which prevents them of growing any larger and some will likely drain (either partly or completely) either during or by the end of the melting season. Other lakes may be completely dammed by ice or by a moraine, with no or very limited output flow of water. Once the water level in such glacial lakes reaches a critical limit the water may breach through the moraine or under the ice and may drain completely over a few days or in a matter of just a few hours. Sudden drainage events like these are called glacial lake outburst floods (GLOFs), or jökulhlaups. The word jökulhlaup comes from Icelandic and literally translated it means glacier run, or glacier flood. (Benn & Evans, 2010; NVE, 2015; NVE, 2021a).

A very simplified illustration of how a glacier dammed glacial lake may cause a GLOF is shown in Figure 2: Water is trapped in a deepening in the terrain between the bedrock and the glacier (Figure 2a). If the lake forms very quickly, the subglacial drainage system will not be able to develop quickly enough to drain the lake, and the lake will build larger and larger as the output of water from the lake is significantly less than the input of meltwater to the lake. As

the water level increases, the water may lift the glacier due to the fact that ice has lower density than liquid water. This may lead to the ice cracking due to tension (Figure 2b). When the water level reaches a critical point, the water will create a subglacial meltwater tunnel beneath the glacier which will drain the lake. Once the water breaks through beneath the ice it may easily melt a gradually larger meltwater tunnel through the ice due to friction, accelerating the drainage further (Figure 2c). After the lake has been drained the meltwater tunnel may close up again due to the pressure and weight of the ice, and the crevasses on the glacier surface may endure (Figure 2d). This is a process which may be repeated the following years as the glacier will reform and refreeze.

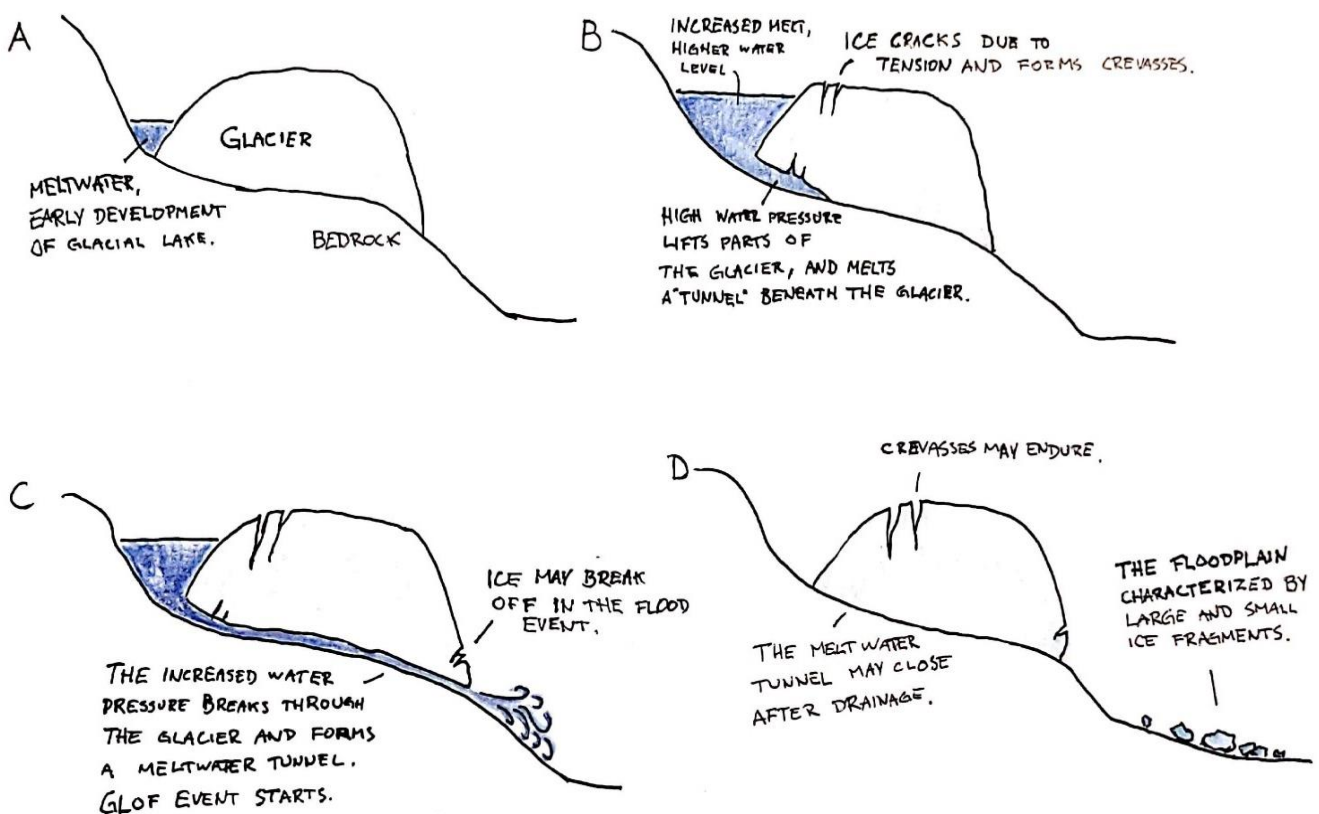


Figure 2: Simplified illustration of how a glacier-dammed lake may cause a GLOF, as is the case at Harbardsbreen.

A GLOF event may also be caused by a moraine dammed lake. A glacial lake which is dammed by a moraine may start to drain once the water finds a way either through or over the moraine wall, which may erode to a gradually larger opening. If the breach in the moraine is large enough and the lake contains a large amount of water a GLOF event is likely to occur. However, once the moraine dammed lake has eroded through the moraine, it is not possible it

will happen again in the same way in this lake as the moraine which dams the lake is no longer able to hold back the water.

1.4 Glaciers and temperature changes in Norway

Glaciers in Southern Norway have shown an overall retreat since the culmination of the little ice age, around AD 1750. Only since the year 2000 most observed glaciers had an annual frontal retreat of more than 100 meters (Nesje, Bakke, Dahl, Lie, & Matthews, 2008), and the melting process has accelerated further during the past decades (Hugonett, et al., 2021). Glaciers in Norway are now at a minimum stage since measurements began around 1900 AD (Andreassen, Elvehøy, Kjøllmoen, & Belart, 2020).

This is reflected by the average annual summer and winter temperatures in Norway. Figure 3 and Figure 4 shows official temperature records from the Western Norway region (which includes the counties Rogaland, Vestland (former Hordaland and Sogn og Fjordane) and Møre og Romsdal) provided by the Norwegian Meteorological Institute, showing summer and winter temperature records respectively. The figures show annual temperature deviations compared to the 1961-1990 normal period, and it is evident that both the summer season and the winter season has seen a significant temperature increase compared to the defined normal period. However, the increase is on average between 1°C and 1.5°C for the summer season, and about 2.5°C for the winter season.

Temperaturavvik fra 1961-1990-normal
Vestlandet – Sommer

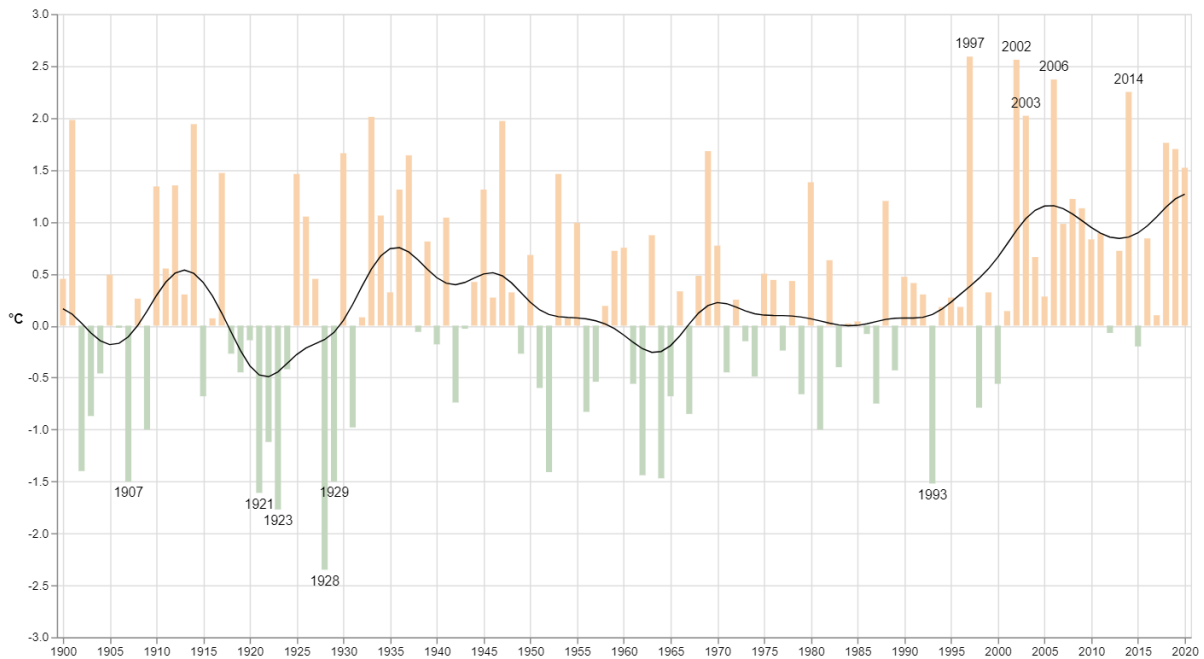


Figure 3: Official temperature records by the Norwegian Meteorological Institute showing summer season temperature deviations compared to the 1961-1990 normal period in the Western Norway region (Vestlandet). The data shows a trend in rising temperatures, yet with large annual variations (Meteorologisk Institutt, 2021).

Temperaturavvik fra 1961-1990-normal
Vestlandet – Vinter

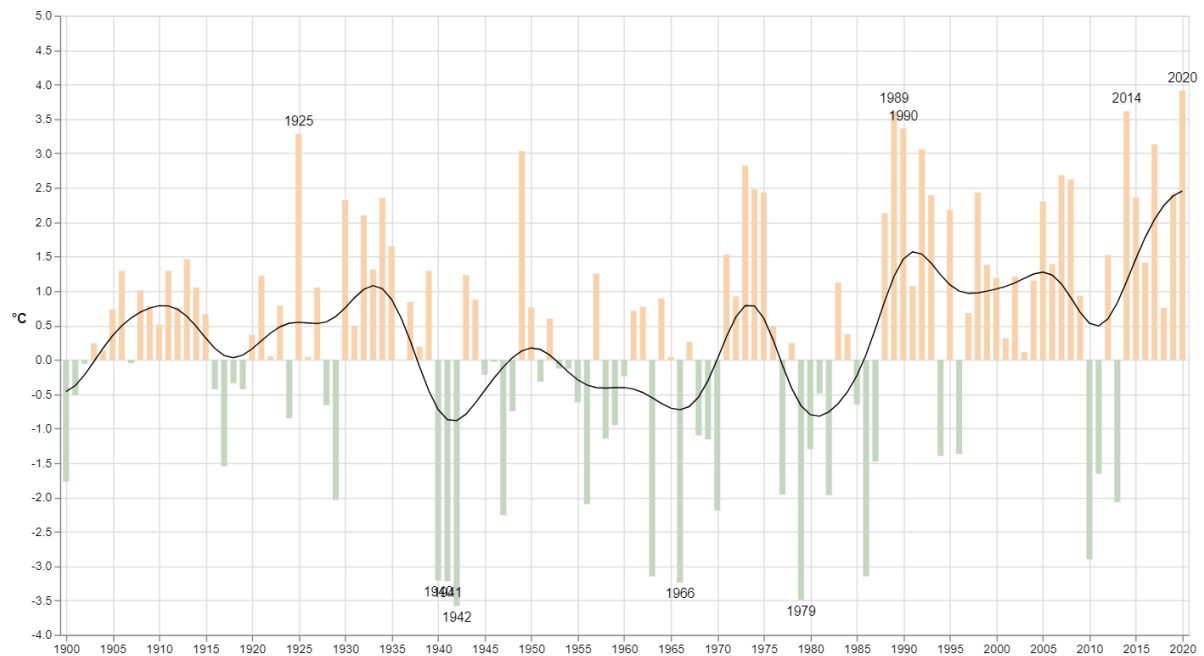


Figure 4: Official temperature records by the Norwegian Meteorological Institute showing the winter season temperature deviations compared to the 1961-1990 normal period in the Western Norway region (Vestlandet). The data shows a trend in rising temperatures, yet with large annual variations (Meteorologisk Institutt, 2021).

1.5 Field location: Harbardsbreen

Harbardsbreen is located in the north-eastern part of Breheimen national park in Luster municipality, Western Norway, just east of Jostedalsbreen (Figure 5), and is known for causing jökulhlaups (Kjøllmoen & Engeset, 2003; NVE, 2010; NVE, 2021b). Harbardsbreen is a plateau glacier which stretches approximately 11 km long in a north to south direction, and up to approximately 5 km across at its widest, and had an area of approximately 25 km² according to the latest published inventory based on Landsat imagery from 2003 (Andreassen, Winsvold, Paul, & Hausberg, 2012). Harbardsbreen's lowest point is at approximately 1250 m.a.s.l., and its highest point is at approximately 1950 m.a.s.l.. However, Harbardsbreen is partly connected to Fortundalsbreen to the north-east, and to Austre Kolleebreen to the north (Figure 6). Combined with these, Harbardsbreen measures approximately 36 km², which makes it the 10th largest glacier in mainland Norway (Thorsnæs, 2020). In this study however, I will only focus on the main parts of Harbardsbreen, not including Fortundalsbreen and Austre Kolleebreen.

In the middle part of Harbardsbreen is a plateau in which the northern and the southern parts of Harbardsbreen meet. Commonly a meltwater lake has formed in the summers on the western side in the middle part of Harbardsbreen, and in more recent years another smaller lake has formed on the eastern side of the glacier, directly across from the other lake (Figure 5d and Figure 6). These lakes are not named, and will from this point onwards in this study be referred to as the Western lake and the Eastern lake, respectively. The glacial lakes of Harbardsbreen are dammed by the glacier on the one side, and by the mountain sides on the other, and are thus classified as ice-marginal lakes, or proglacial lakes, and they are located at an altitude of approximately 1400 to 1450 m.a.s.l.. The lakes drain through subglacial meltwater tunnels beneath the glacier, and the assumed drainage path is shown in Figure 6. During the past decades there have been registered several GLOFs from these lakes, of which the largest ones in recent years occurred in 2010 and 2015 (NVE, 2021a; NVE, 2021b). Figure 7 shows helicopter photos of the Western lake on September 2nd 2020, after the lake has been drained. The photos show in high detail large and extensive crevasses which circle the area which the lake was before it drained. They also show large pieces of broken ice where the lake was.

Located in the valley below Harbardsbreen is a dammed, regulated hydropower reservoir (Fivlemyrane) owned by the company Hydro (Figure 6). If a GLOF should come unwarned, this dam may overflow, causing flooding in Fortunsdalen. However, if the GLOF is warned and the reservoir is regulated accordingly, a GLOF may have a positive effect by filling the

reservoir, meaning the power company can produce more electricity. More knowledge about the lakes of Harbardsbreen is thus both needed and beneficial for the power company, the inhabitants in Fortunsdalen, as well as for future research on this topic.

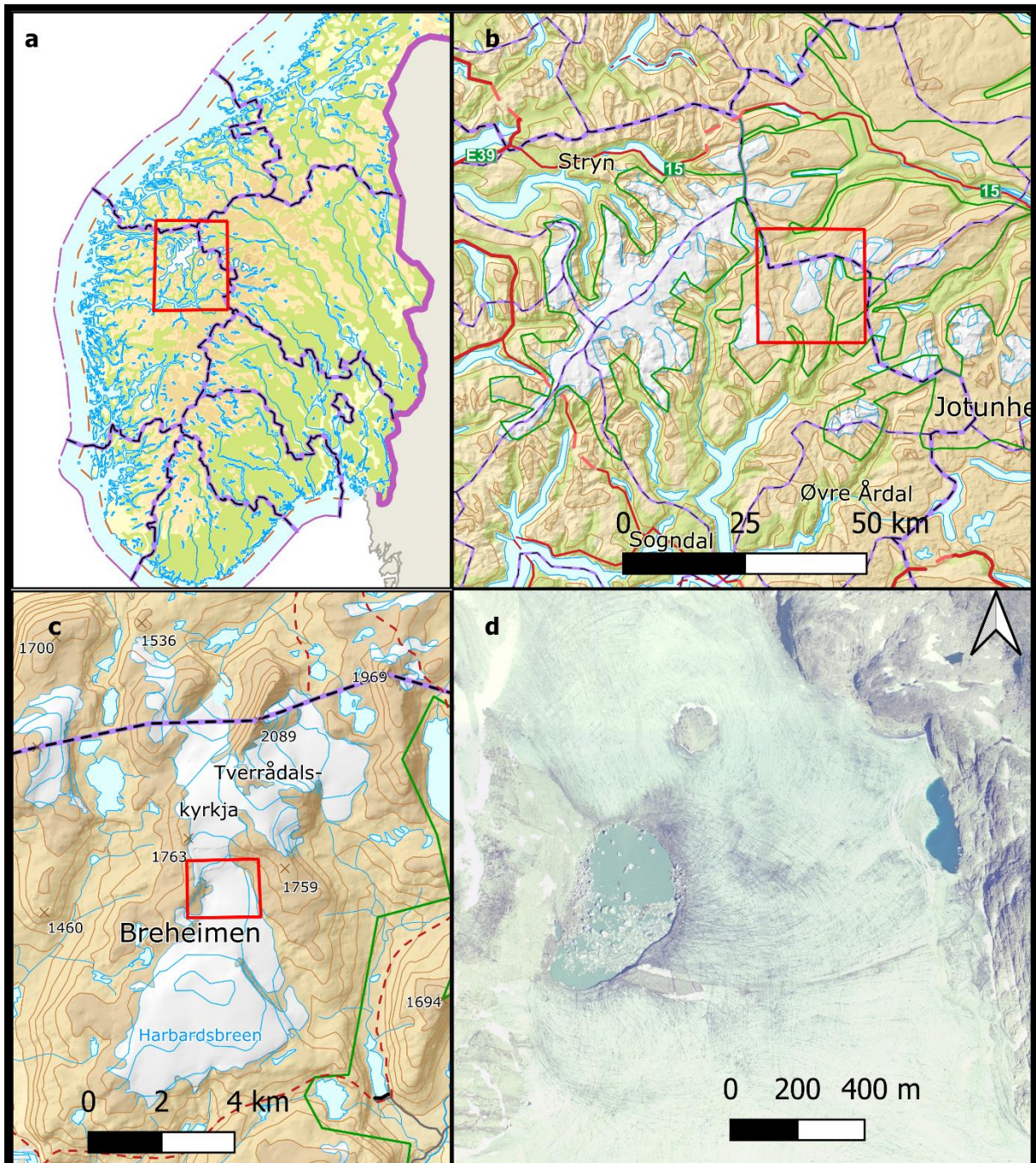


Figure 5: Overview map of Harbardsbreen location and the glacial lakes. (d) shows an orthophoto of the lakes as of 12.08.2004. Please note the difference in colors in the two lakes. (Kartverket/NorgeiBilder)

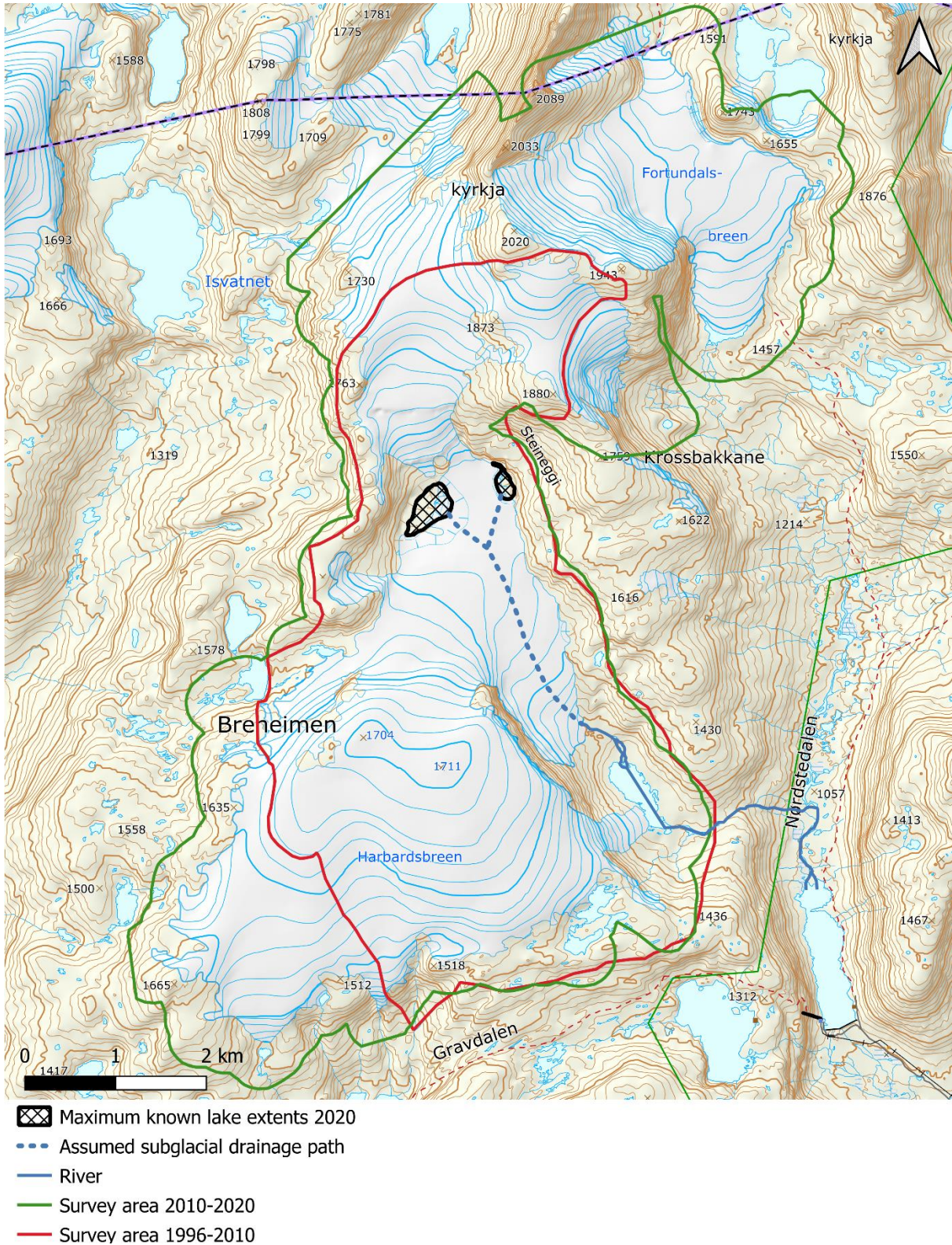


Figure 6: Overview map of Harbardsbreen, showing the maximum known lake extents of 2020 as well as the assumed drainage path beneath the glacier. The survey area for the period 1996-2010 and 2010-2020 is also drawn on the map. Please note that the northernmost part of the glacier (Austre Kollebreven) is not covered by neither the 2010 nor the 2020 LiDAR survey. To the bottom right of the map one can see the dammed and regulated lake Fivlemyrane, which is downstream of Harbardsbreen. (Background map: Kartverket)

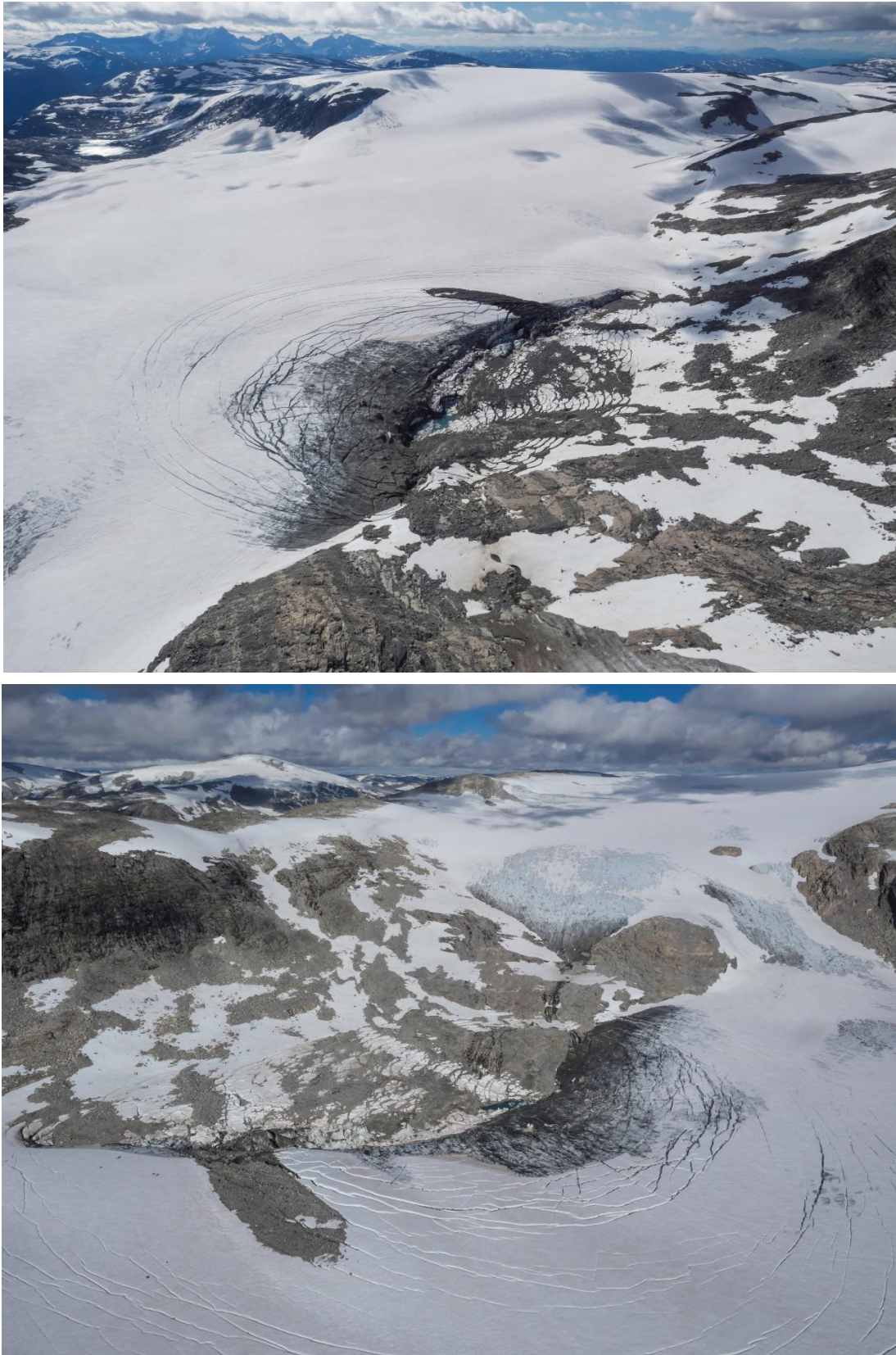


Figure 7: The drained Western lake, captured from helicopter on 02.09.2020, facing south (top) and north (bottom). Please note the crevasses which follow a circular shape around where the lake was located before it drained. Photo: Thorben Dunse.

1.6 Registered GLOF events in Norway

NVE (2021b) has a publicly available data record of registered and documented GLOF events in Norway. In total, they currently monitor 27 glaciers for GLOF activities, including Harbardsbreen. The database shows a significant change in the frequencies of registered GLOF events in Norway. Combining the data from all 27 locations and sorting this into 30-year periods one can see a clear trend of a higher frequency of registered GLOF events in later years, as shown in Figure 8 below, and a detailed view of the last 30-year period is shown in Figure 9 (data downloaded and valid as of March 8th, 2021).

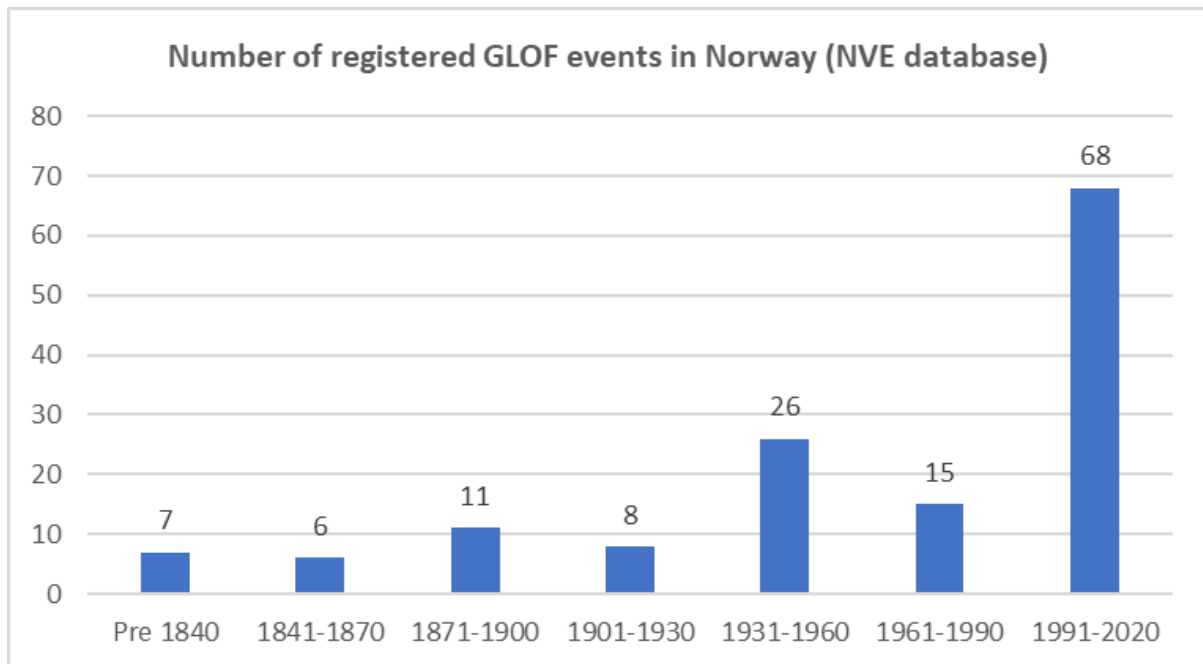


Figure 8: The total number of registered GLOF events in Norway divided into 30-year periods. Data is collected from NVE's GLOF database (NVE, 2021b).

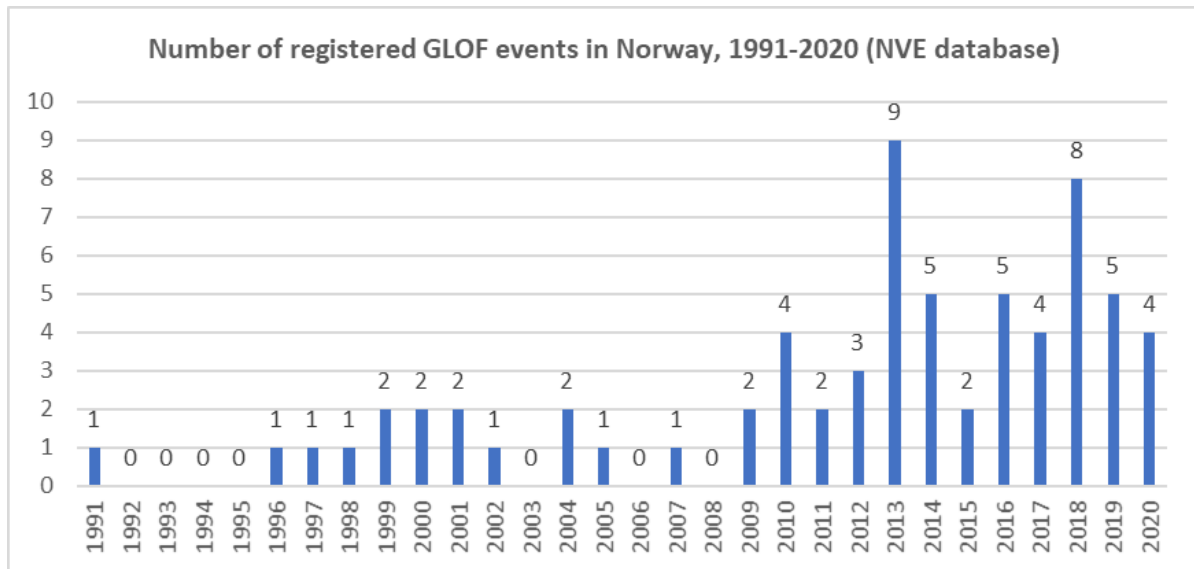


Figure 9: The total number of registered GLOF events in Norway for the last 30-year period, 1991-2020. Data is collected from NVE's GLOF database (NVE, 2021b).

1.7 Registered GLOF events at Harbardsbreen

All documented GLOF events at Harbardsbreen are shown in Table 1. Please note that the dates until 2001 are set as approximate, and the date in 2012 is unknown. Satellite photos and orthophoto of the lakes from 2020, 2015 and 2010 are shown in Figure 10, Figure 11 and Figure 12.

Table 1: Documented GLOF events at Harbardsbreen (Kjøllmoen & Engeset, 2003; Kjøllmoen B., 2011; Kjøllmoen B., 2016; NVE, 2021b).

Year	Date	Estimated discharge volume, million m ³	Comment
2020	06/24	-	(Figure 10)
2015	08/21	5.5	(Figure 11)
2012	Unknown date	0.6	Possibly in early July
2010	08/04	5.5	(Figure 12)
2001	09/01 (approx.)	-	Between Aug. 23 rd and Sept. 19 th 2001
2000	10/01 (approx.)	-	Between Sept. 13 th 2000 and Feb. 16 th 2001
1998	10/01 (approx.)	-	Between Sept. 23 rd 1998 and May 8 th 1999
1997	10/01 (approx.)	-	After Sept. 24 th 1997
1996	10/01 (approx.)	-	Between Sept. 14 th 1996 and Feb. 1 st 1997

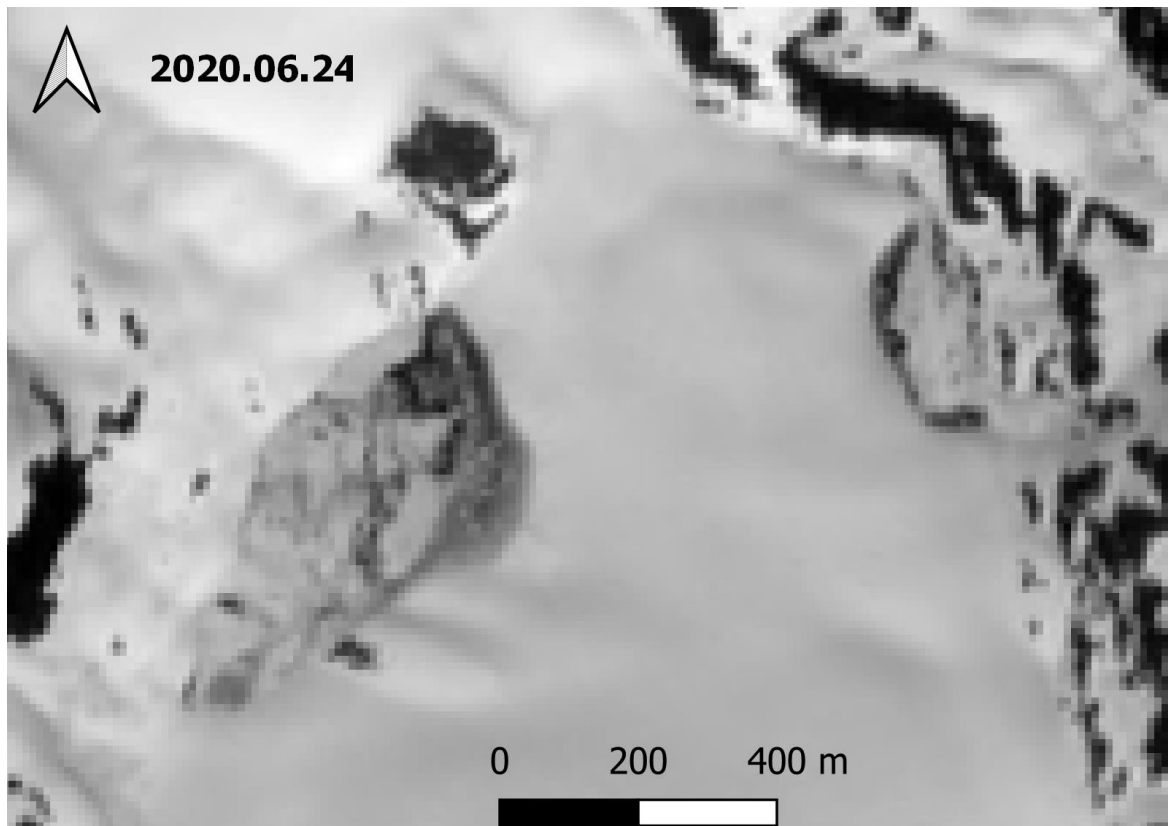


Figure 10: Sentinel-2 satellite photo of the lakes as of August 24th 2020 (day of the registered GLOF).

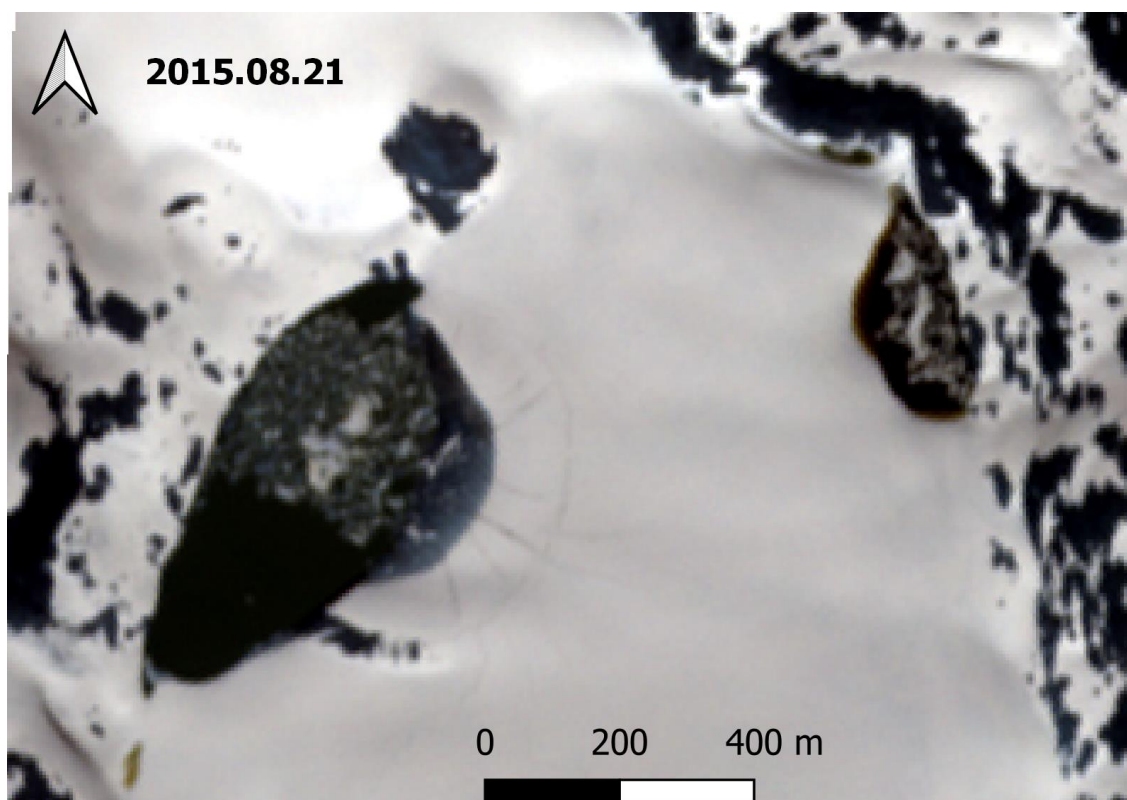


Figure 11: RapidEye satellite photo of the lakes as of August 21st 2015 (day of the registered GLOF).

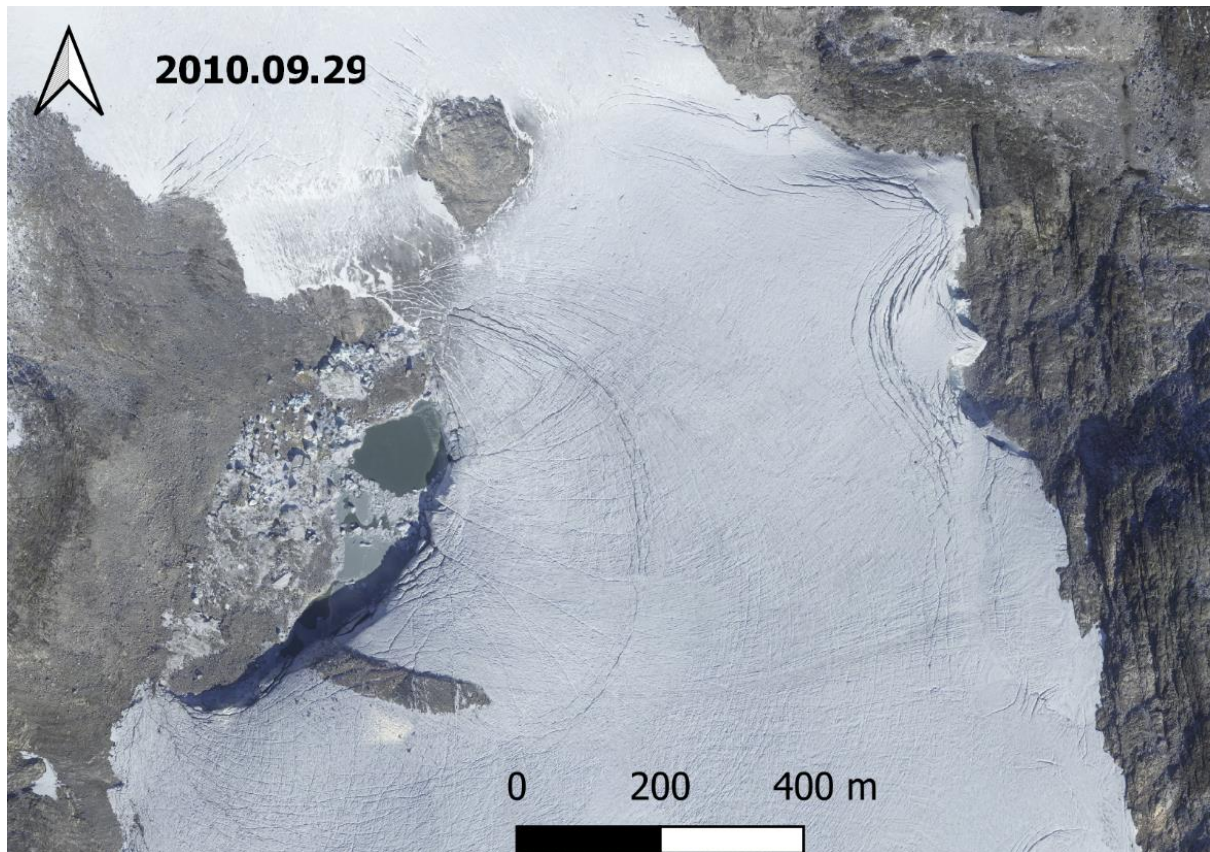


Figure 12: High resolution orthophoto of the lakes as of September 29th 2010. The Western lake's maximum extent is still visible by the icy edge to the left of the Western lake, which still has some water in it after getting drained in the GLOF event on August 4th 2010. (©NorgeiBilder)

1.8 Previous research

Several studies have been done at Harbardsbreen prior to this study. Mass balance investigations have been made for the periods 1966-1996 (Kjøllmoen B. , 1997), 1997-2001 (Kjøllmoen & Engeset, 2003) and 1996-2010 (Andreassen L. M., 2013). They found a significant negative mass balance of -0.28 m, -0.23 m and -0.82 m water equivalents per year respectively. However, these studies did not cover the entire surface area of Harbardsbreen, as the elevation data from 1966 and 1996 only covers the main part of Harbardsbreen (Figure 6). NVE has also logged GLOF activities at Harbardsbreen in their GLOF database (NVE, 2021b). Ice thickness measurements using radar was done in 1996 on the plateau area between the lakes in the middle part of Harbardsbreen, which found a deepening in the subglacial topography in this area, and found the ice thickness to be up to 160 meters (Kjøllmoen & Engeset, 2003).

Other studies have also used satellite imagery (Sentinel-1 and Sentinel-2) to map glaciers and glacial lakes in Norway and Svalbard, including Nagy & Andreassen (2019), Kjølmoen et. al. (2020), and Andreassen et. al. (2021). However, the use of satellite imagery to map glacial changes and changes in glacial lakes over time has not been done at Harbardsbreen prior to this study.

1.9 Research objectives

In this research project I will investigate the development of the lakes of Harbardsbreen and link this activity to weather data. I will use satellite data from Planet Labs and Copernicus Open Access Hub to present a multidecadal time series of the evolution of the lakes. For the time period 2010 to 2020 I will focus on making an as detailed as possible mapping of the lakes' annual developments, and link this to available weather data to find possible connections between this and recent GLOF events. I will also use elevation data to calculate the mass balance between 2010 and 2020, and find a link between the long-term lake development and glacier mass balance. I will also aim to find a formula for an early warning of a GLOF event at Harbardsbreen.

2 Data and methods

2.1 Satellite data

For this project I have used daily satellite imagery provided by Planet Labs to make an as detailed as possible time series of the development of the lakes of Harbardsbreen over the past decade (2010-2020), as well as a long-term overview of the development of the lakes since 1972 using the Copernicus Open Access Hub to access Sentinel-2 and Landsat data for the period of 1972 to 2020. An overview of the different satellite data sources used in this study is presented in Table 2.

Previous studies which have used Sentinel and Landsat data often rely on automatic or semi-automatic methods for mapping large areas and potentially a large number of glaciers and lakes, e.g. Andreassen et.al. (2021). However, manual corrections commonly have to be made, and very small and/or ice-covered lakes may not be registered properly only using automatic methods. In this study, however, I will solely focus on Harbardsbreen, of which the lakes form in a small area and are comparably small to other glacial lakes. Because of this, I chose to do all the mapping manually in QGIS using available satellite imagery from various sources, as presented in Table 2. For most of the cloud free imagery from Planet and Sentinel-2 it was very simple to map the lakes' extents manually only based on the visibility of the lakes' borders in the imagery. However, in some images the borders of the lakes were not easily defined. This could be because of partly snow and ice cover, or that the bedrock had very similar color as the water body. In these cases, I found the extents of the lakes by finding the normalized difference water index (NDWI) using the raster calculator in QGIS and the green and the near-infrared (NIR) bands (band 2 and band 4) of the multispectral imagery which Sentinel-2 provides. The equation for finding the NDWI is:

$$NDWI = \frac{(Green - NIR)}{(Green + NIR)}$$

This technique creates a false-color image in which water bodies will have the color code of values ≥ 0.3 (McFeeters, 1996). However, this method is not always correct as some shadows also may be registered with the same values as water bodies.

2.1.1 Planet Labs

Planet Labs (www.Planet.com) was founded in 2010 with the goal of providing daily satellite imagery of the entire Earth's surface. Their first satellite, Dove 1, was launched in a sun synchronous orbit in 2013. Only four years later, in 2017, Planet Labs reached their goal of covering the earth with daily imagery by steadily increasing their satellite capacity. Today Planet Labs have more than 200 satellites in polar orbits, providing high resolution satellite imagery of the entirety of the Earth's surface every day at a resolution of 3 by 3 meters. Through Planet Labs' data records (www.Planet.com/explorer) one can access satellite data from several sources. These include Planet Labs' own PlanetScope and RapidEye imagery, as well as Sentinel-2 and Landsat 8. However, Planet Labs' data records only provide imagery dating back to 2009, as the RapidEye satellites (five in total) were put into orbit in 2008 and were operational from February 2009. Image frequency is thus poorer in the earlier years of this record as they did not have full daily imagery coverage until 2017. It is required to apply to create an academic account in order to download satellite data from Planet, however it is possible to self-register for a free trial account, but this will have restrictions on the quantity of downloads.

2.1.2 Copernicus Open Access Hub

To download satellite data dating pre 2010 I used the Semi-Automatic Classification Plugin in QGIS to access the Copernicus Open Access Hub. This service requires to register a free SciHub account in order to download satellite data. Once registered, you can get access to data from Sentinel (1st to 3rd generation) and Landsat (1st to 8th generation) among other sources.

The first generation of Landsat was launched in 1972 and was operational until 1982, which is very valuable for having as historic references. However, both the time resolution and the spatial resolution of the imagery is not the best in the earliest years of the existence of Landsat. Before 1984, when the Landsat 5 satellite was launched, the Landsat satellite data have a spatial resolution of 60 by 60 meters per pixel. Compared to the 3 by 3 meters resolution of the daily PlanetScope data available today you can tell there has been a significant improvement in the technology the past decades. The Landsat program is still active today, and the Landsat 7 and Landsat 8 satellites are still operational today after their launch in 1999 and 2013 respectively, and have a spatial resolution of 30 by 30 meters per pixel.

The three first generations of Sentinel satellites exist in pairs. The first satellite in the Sentinel program, Sentinel-1A, was launched in April 2014, and was followed by its twin satellite Sentinel-1B in April 2016. The first-generation Sentinel satellites provide radar imaging for land and ocean services. In June 2015, the Sentinel-2A satellite was launched, followed by Sentinel-2B in March 2017. Sentinel-2 provides multispectral imagery of high resolution (10 by 10 meters per pixel) for land monitoring. Sentinel-2 imagery has previously been used in several studies related to glacial changes and mapping of glacial lakes (e.g. Nagy & Andreassen (2019)) due to both its high-resolution imagery as well as relatively high image frequency in higher latitude areas due to the satellites' polar orbits.

Table 2: Overview of satellites used in this study (Landsat 6 never reached orbit).

Satellite	Launch year	End of service	Years of service	Image resolution [m]	Image frequency at field location (approx.)
Landsat 1	1972	1978	6	60x60	1-3 times a month
Landsat 2	1975	1982	7	60x60	1-3 times a month
Landsat 3	1978	1983	5	60x60	1-3 times a month
Landsat 4	1982	1993	11	60x60	1-3 times a month
Landsat 5	1984	2013	29	30x30	1-3 times a month
Landsat 7	1998	Still operational	23 →	15x15/30x30*	Once a week
Landsat 8	2013	Still operational	8 →	15x15/30x30*	Once or twice a week
RapidEye	2008	2020	12	5x5	1-3 times a month
Sentinel-2	2015	Still operational	6 →	10x10	Every 1-3 days
Doves** (PlanetScope)	2013	Still operational	8 →	3x3	Daily since 2017, up to several images per day

*Panchromatic/multispectral

**First satellite launch followed by several more. Currently there are more than 180 Dove satellites in orbit.

2.2 Glacier extent

I manually mapped the extent and area of Harbardsbreen in QGIS using the latest available satellite photos from the summer season which were snow free in 2010 (September 6th) and in 2020 (August 26th). However, because Harbardsbreen was still snow covered at the end of the summer season in 2020 the mapped area of Harbardsbreen is likely overestimated as the border between the snow-covered glacial ice and the snow-covered bedrock was difficult to find. Thus, additionally I also mapped the glacier's area from early autumn 2019 (August 26th) as a reference, as the entire glacier was completely snow free on this date due to extensive snow and ice melt this summer. However, I still used the measured area for 2020 when I calculated the elevation change and mass balance.

2.3 Elevation change and mass balance

The original plan for collecting elevation data was to do this by using a drone with a laser scanner at the field location in order to get a high-resolution elevation model (centimeter scale resolution). Previous research on Norwegian glaciers and glacial lakes has used this technique and found it both useful and highly accurate, e.g. Andreassen & De Marco (2018). Unfortunately, the weather conditions did not allow this kind of field work in our available time window in early to mid-September 2020 (before the first snowfall), and had to be cancelled. Thus, I had to use third party elevation data.

Elevation data from 2020 was collected from www.hoydedata.no, a web service provided by Kartverket (The Norwegian Mapping Authority). The latest available elevation data from different locations in Norway are free to download through this service as digital elevation models (DEM) or digital pointclouds. The latest LiDAR scanning survey was executed on August 18th 2020 by Terratec (Terratec, 2020).

My supervisor Liss M. Andreassen, NVE, provided me with elevation data from September 29th 2010, as well as from 1996 and 1966 for historic references. The data from 2010 was saved as LiDAR files (.las), also provided by Terratec (Terratec, 2020), which I had to convert to a DEM using the LAStools plugin in QGIS. The elevation data from 1996 and 1966 were digitalized contour lines from maps, which I used the GRASStools plugin in QGIS to convert the contours (vector data) to a DEM (raster data).

The surface elevation change of Harbardsbreen in the period 2010 to 2020 was found using the raster calculator tool in QGIS. The DEM from 2010 was subtracted from the DEM from 2020:

$$\text{Elevation change 2010 to 2020} = \text{DEM}_{2020} - \text{DEM}_{2010}$$

This gives total changes in surface elevation of the glacier, including ice, firn (snow that has survived at least one summer season) and snow for every pixel in the DEM raster files. The volume change was found using the Raster Surface Volume tool in QGIS, and dividing this volume by the mean measured glacier extent from 2010 and 2020 (Zemp, et al., 2013; Andreassen, Elvehøy, Kjøllmoen, & Engeset, 2016) I found the average elevation change for the entire measured area of Harbardsbreen over the time period of 2010 to 2020.

$$\text{Average elevation change} = \frac{\text{Total volume change}}{\text{Average area}}$$

Doing the same calculation using the extreme values of the error margins for both the measured glacier area and volume change I also found the uncertainty for the average elevation change.

To find the mass balance of the glacier I need to know the density of the ice, firn and snow. Glacial ice usually has a density which varies between 830 and 917 kg/m³ depending on the purity of the ice (Cuffey & Paterson, 2010). Assuming an average, consistent density of all the ice, firn and snow combined one can estimate the mass loss in meters of water equivalents (m.w.e.). Huss (2013) recommends using 850 ± 60 kg/m³ for periods longer than 5 years with stable mass balance gradients, the presence of a firn area as well as volume changes significantly different from zero. This estimated value has been used in several studies, including previous work on Harbardsbreen performed by Andreassen, L. M. (2013). An average ice density of 850 ± 60 kg/m³ means that a glacier which has melted 10 meters vertically has had a mass loss of 8.5 ± 0.6 m water equivalents.

2.4 Weather data

Weather data was collected from SeNorge (www.SeNorge.no), a free and public web service which provides interpolated weather data for any 1 by 1 km grid cell in mainland Norway (Lussana, Tveito, Dobler, & Tunheim, 2019). Interpolated data means that the spatial data is estimated from what data records are available from surrounding weather stations in

Norway, and the data has also been adjusted for elevation. This gives a complete data record for any given location in Norway, and the service provides weather data records ranging back to 1957. The service is developed by NVE in collaboration with Meteorologisk Institutt (The Norwegian Meteorological Institute), and is both well-known and trusted by Norwegian scientists as a data source.

However, the geographic spread of weather stations varies, and there are generally fewer stations located in high-altitude areas. Thus, in areas with long distances between the weather stations the interpolated data may not be accurate. However, there are two weather stations in mountain areas relatively close by the field area of Harbardsbreen. These are Spørteggbu (1566 m.a.s.l.) and Sognefjellhytta (1413 m.a.s.l.), which are located approximately 19 and 23 km from the lakes of Harbardsbreen respectively. In addition, there are two stations located in Jostedalen (243 and 305 m.a.s.l.), approximately 22 km from Harbardsbreen, which are the two closest stations in non-mountain areas. Spørteggbu is a relatively new station which only provides data back to 2017, while Sognefjellhytta on the other hand provides nearly complete weather data dating back to 1979. Given that the weather station at Sognefjellhytta is both in relatively close proximity to Harbardsbreen, as well as being at the approximate same elevation as the lakes of Harbardsbreen, I will argue that the interpolated data from SeNorge is quite representative for actual values at the area of interest at Harbardsbreen. Kjølmoen & Engeset (2003) also compared the monthly mean temperatures from Sognefjellhytta with a temperature logger which was put up on the east side of Harbardsbreen in a shorter period from 1997 to 2001, and found the temperature readings to be very similar to the ones at Sognefjellhytta. I downloaded the data from the 1 by 1 km grid cell which covered the Western lake the best: UTM 33N, X: 112640, Y: 6862612.

2.4.1 Cumulative positive degree days (PDD)

Cumulative positive degree days (PDD) is an indicator of how intensive the available heat energy for melting snow and ice is over time. PDD is defined as the sum of the mean daily temperature measured in °C for all days which the mean temperature is higher than 0°C ($PDD = \sum \bar{T}_d$), and has the unit of °C (Benn & Evans, 2010). As an example, if the average daily temperature is 5°C for 20 consecutive days, you will have a total value of 100 positive degree days. I used the temperature data to find cumulative positive degree days for the area of interest. I chose to count the annual data from March to October to see if there were any years

the melting season started very early or ended very late. The data was also used to present a graph showing annual PDD values as well as linking the development of the Harbardsbreen lakes and potential GLOF events to the estimated PDD values for the relevant dates.

2.4.2 Precipitation

I used the precipitation data to see if there has been a significant increase in annual precipitation since the beginning of the data records (1957). I also filtered the data to show precipitation at temperatures higher than or equal to 0.5°C, which would be indicative of precipitation as rain in the summer season (April to September), and at temperatures lower than 0.5°C, indicative of precipitation as snow (October to March).

2.5 Software

I used the free mapping software QGIS, software version 3.10 (long-term release), to handle the satellite data and spatial data for this project and to map the extent of the lakes and of the glacier. The measured area and perimeter of the lakes were transferred to Microsoft Excel for further analyses. I also used Microsoft Excel to present the necessary graphs and figures.

2.6 Errors and uncertainties

2.6.1 Satellite data and cloud cover

The cloud cover percentage filter in Planet is not reliable. Very cloudy images could be marked with less than 5% cloud cover, and some almost cloud free images were marked with more than 30% and up to 40% cloud cover. Also, the area of interest is relatively small, and even in heavy cloud covers there may be scattered clouds, meaning there is still a chance for the area of interest to not be cloud covered and the imagery will still provide useful data. Hence, the cloud cover percentage filter in Planet's images was maximized from 0% to 100% cloud cover, to not miss available cloud free images. Still, it is possible that I have missed some days of good data as the preview in www.Planet.com/explorer could be very different from the downloaded file, as could often be the case for Sentinel-2 and 4-band PlanetScope imagery.

2.6.2 Lake and glacier area

The error margin for the measured lake area was found using this formula, as described by Shukla, Garg, & Srivastava (2018): $U_l = N \times \frac{A}{2}$, where U_l is the uncertainty in the measured lake area, N is the number of pixels around the perimeter of the lake, and A is the area of one pixel. Please note that the area or the shape of the lake is not considered in this formula, only the perimeter of the lake and the pixel size. As an example, a lake measured which has a measured perimeter of 1000 meters from a satellite photo with a resolution of 5 by 5 meters per pixel will give an uncertainty of $\frac{1000m}{5m/pixel} \times \frac{25m^2/pixel}{2} = \pm 2500m^2$. This means that a circular lake will have a smaller relative uncertainty than an elongated, narrow lake with the same perimeter, as the area of the elongated lake is significantly smaller than the circular one. Theoretically the relative error margin could be larger than the area of the lake itself, however this was not the case for any measurements I did in this study. I also used this formula to find the error margin when measuring the area of Harbardsbreen.

There are also uncertainties to how accurately I have been able to map the lakes. Some of the satellite imagery is of poorer resolution (e.g. Landsat 1, 2, 3 and 4 which is 60 by 60 meters per pixel), which makes it hard to define the lakes' borders. In newer satellite data (e.g. PlanetScope) this is less of a problem due to higher spatial resolution. Still, it may at times be very difficult to define the lakes' borders if they are partly ice covered and the glacier and the bordering bedrock are snow covered. In difficult cases I used contour lines which I had made from the elevation data to verify the lake borders along the mountain side. If I found that what I had thought was the lake border suddenly was several meters to tens of meters higher in elevation in one place than another I had to make adjustments to the measured lake border. This was not used to define the lakes' borders towards the glacier, as the glacier may change its position and elevation from year to year as well as through the summer season. Still, this helped define the lake borders along the mountain side in some cases.

2.6.3 Weather data

The temperature and precipitation data provided by SeNorge are, as mentioned, not direct measurements, but interpolated data from surrounding weather stations. In other words, they are estimations, and should be considered so. Therefore, I will interpret the temperature and

precipitation data as indications more than exact values. Still, this is a trusted service and data source among Norwegian scientists.

2.6.4 Elevation data

The DEMs from 2010 and 2020 both have an estimated vertical error margin of ± 10 cm. This error margin was combined with the error margin related to the measurement of the area of the glacier when I converted the elevation change to mass loss in water equivalents. To do this I estimated both the highest and lowest possible outcomes using the extreme ends of the error margins before converting the results to water equivalents.

3 Results

3.1 Maximum known lake extents

I had satellite data available dating back to 1972, the year of the launch of Landsat 1. The earliest year the Western lake appeared in the imagery was in 1973. Existence of the lake prior in earlier years is not known, but aerial imagery of the glacier from 1966 shows that the Western lake was present at the time of photographing, on July 19th 1966, as described by Kjølmoen & Engeset (2003). This indicates that the satellite record is not long enough to conclude if this is the earliest appearance of the lake(s) on Harbardsbreen.

Figure 13 shows the measured annual maximum known glacial lake extents of Harbardsbreen. Some years the lake(s) were not visible in the imagery due to a combination of poor time resolution and cloud cover, thus I had no evidence of any development of the lake(s). These years have been marked with “(N/A)”, meaning “not available”, and the lake area was set to zero. Years with documented cases of GLOF events are marked with an asterisk (*) to visualize the frequency of GLOF events at Harbardsbreen through time. Documented GLOF events occurred in 1996, 1997, 1998, 2000, 2001, 2010, 2012, 2015 and 2020 (NVE, 2021b). However, in 2012 I had no evidence of the lake development as the satellite data was limited in time resolution and the images which were available were heavily affected by thick cloud covers, providing no useful data this season except two images on August 15th and 27th which both show the Western lake in its drained state, indicating that a possible GLOF event must have happened before August 15th. Thus, the year 2012 is marked both with an asterisk, and “(N/A)”. In 2016 and in 1999, however, it was evident that neither the Western nor the Eastern lake formed in the summer season, and has thus been marked accordingly with a lake area of zero. In 2014 only the Eastern lake formed, and not the Western lake. Apart from 1999, 2014 and 2016, the Western lake has formed every year which has had sufficient satellite data since the beginning of the records (1972).

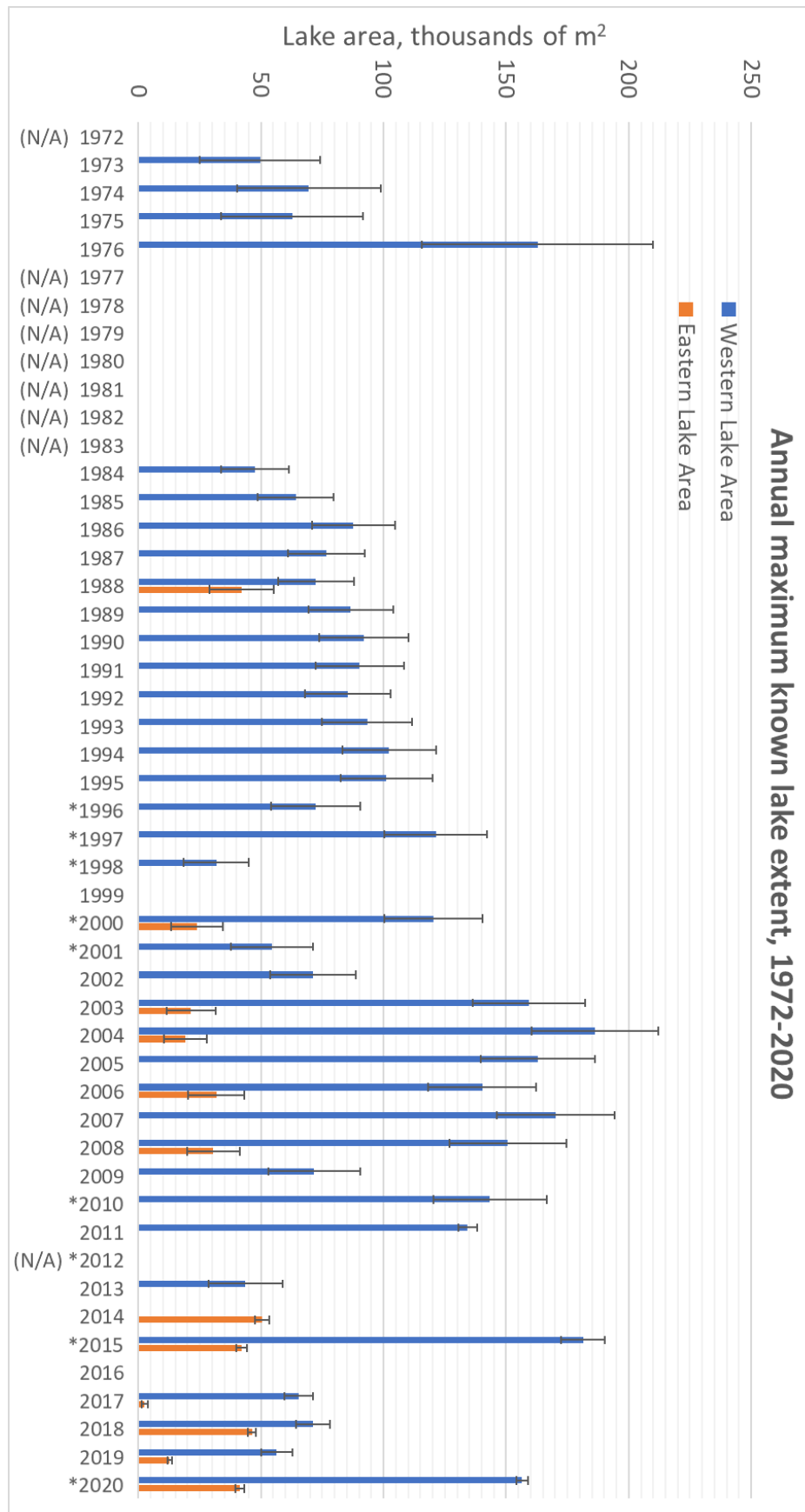


Figure 13: Annual maximum known glacial lake extents of Harbardsbreen, 1972-2020. Years in which GLOF events are documented are marked with an asterisk (*). Years with not enough data to determine the presence and area of the lakes are marked with "(N/A)". Neither of the lakes developed in 1999 and in 2016.

3.2 PDD values for drainage events

Figure 14 shows the cumulative PDD for GLOF and drainage events from 2010-2020. Exact numbers are used for known and documented GLOF events. For the other years, the error margins stretch from the date of the largest known lake area to the first evidence of the drained lake(s).

Figure 15 shows cumulative PDD values from 2010-2020. The figure clearly shows that 2018 overall has been the warmest summer season in this period with the earliest start, and that 2015 was the coldest season with the latest start. However, the starting point of the melting season varies a lot from year to year (normally ranging from early May to mid-June). To compensate for this, all the data series were set to start at the day which the PDD value had reached 20 PDD (Figure 16). The threshold value of 20 PDD was selected after counselling with my supervisor Thorben Dunse (HVL). This threshold value of 20 PDD was set to mark the start of the melting season, as the first few days of temperatures above zero likely will lead to melt and refreeze processes, and not melt and runoff. Comparing the development of the cumulative PDD from the years 2010-2020 by this standard shows a very different result than Figure 15. 2015 proves to not be the coldest year after the melting season has started, but apparently around average – even if the melting season did not start until mid to late June this year.

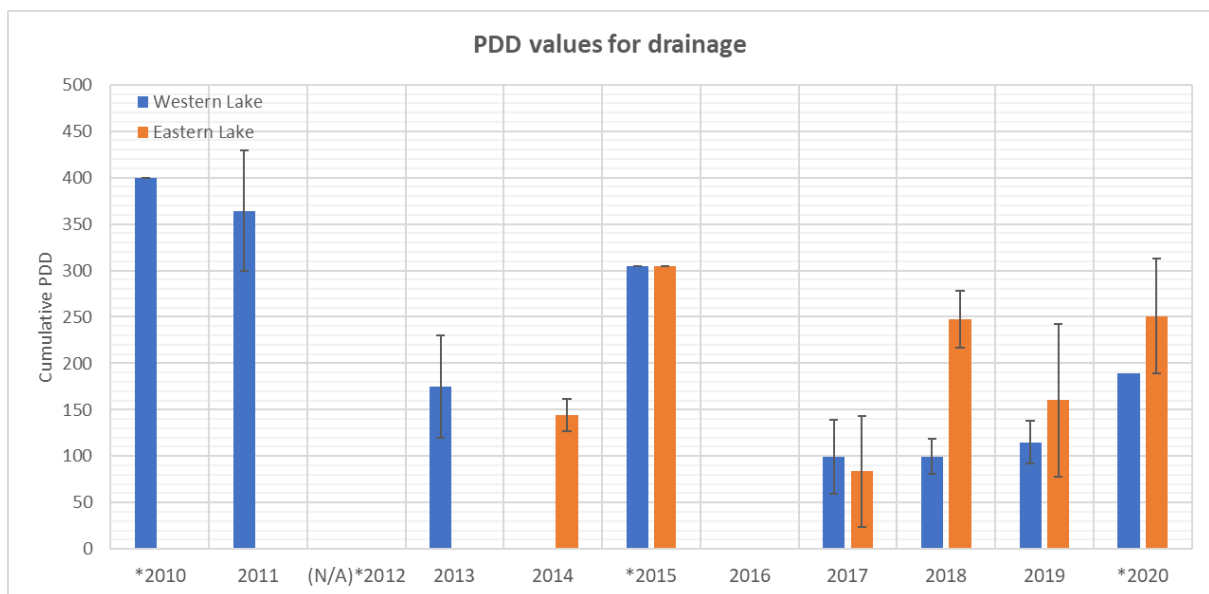


Figure 14: Cumulative PDD values for GLOFs and drainage events. Years with known dates of GLOF events are marked with an asterisk (*), of which exact values have been used.

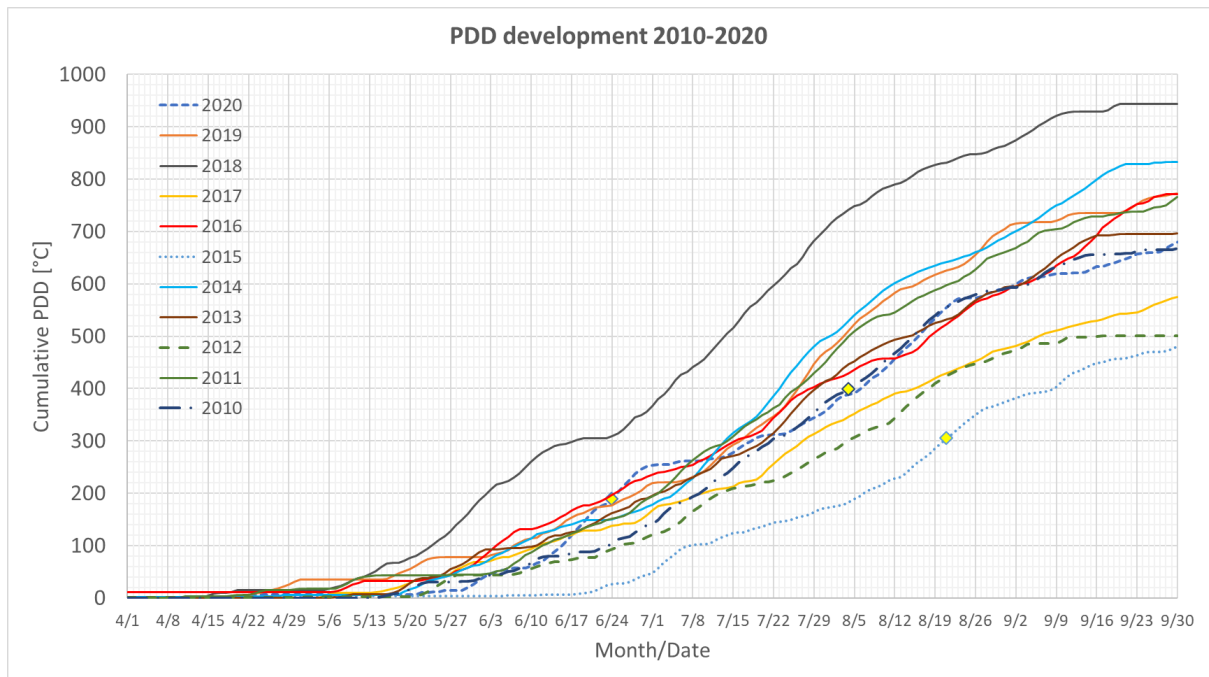


Figure 15: PDD values by date, 2010-2020. Known GLOF events are marked in yellow diamonds (2020, 2015 and 2010).

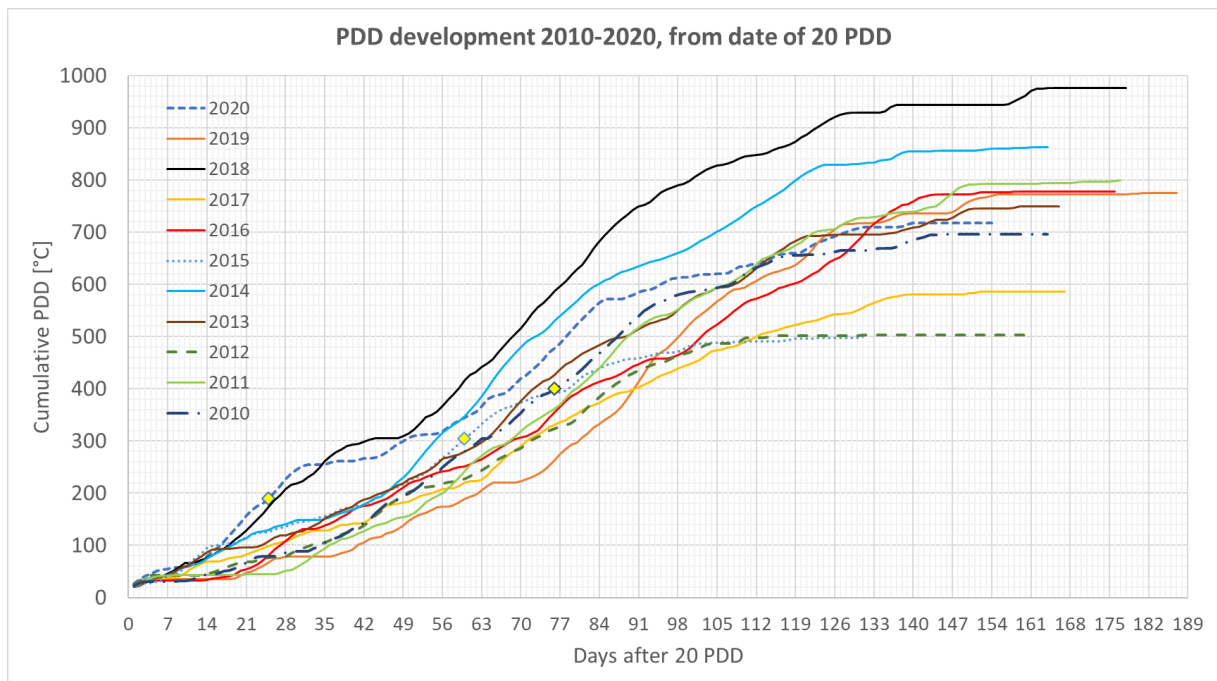


Figure 16: PDD values normalized by the first date of 20 PDD as a reference starting point of the melting season. The x-axis shows the number of days after this reference point. Known GLOF events are marked in yellow diamonds (2020, 2015 and 2010).

3.3 Temperature and precipitation

3.3.1 Temperature

The temperature data provided by SeNorge shows that the melting season has become longer and/or more intense the past decades. Figure 17 shows cumulative positive degree days throughout the summer season. With a few exceptions, typically the first positive degrees of the season would not be apparent before mid to late April and the melting season would typically end in September, which was expected. As Figure 17 shows, in the 1960's and 1970's the average seasonal PDD value was around 600 PDD. A small reduction is seen in the 1980's with an average of around 500 PDD. Since the 2000's the average has risen to around 700 PDD, an approximately 40% increase compared to 1980's values. These results correspond well to official climate data from the Norwegian Meteorological Institute (Meteorologisk Institutt), as shown in Figure 3 and Figure 4.

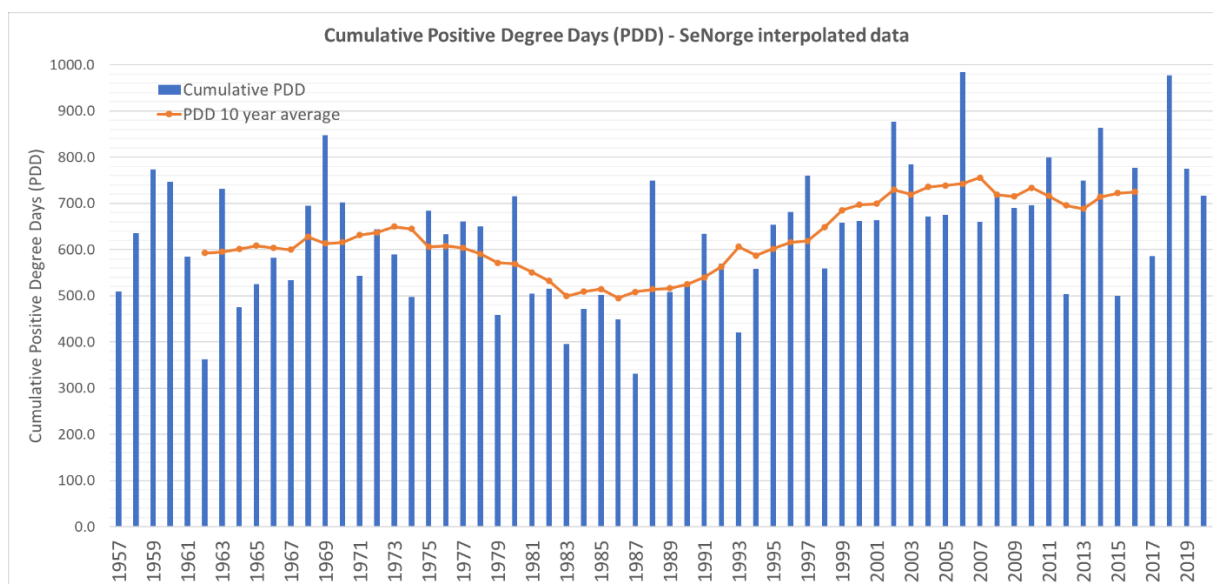


Figure 17: Annual cumulative positive degree days (PDD) from 1957 to 2020 for the field area on Harbardsbreen. The data shows that the melting season has, on average, become significantly longer and/or more intense since the 1980's.

Figure 18 shows the 10-year average of the annual number of days with temperatures above 0°C, and the average daily temperature per day with temperatures above 0°C. As the figure shows, the average number of days warmer than 0°C is approximately the same in the last decade as in the first decade of the time series, averaging at around 140 days. In the 1980's the

average number of days warmer than 0°C was closer to 120 days, which makes for an increase of approximately 16% since the 1980's. On the other hand, the average temperature per day with temperatures above 0°C has risen from just over 4°C, to just above 5°C.

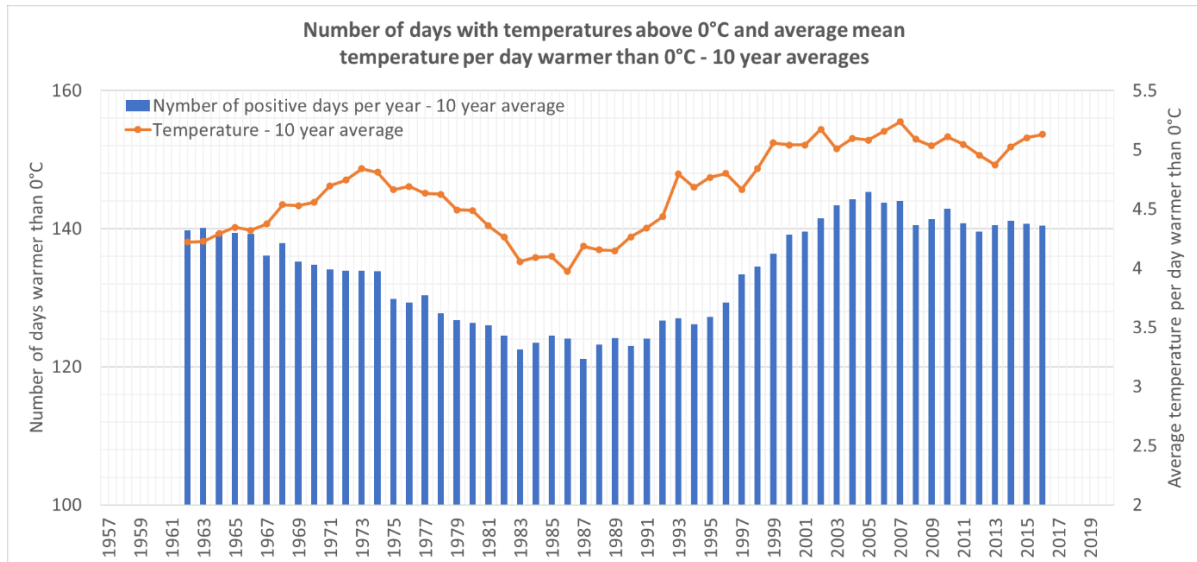


Figure 18: 10-year averages of the annual number of days with temperatures above 0°C and the average temperature per day with temperatures above 0°C. Please note that the y-axes have been cut to make the figure more presentable.

3.3.2 Precipitation

I used the interpolated precipitation data from SeNorge to find annual precipitation values. As Figure 19 shows, there is no significant change in the center weighted 10-year average values, and thus the expected amount of annual precipitation is approximately the same as it was at the beginning of the records in 1957. Adding a trendline to the graph it shows a slightly decreasing trend, however this is not significant enough to conclude that this is the case.

Figure 20 shows the estimated annual precipitation which falls as snow, and Figure 21 the estimated annual precipitation which falls as rain. This has been filtered with a mean daily temperature limit set at 0.5°C – any precipitation registered on a day with mean temperature 0.5°C or warmer has been identified as rain, and precipitation registered on a day with mean temperature colder than 0.5°C has been identified as snow. There are no clear trends in the 10-year average values for precipitation as snow but there are large variations from year to year.

Figure 21 may show a slight increase in annual precipitation as rain since the 2000's, however, the average values are not significantly different from those at the start of the record.

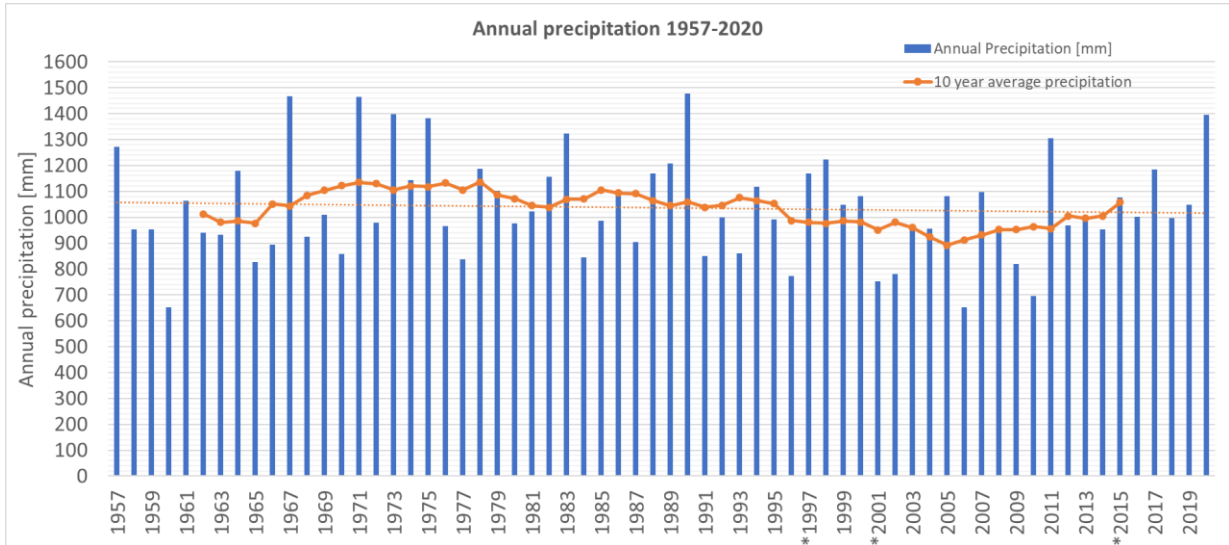


Figure 19: Annual precipitation at the area of interest at Harbardsbreen. Years with known GLOF events are marked with an asterisk (*).

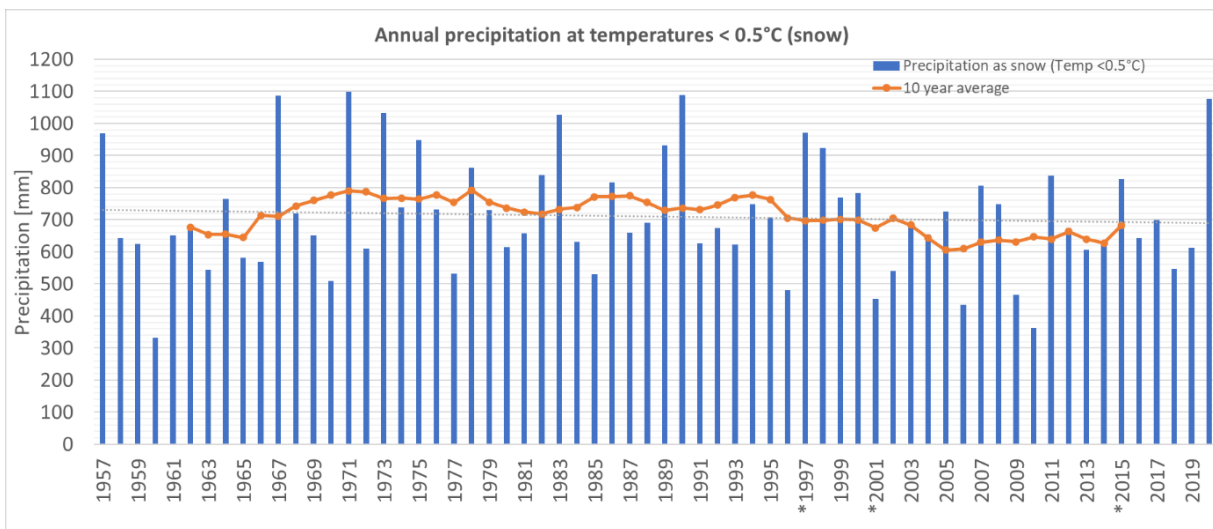


Figure 20: Annual precipitation at mean daily temperatures < 0.5°C, indicative as snow. Years with known GLOF events are marked with an asterisk (*).

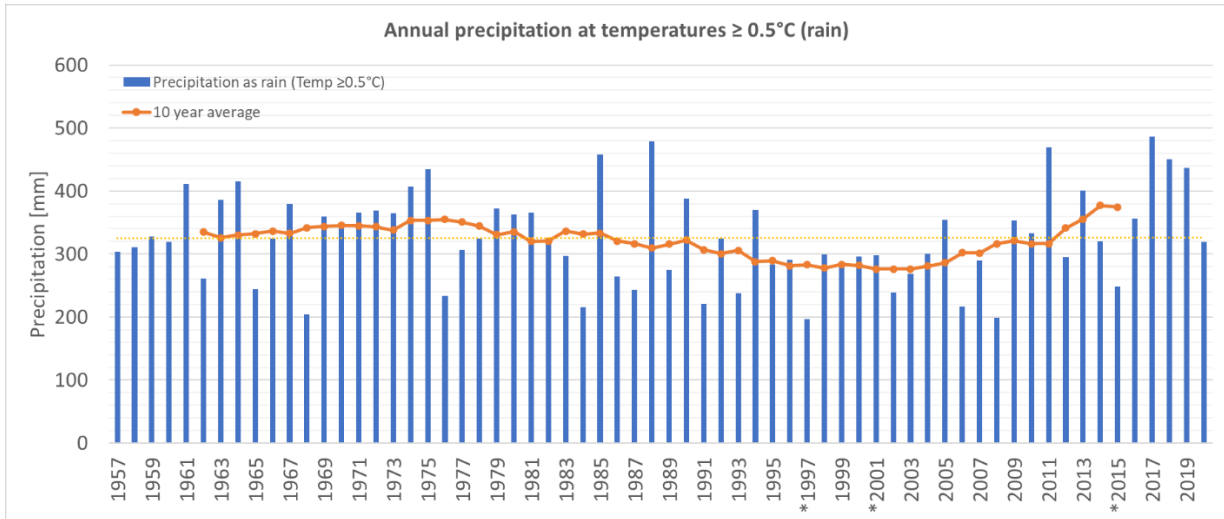


Figure 21: Annual precipitation at mean daily temperatures $\geq 0.5^{\circ}\text{C}$, indicative as rain. Years with known GLOF events are marked with an asterisk (*).

A detailed view of the cumulative precipitation as rain for the period 2010-2020 is shown in Figure 22 below. All the data series in this figure are set to start at the day which the PDD value had reached 20 PDD, the same date as the defined starting point for the melting season for the different years respectively, as already shown in Figure 16.

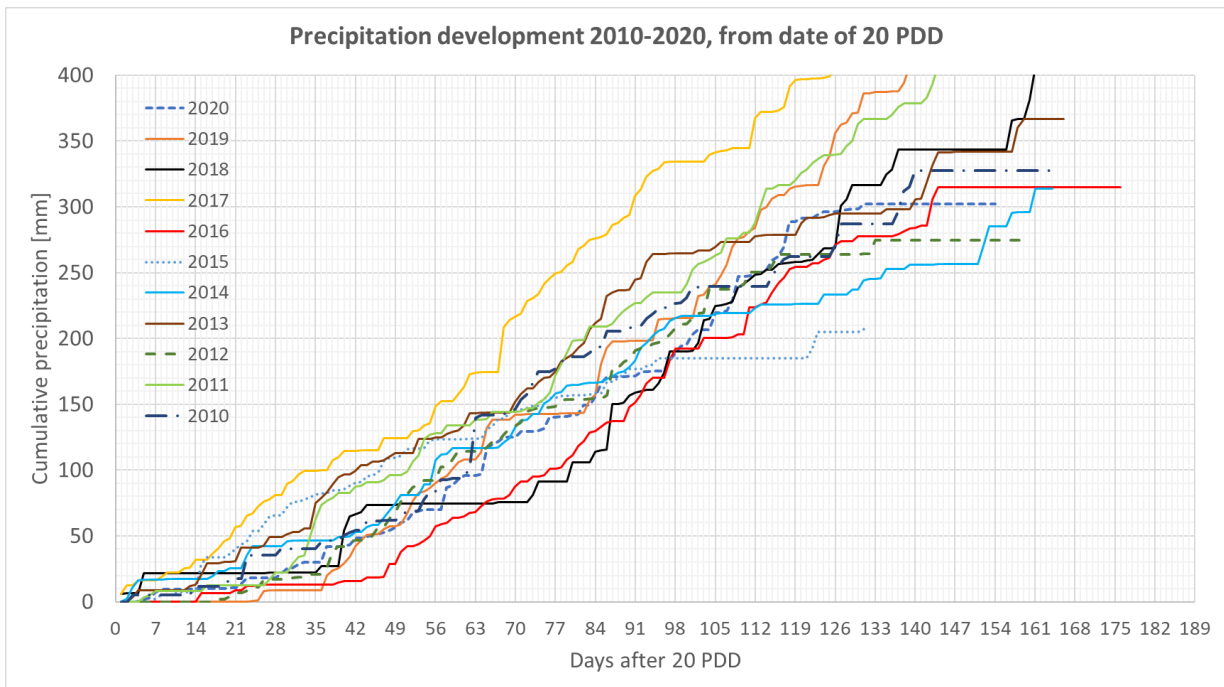


Figure 22: Detailed cumulative precipitation as rain from 2010-2020. The series are set to start at the day which the PDD had reached at least 20 PDD, which has been set as a threshold value for the start of the melting season, as explained in section 3.2.

3.4 Lake area and PDD

To find possible correlations between temperature, lake area development and GLOF events I made a graph showing PDD on the x-axis and lake area on the y-axis for both the Western and the Eastern lake (Figure 23 and Figure 24).

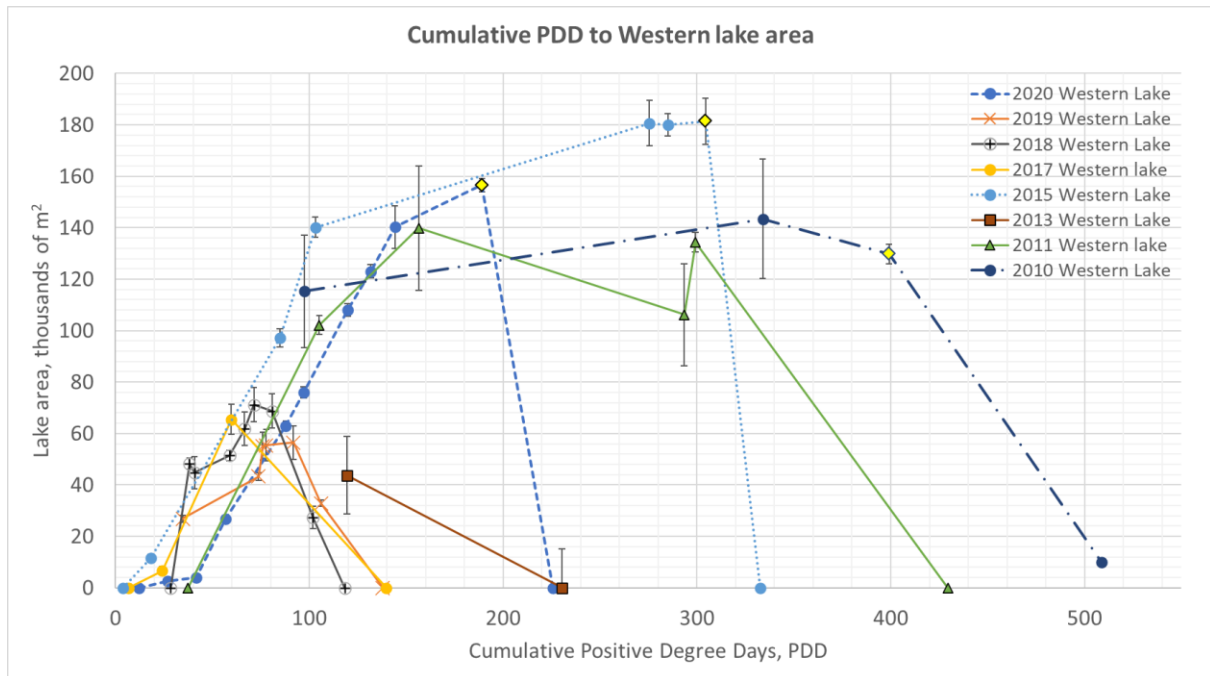


Figure 23: Development of the Western lake 2010-2020, showing the lake area change to cumulative positive degree days. The figure shows the development of the lake until the last measurement before a significant negative change in the lake area. Documented GLOF events are marked with a yellow diamond (2010, 2015 and 2020). Please note the different scale on the y-axis compared to Figure 24.

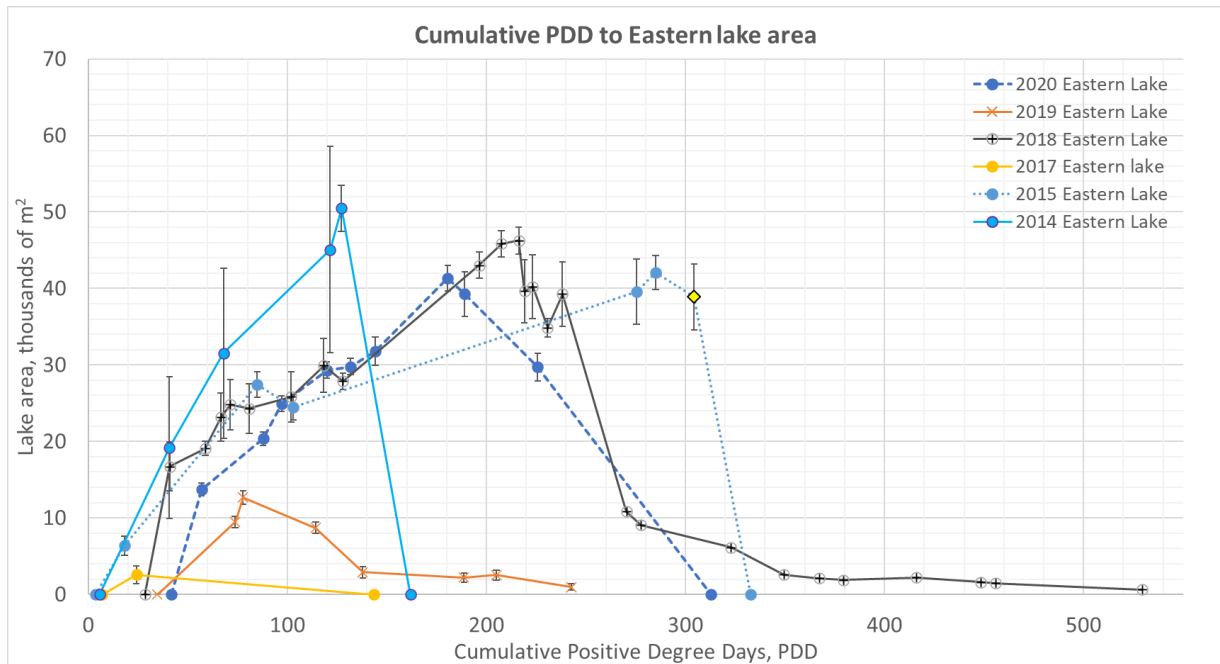


Figure 24: Development of the Eastern lake 2010-2020, showing the lake area change to cumulative positive degree days. The figure shows the development of the lake until the last measurement before a significant negative change in the lake area. Documented GLOF event is marked with a yellow diamond (2015). Please note the different scale on the y-axis compared to Figure 23.

3.5 Detailed lake developments 2010-2020

3.5.1 Detailed graphs

For the period 2010-2020 (11 years), I did an as detailed as possible study of the development of the glacial lakes of Harbardsbreen, presented in Figure 25 to Figure 35. Here I show the lake extents, cumulative PDD as well as cumulative precipitation as rain (precipitation of which daily average temperatures $> 0.5^{\circ}\text{C}$). To illustrate the change in the ice cover of the lake, the graphs are shown with a square if the lake is more ice covered than not, a triangle if the lake is less than 50% ice covered and/or has a broken ice cover, and a circle if the lake is ice free. Additionally, the marker is colored yellow for dates of known GLOF events in 2010, 2015 and 2020. As more and more satellites are available, and thus more and more imageries, the time resolution of the data series become increasingly better in the last half of the decade.

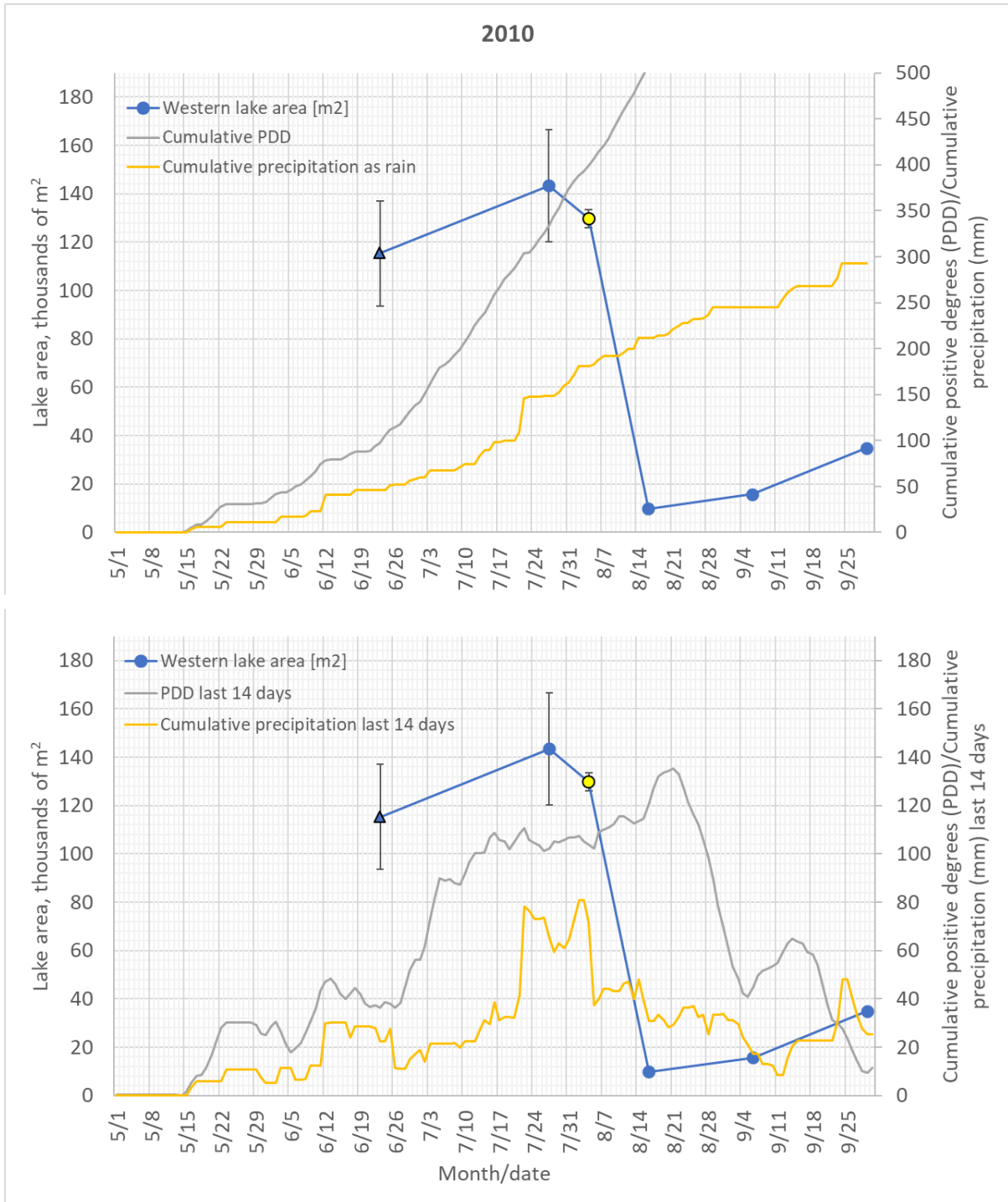


Figure 25: Detailed lake development on Harbardsbreen in 2010 with corresponding cumulative PDD and cumulative precipitation as rain (top) and cumulative PDD and cumulative precipitation as rain for the last 14-day period, which shows the intensity of temperature and precipitation (bottom). Yellow marker marks date for known GLOF event (04.08.2010). Square: lake is more ice covered than not, Triangle: less than 50% ice cover and/or broken ice cover, Circle: Ice free lake.

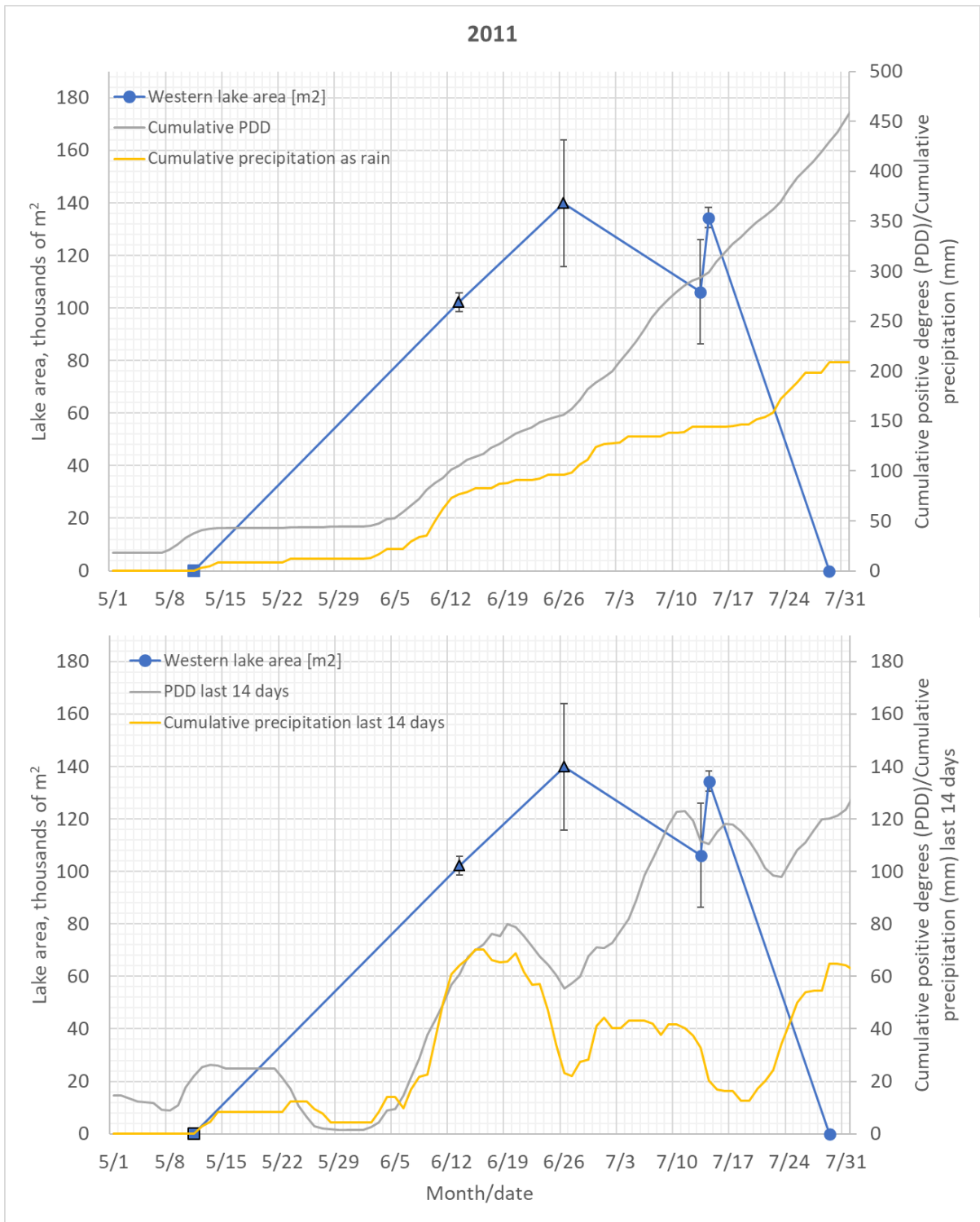


Figure 26: Detailed lake development on Harbardsbreen in 2011 with corresponding cumulative PDD and cumulative precipitation as rain (top) and cumulative PDD and cumulative precipitation as rain for the last 14-day period, which shows the intensity of temperature and precipitation (bottom). Square: lake is more ice covered than not, Triangle: less than 50% ice cover and/or broken ice cover, Circle: Ice free lake.

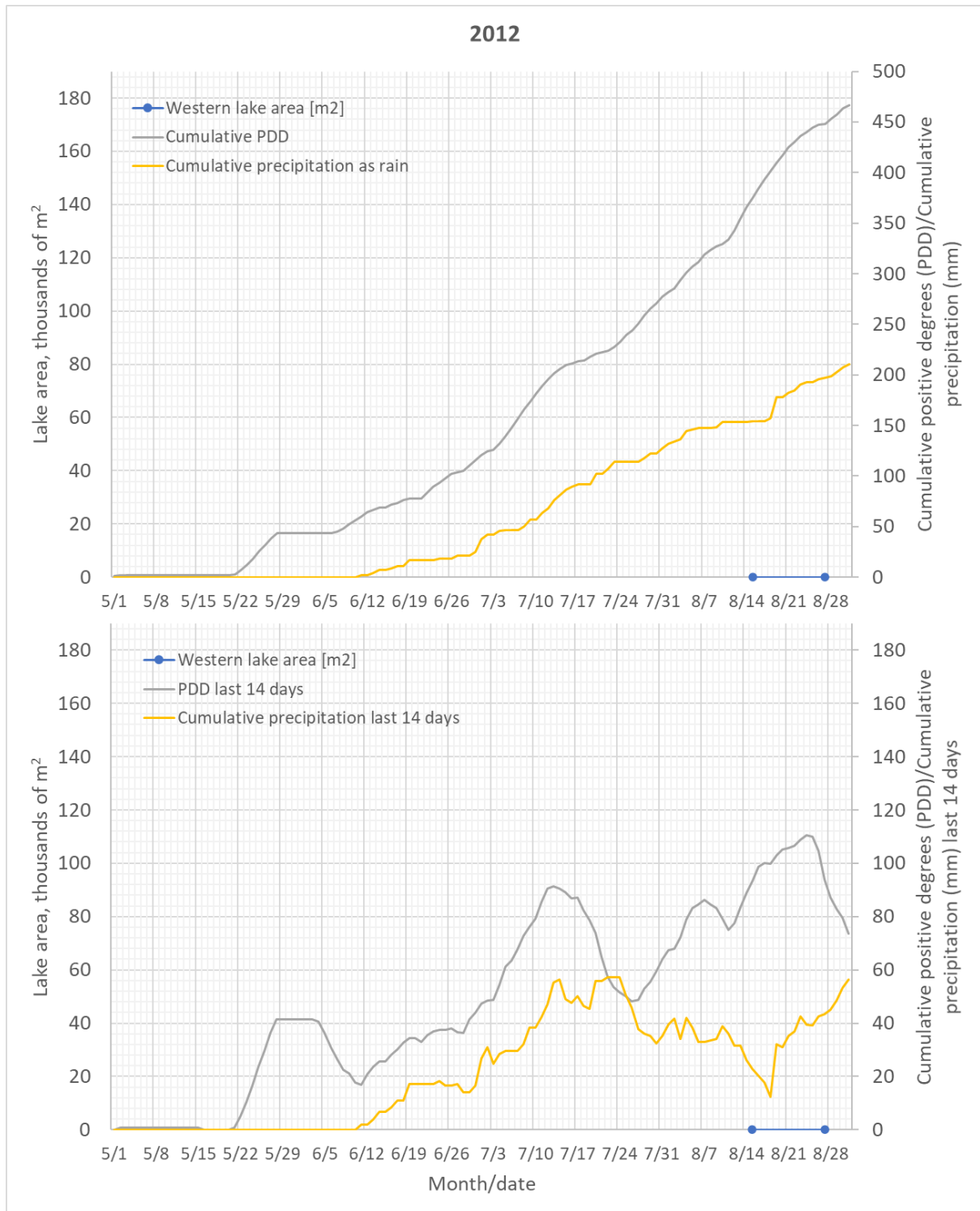


Figure 27: Detailed lake development on Harbardsbreen in 2012 with cumulative PDD and cumulative precipitation as rain (top) and cumulative PDD and cumulative precipitation as rain for the last 14-day period, which shows the intensity of temperature and precipitation (bottom). The NVE GLOF database (NVE, 2021b) has registered a GLOF event at Harbardsbreen in 2012 (unknown date, but probably early July (Kjøllmoen B., 2016)). However, as mentioned in section 3.1, I have no imageries to document the lake(s) development this year, except footage from August 15th and 27th which shows the Western lake in its drained state. Still, the intensity peak of the 14-day cumulative PDD value of over 90 PDD in mid-July supports the theory of the potential GLOF event occurring around this time.

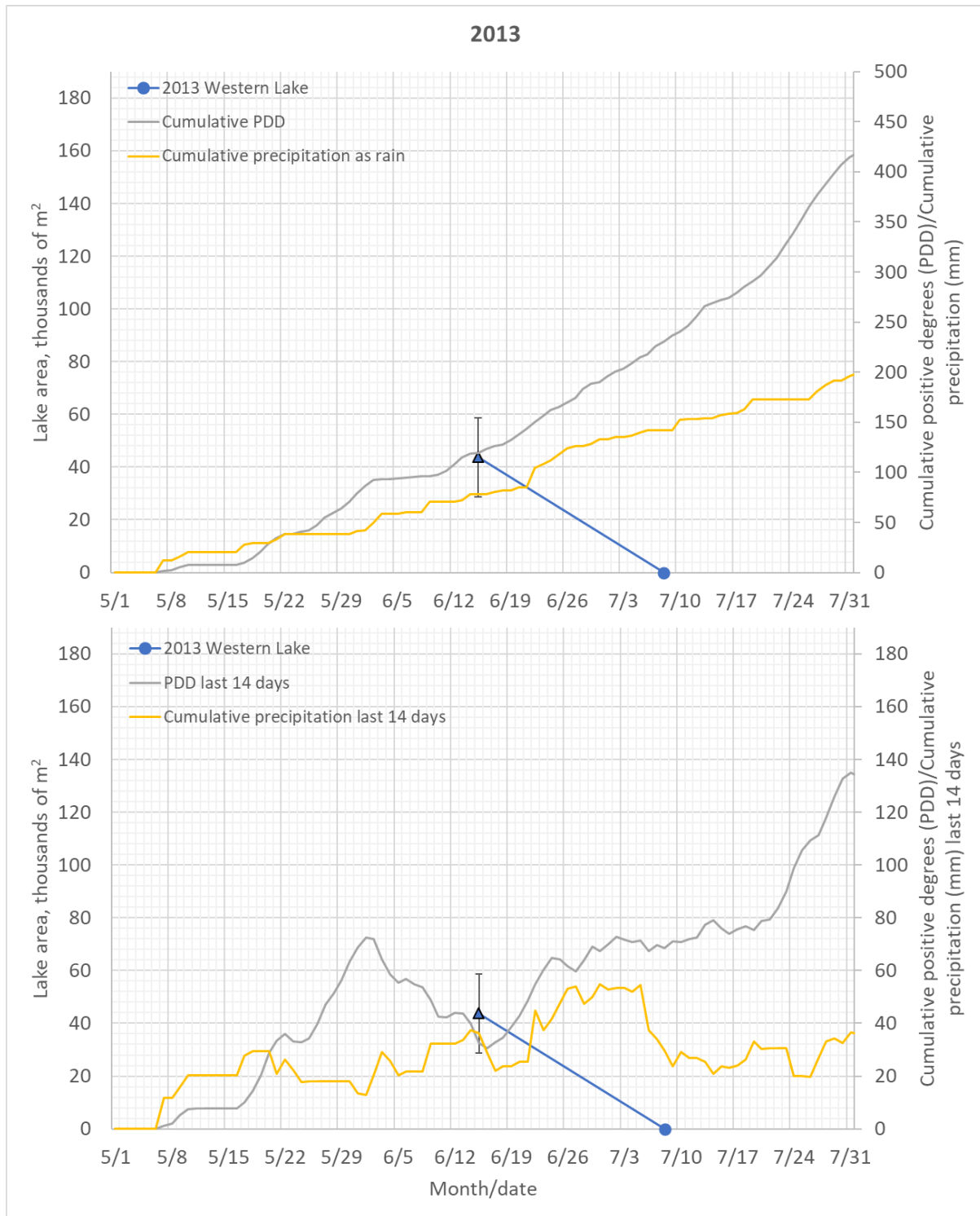


Figure 28: Detailed lake development on Harbardsbreen in 2013 with corresponding total cumulative PDD and cumulative precipitation as rain (top) and cumulative PDD and cumulative precipitation as rain for the last 14-day period, which shows the intensity of temperature and precipitation (bottom). Square: lake is more ice covered than not, Triangle: less than 50% ice cover and/or broken ice cover, Circle: Ice free lake.

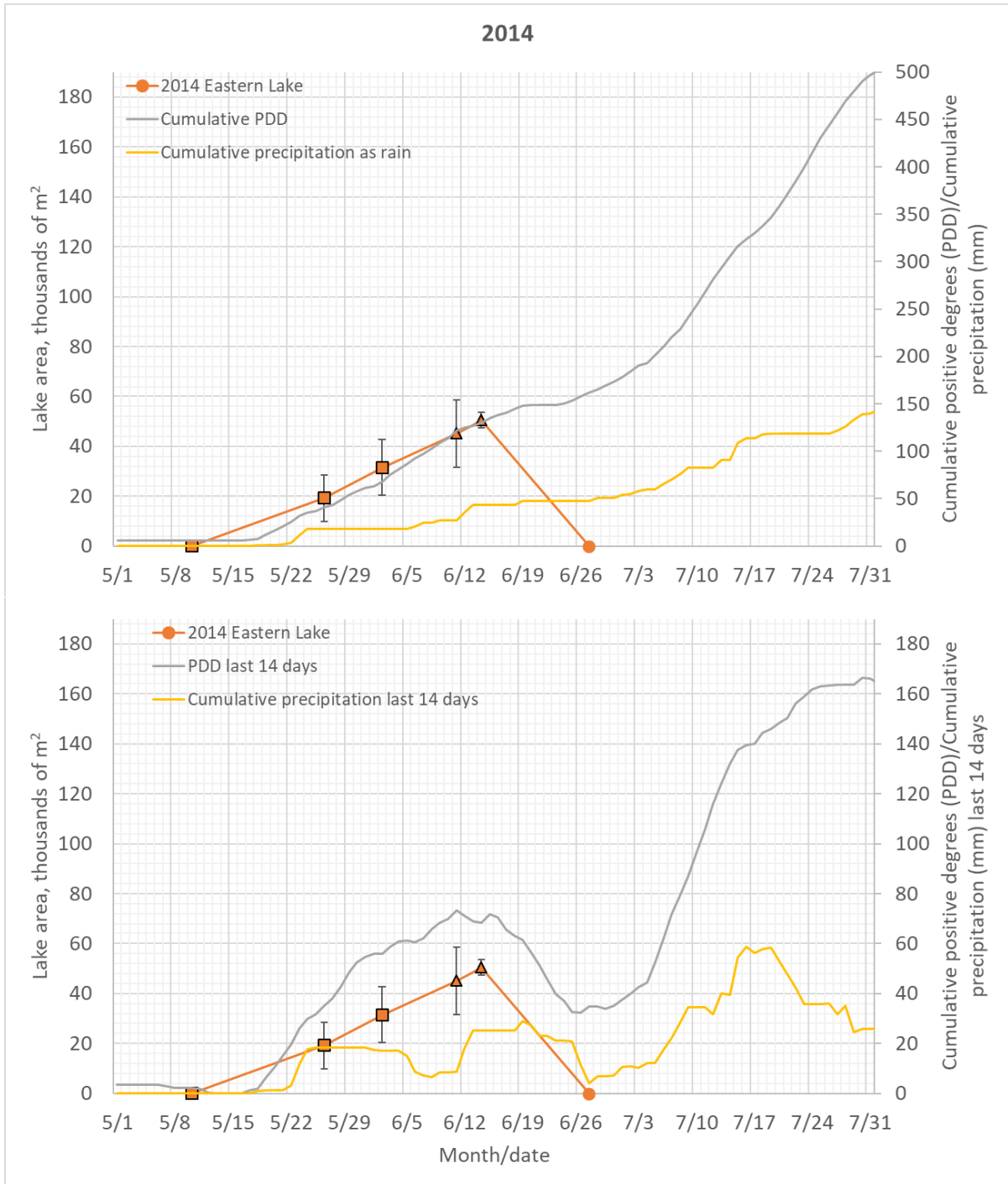


Figure 29: Detailed lake development on Harbardsbreen in 2014 with corresponding total cumulative PDD and cumulative precipitation as rain (top) and cumulative PDD and cumulative precipitation as rain for the last 14-day period, which shows the intensity of temperature and precipitation (bottom). Square: lake is more ice covered than not, Triangle: less than 50% ice cover and/or broken ice cover, Circle: Ice free lake.

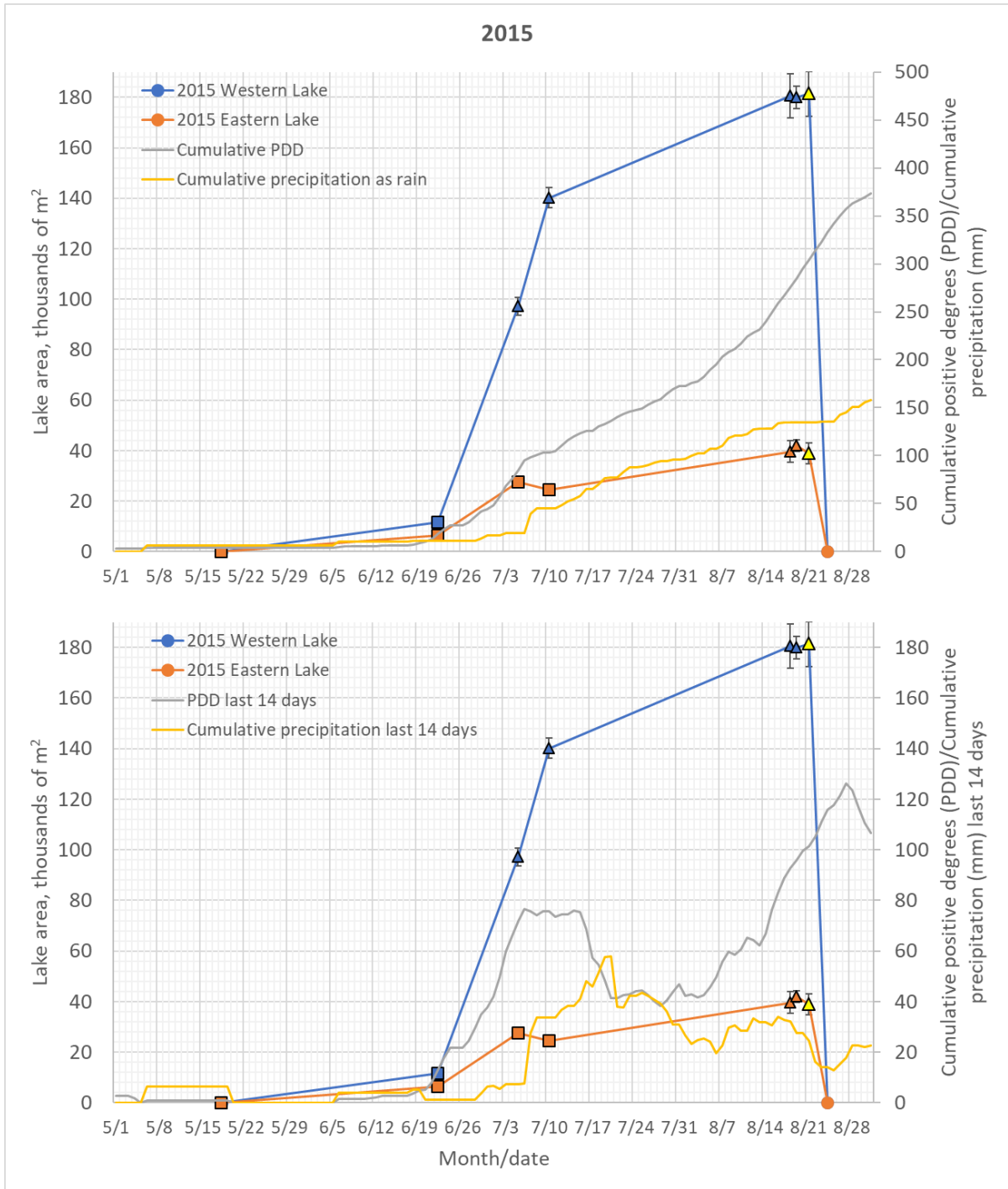


Figure 30: Detailed lake development on Harbardsbreen in 2015 with corresponding total cumulative PDD and cumulative precipitation as rain (top) and cumulative PDD and cumulative precipitation as rain for the last 14-day period, which shows the intensity of temperature and precipitation (bottom). The yellow marker marks date of known GLOF event (21.08.2015). Square: lake is more ice covered than not, Triangle: less than 50% ice cover and/or broken ice cover, Circle: Ice free lake.

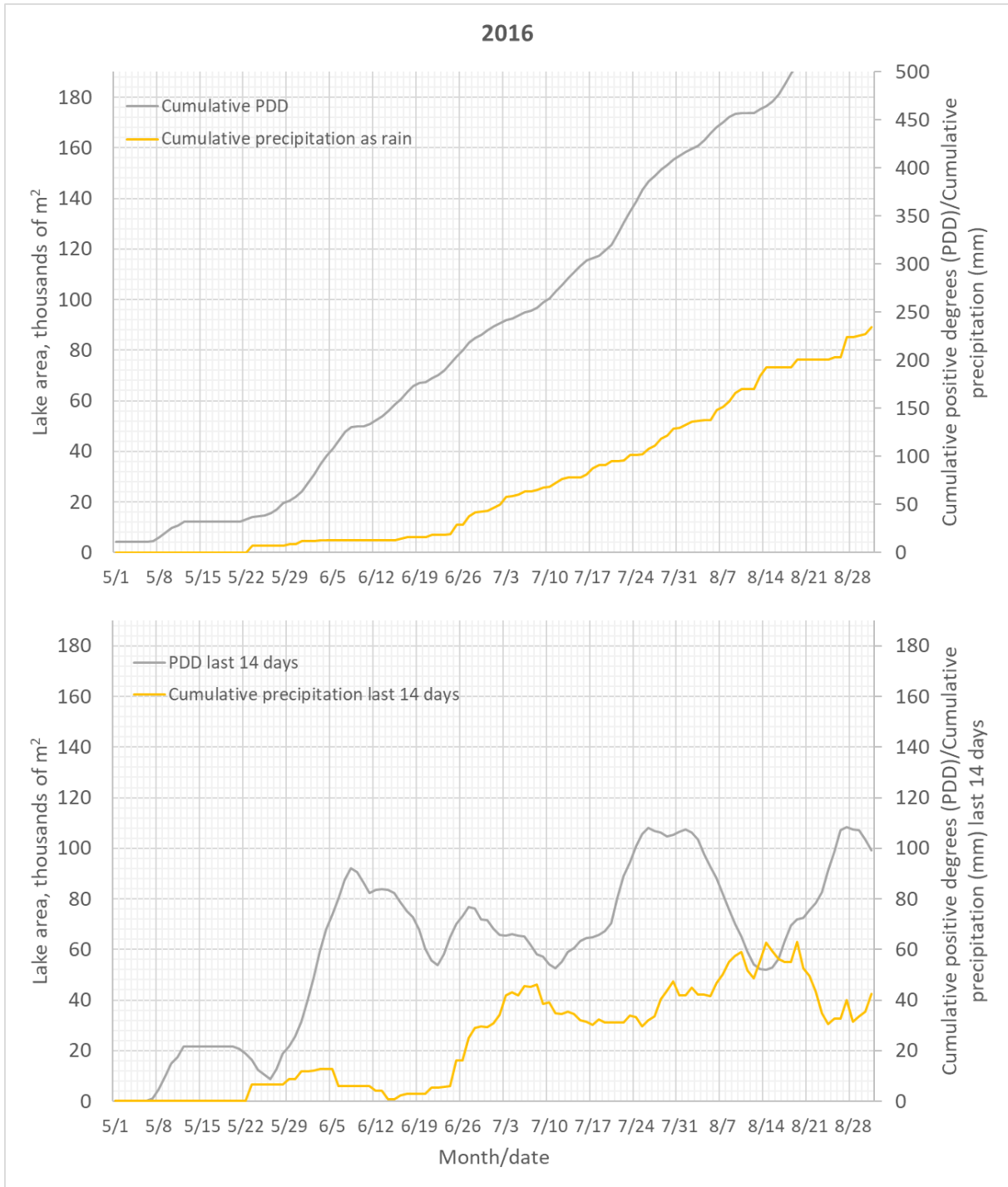


Figure 31: Total cumulative PDD and cumulative precipitation as rain, 2016 (top) and cumulative PDD and cumulative precipitation as rain for the last 14-day period, which shows the intensity of temperature and precipitation (bottom). As discussed in section 3.1 satellite imagery shows that neither of the lakes of Harbardsbreen developed this year. Square: lake is more ice covered than not, Triangle: less than 50% ice cover and/or broken ice cover, Circle: Ice free lake.

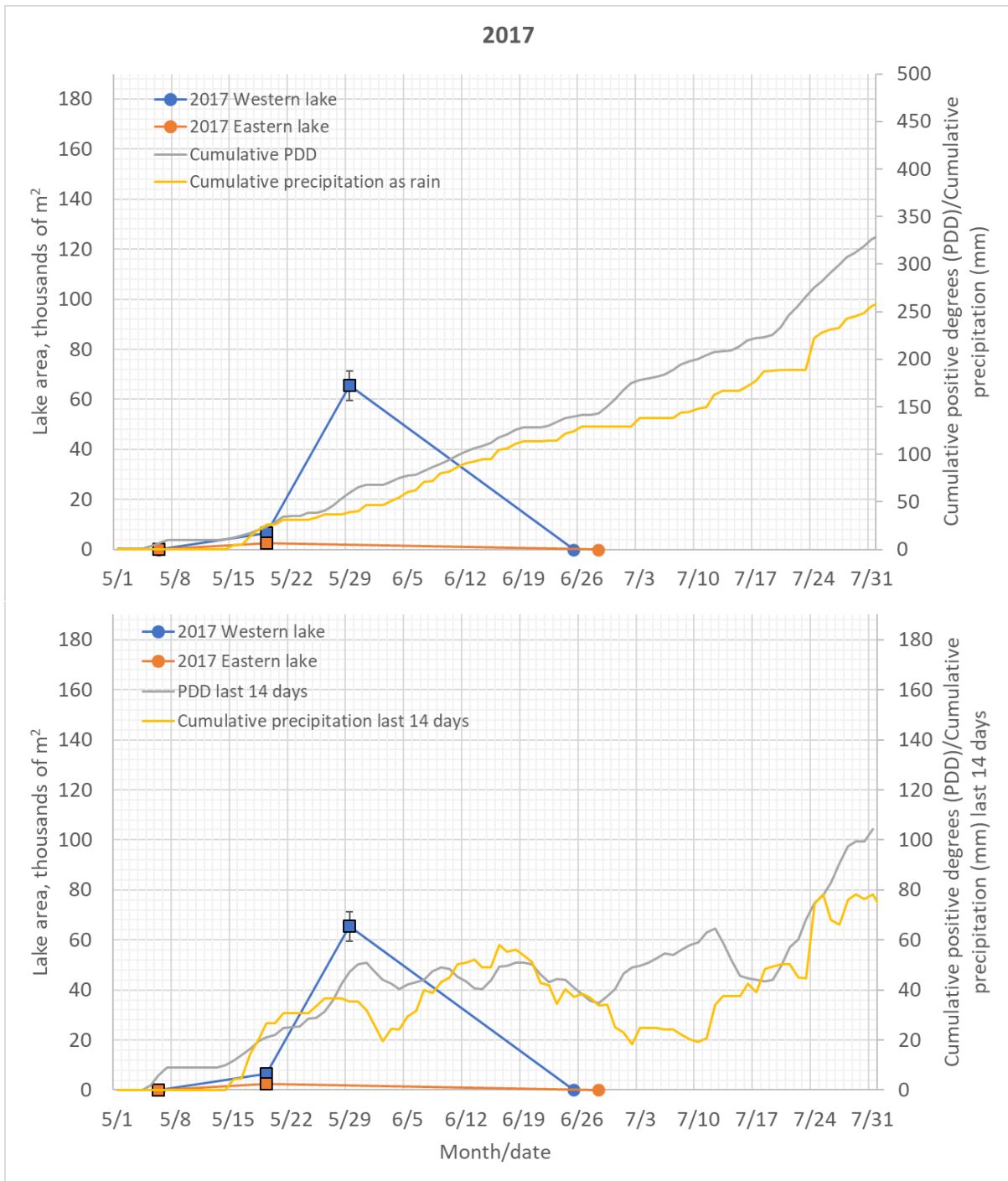


Figure 32: Detailed lake development on Harbardsbreen in 2017 with corresponding total cumulative PDD and cumulative precipitation as rain (top) and cumulative PDD and cumulative precipitation as rain for the last 14-day period, which shows the intensity of temperature and precipitation (bottom). Square: lake is more ice covered than not, Triangle: less than 50% ice cover and/or broken ice cover, Circle: Ice free lake.

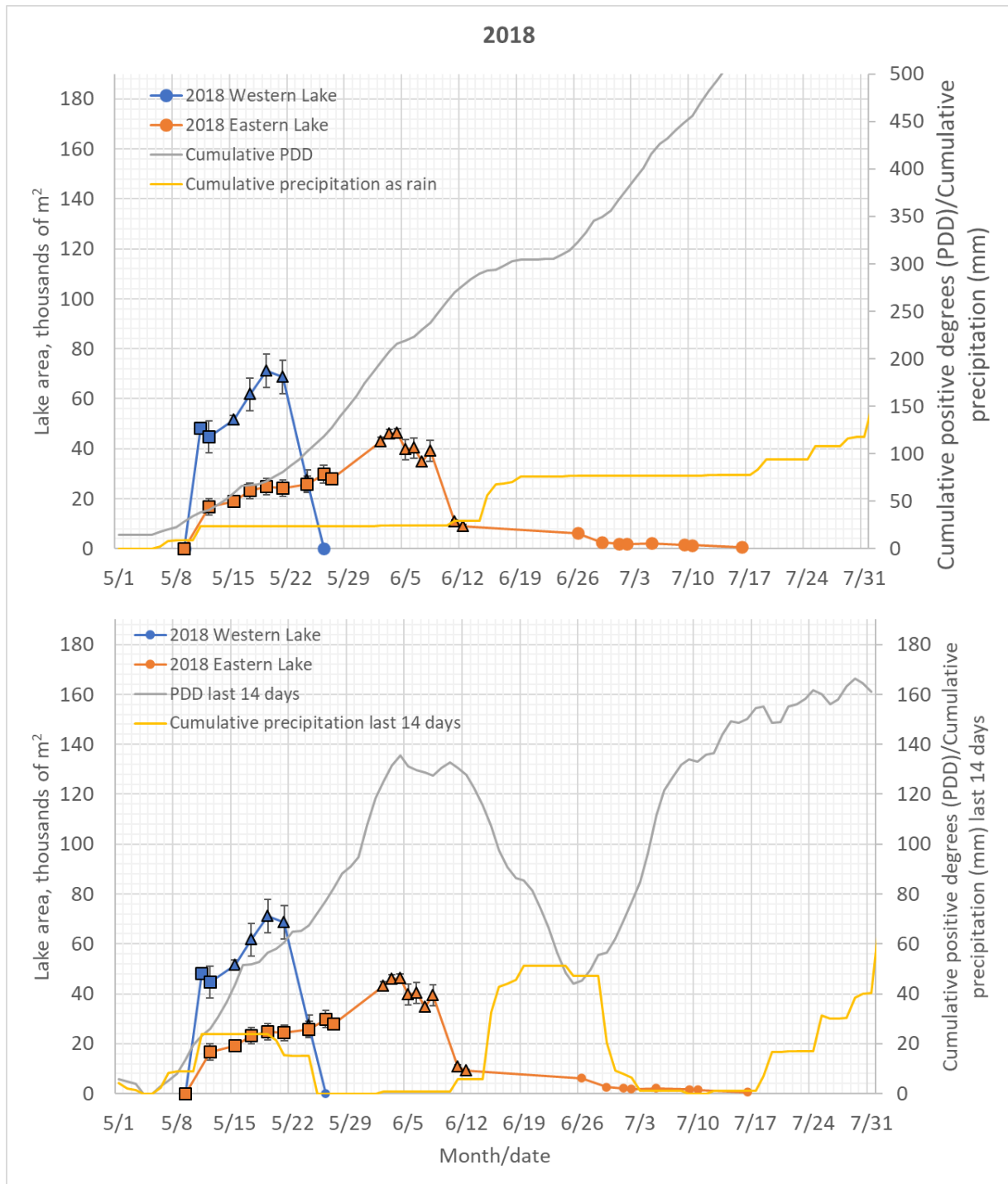


Figure 33: Detailed lake development on Harbardsbreen in 2018 with corresponding cumulative PDD and cumulative precipitation as rain (top) and cumulative PDD and cumulative precipitation as rain for the last 14-day period, which shows the intensity of temperature and precipitation (bottom). Square: lake is more ice covered than not, Triangle: less than 50% ice cover and/or broken ice cover, Circle: Ice free lake.

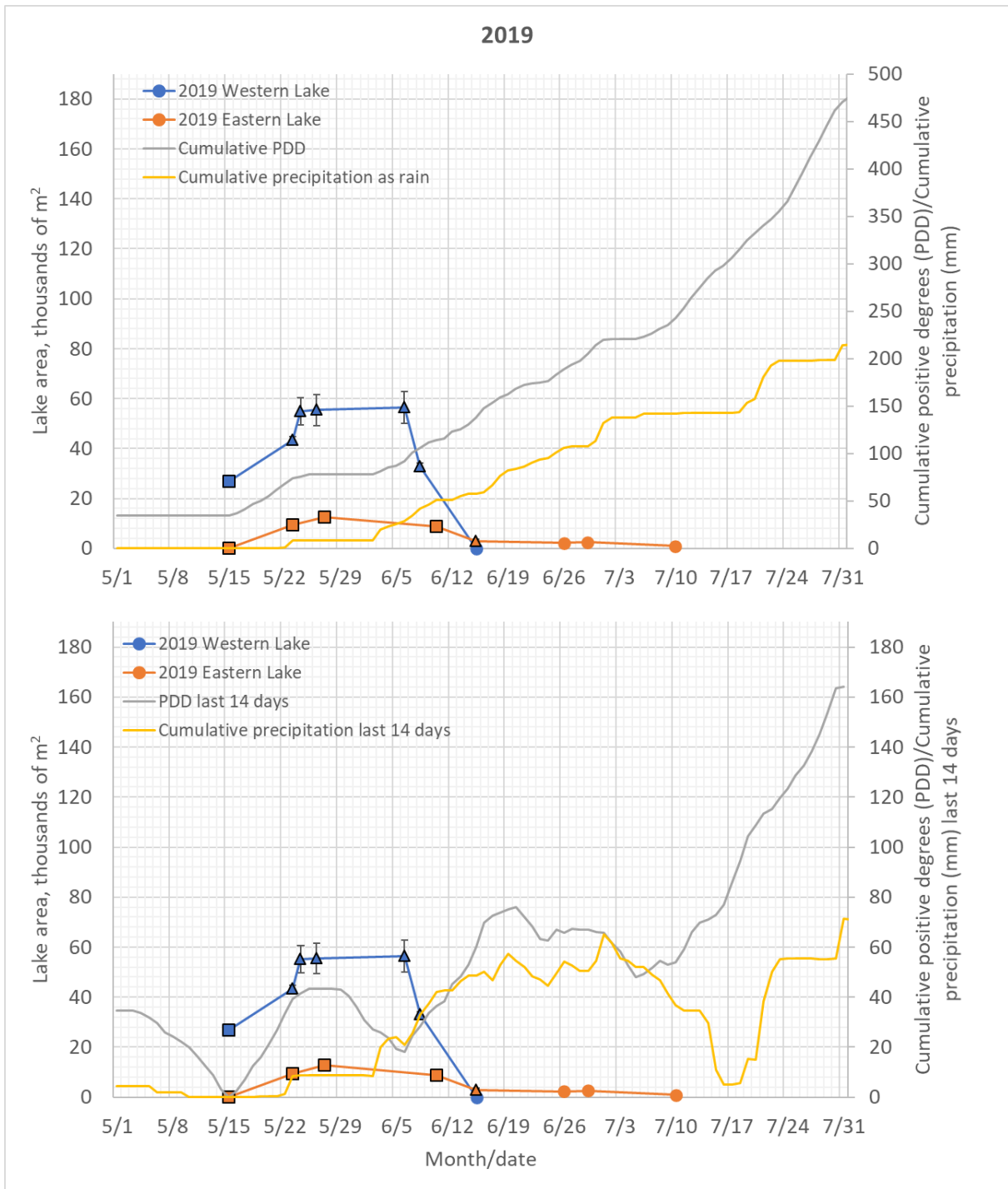


Figure 34: Detailed lake development on Harbardsbreen in 2019 with corresponding cumulative PDD and cumulative precipitation as rain (top) and cumulative PDD and cumulative precipitation as rain for the last 14-day period, which shows the intensity of temperature and precipitation (bottom). Square: lake is more ice covered than not, Triangle: less than 50% ice cover and/or broken ice cover, Circle: Ice free lake.

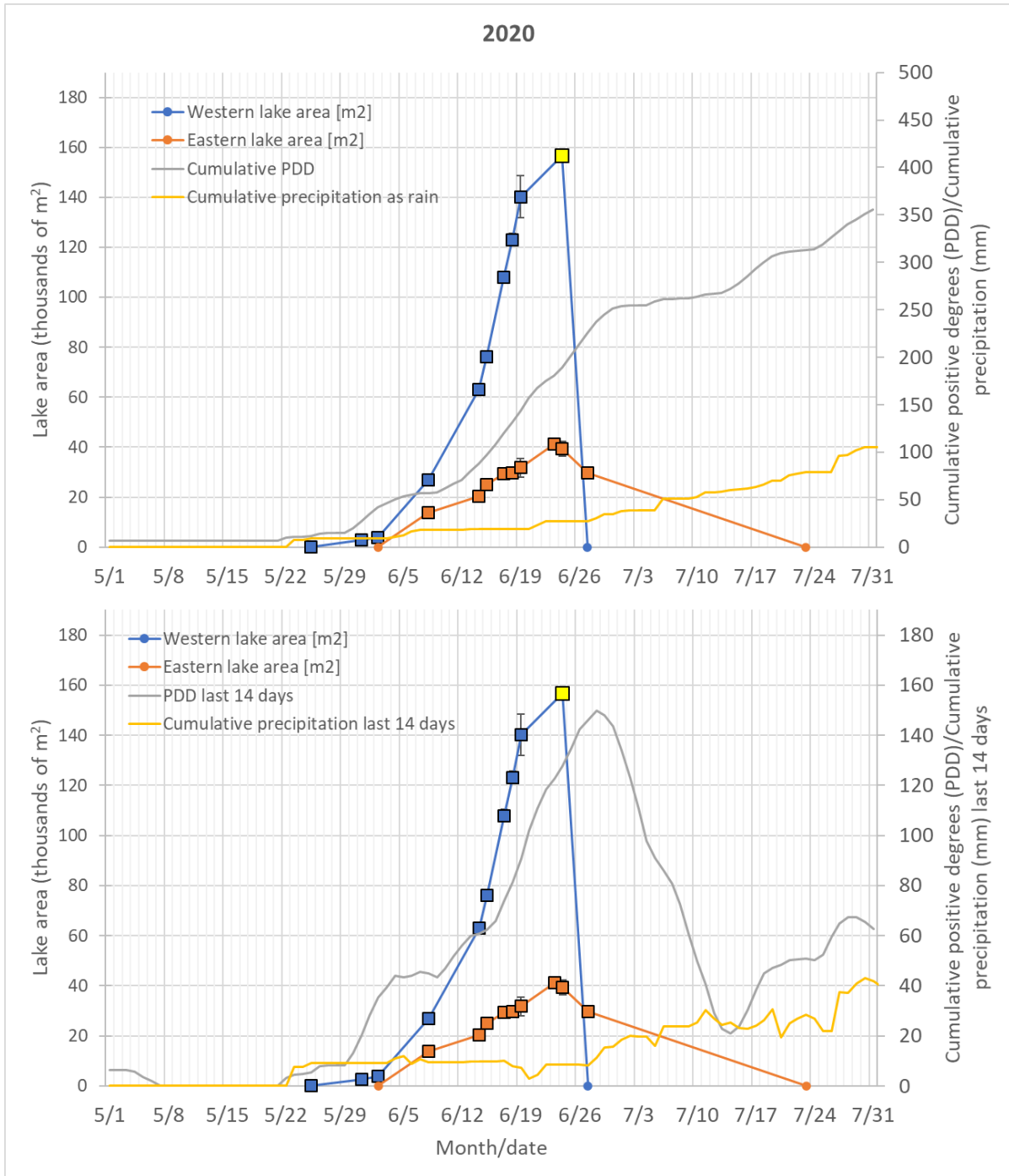


Figure 35: Detailed lake development on Harbardsbreen in 2020 with corresponding cumulative PDD and cumulative precipitation as rain (top) and cumulative PDD and cumulative precipitation as rain for the last 14-day period, which shows the intensity of temperature and precipitation (bottom). The yellow marker marks date of known GLOF event (24.06.2020). Unfortunately, the Eastern lake was not covered by the satellite imagery on this date. Square: lake is more ice covered than not, Triangle: less than 50% ice cover and/or broken ice cover, Circle: Ice free lake.

Combining all the detailed lake area graphs by date (Figure 36 and Figure 37), it is evident that the time of the development of the lakes varies significantly from year to year.

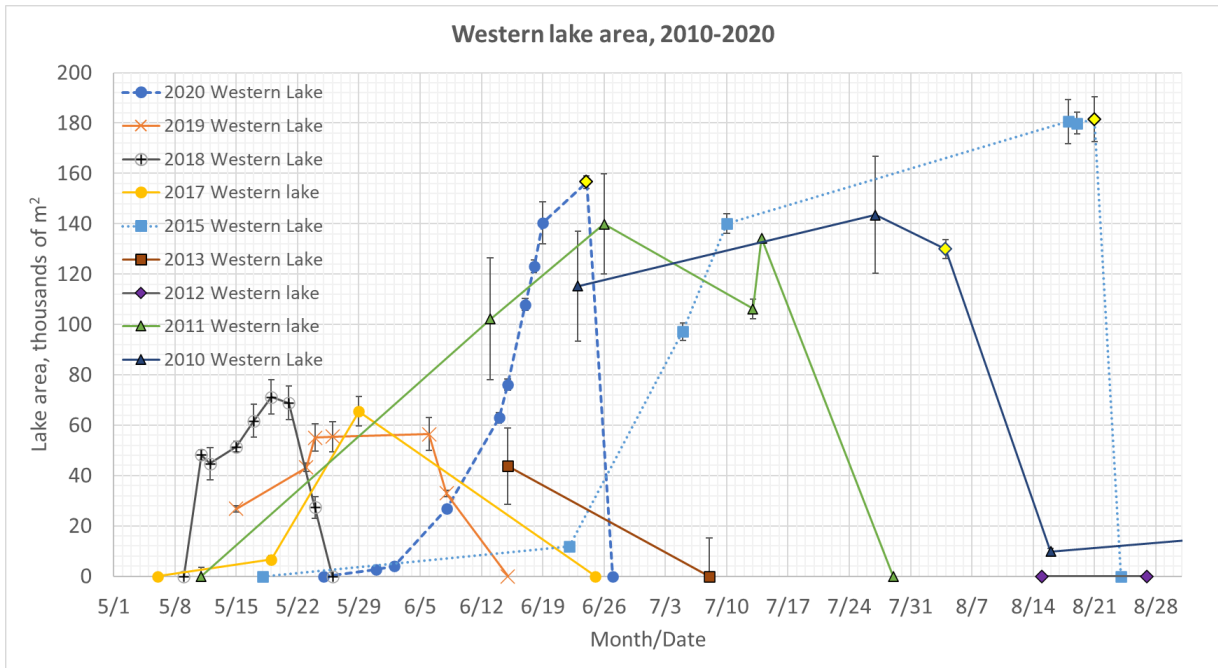


Figure 36: Combined detailed development of the Western lake 2010-2020 by date. The yellow diamonds mark the known GLOF events in 2010, 2015 and 2020.

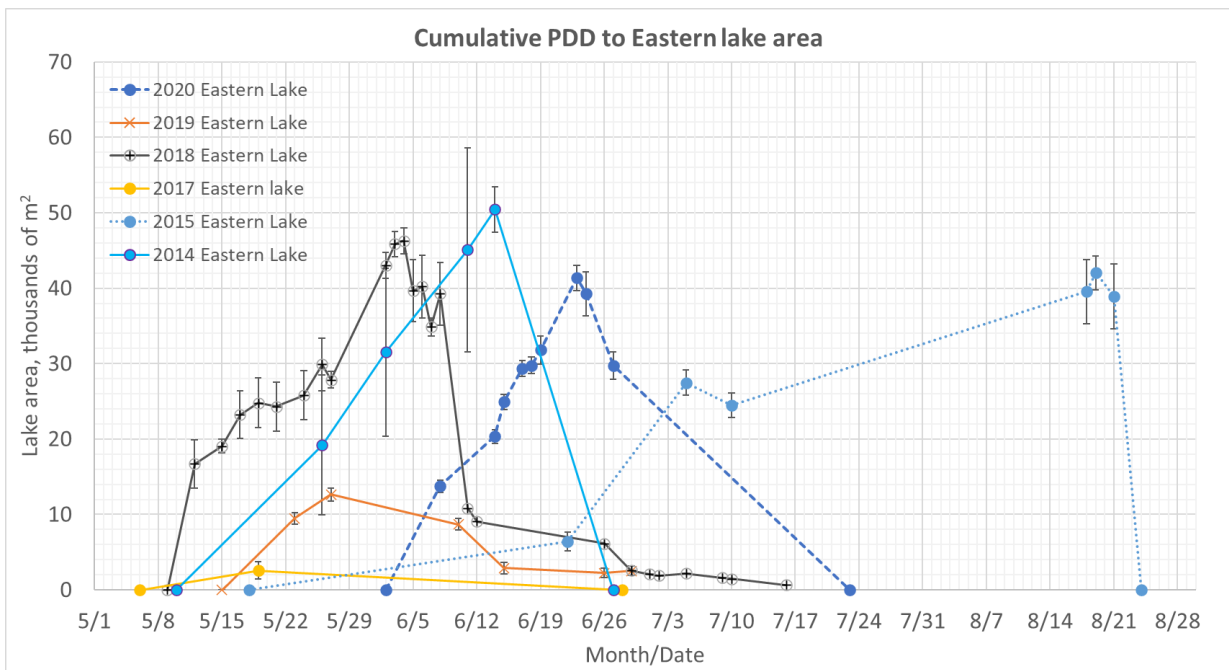


Figure 37: Combined detailed development of the Eastern lake 2010-2020 by date.

To better illustrate how the lakes can develop throughout the summer I made a mosaic of Sentinel-2 and PlanetScope 4-band images for the summer season of 2018 (Figure 38).

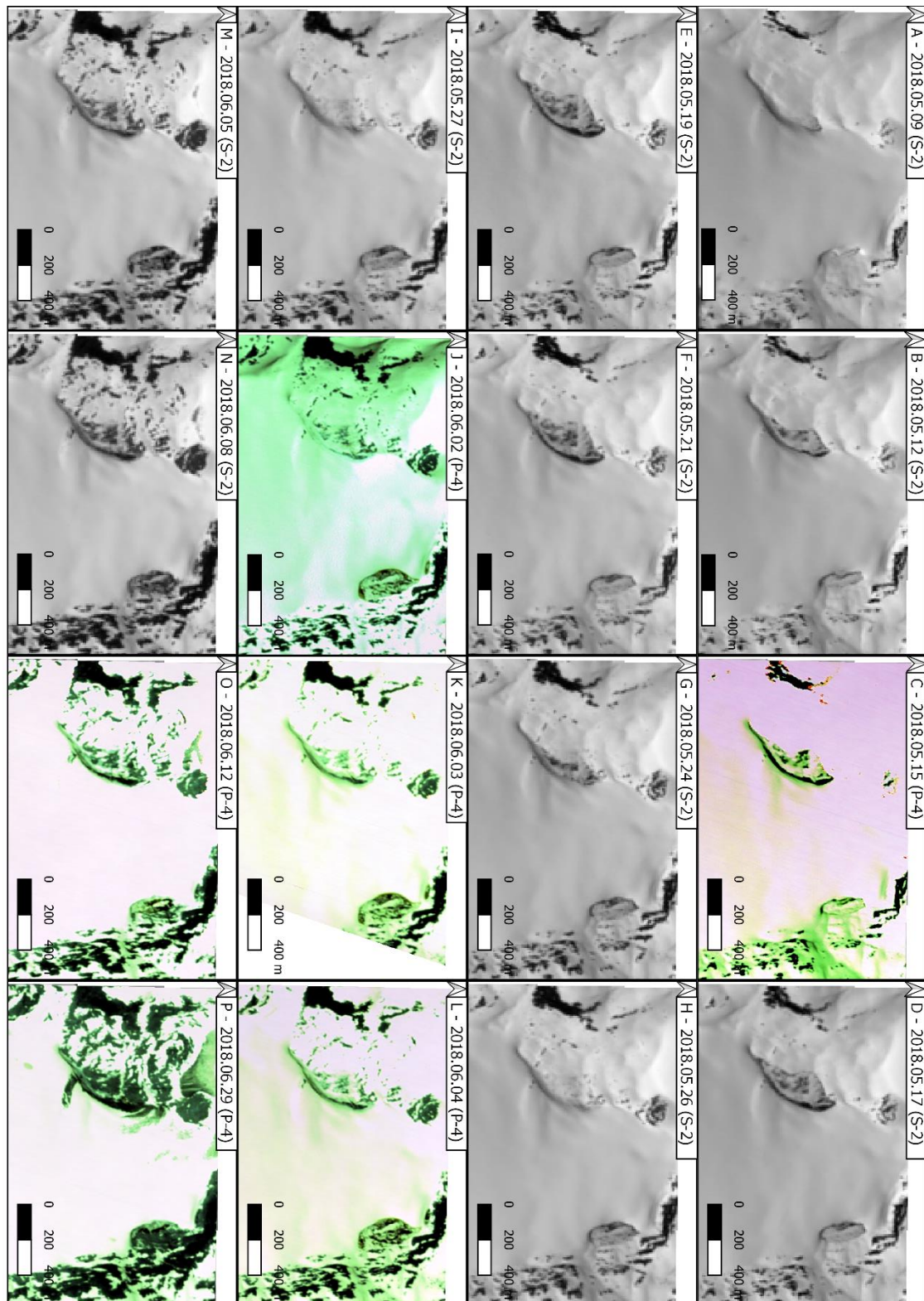


Figure 38: Mosaic of Sentinel-2 (S-2) and 4-band PlanetScope (P-4) imagery from 2018. The Western lake reached its maximum known extent on May 19th/May 21st (E+F) and was drained by May 26th (H). The Eastern lake reached its maximum known extent on June 4th (L) and drained more slowly. The Eastern lake had drained nearly completely by June 29th (P).

3.6 Lake volume

I used the newest available elevation model from 18.08.2020 to find the volumes of both the Western and the Eastern lake. I selected only the area around the lakes respectively and used the Raster Surface Volume tool in QGIS to find the lake volumes in 5 meters elevation intervals and present this in a graph. While doing this I also found the Western lake had a depth of up to approximately 40 meter in 2020, and the Eastern lake around 30 meters. The results show a virtually linear relation between lake volume and lake area for both the Western and the Eastern lake (Figure 39 and Figure 40). However, this result is only valid for measurements from 2020 as the glacier will melt, move and change from year to year. For other years this model would only be approximate. At the time the elevation model from 2010 was made, the Western lake was still not completely drained, and a significant amount of water was still in the lake. This made it unsuitable for measuring the lake volume as I could not measure the full potential volume of the lake.

The plots in Figure 39 and Figure 40 show a trendline function of $y = 12.017x - 89452$ ($R^2 = 0.9914$) for the Western lake and $y = 14.619x - 62480$ ($R^2 = 0.9721$) for the Eastern lake. The R^2 -value is a dimensionless number ranging from 0 to 1, and indicates how well the function fits the data points. An R^2 -value of 1 means a perfect fit. Using these functions, I converted the measured area of the lakes for the period 2010-2020 (Figure 41).

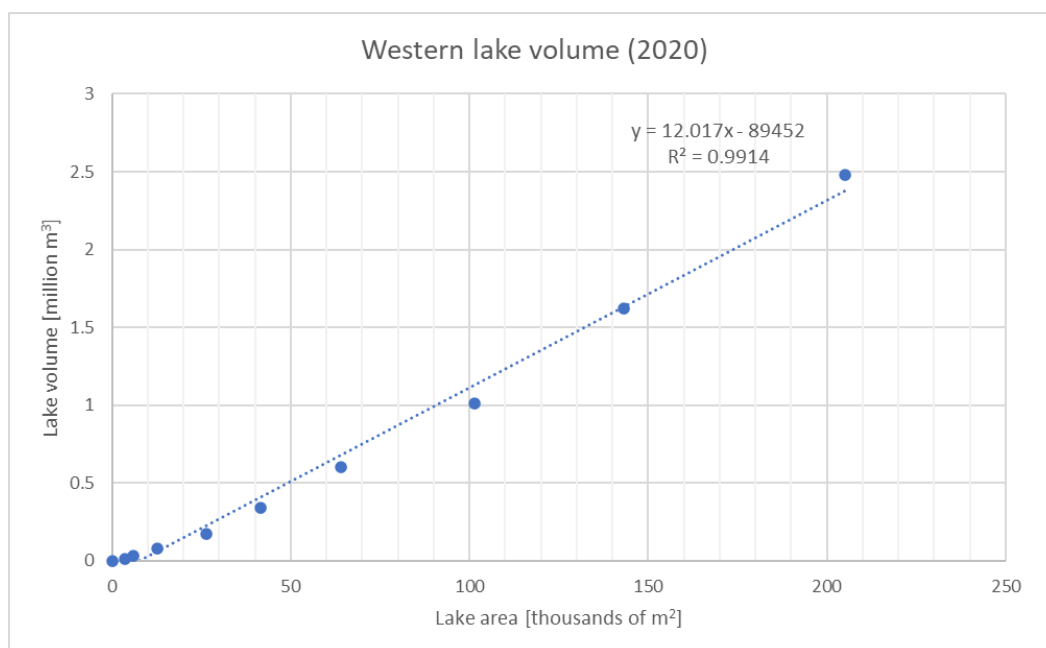


Figure 39: Western lake volume to lake area (from elevation model from 18.08.2020).

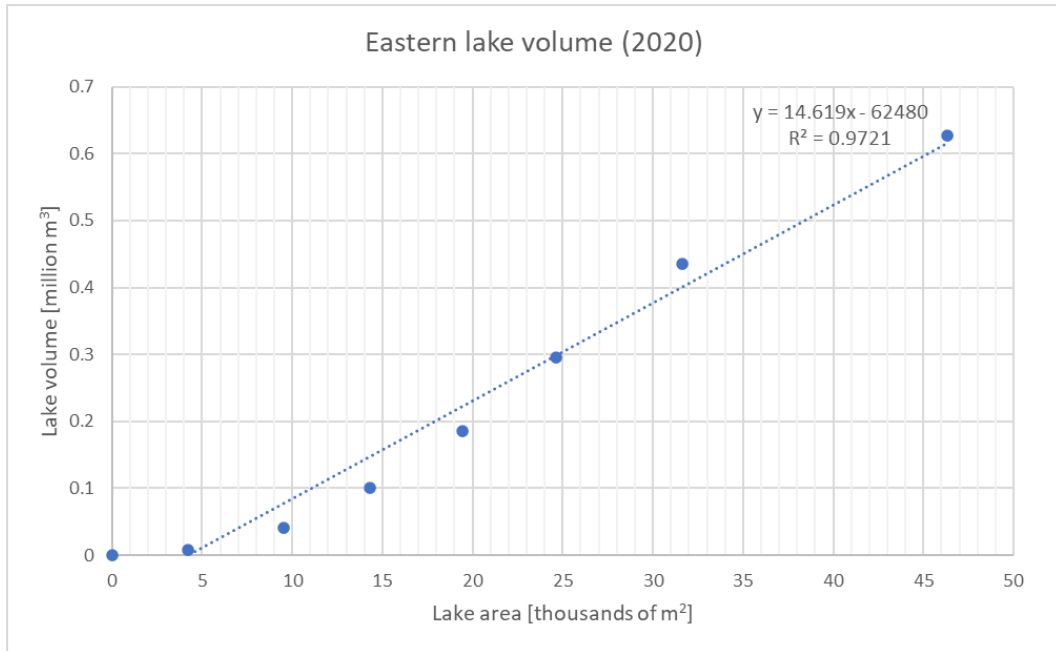


Figure 40: Eastern lake volume to lake area (from elevation model from 18.08.2020).

I used the functions to estimate both the Western and the Eastern lake’s maximum volume, based on the maximum known lake extents, for the period 2010 to 2020. The results are shown in Figure 41 as a stacked column diagram. Please keep in mind that the model is based on the digital elevation model (DEM) from 2020, and the estimated volume in other years are as a consequence not accurate, but rather estimations.

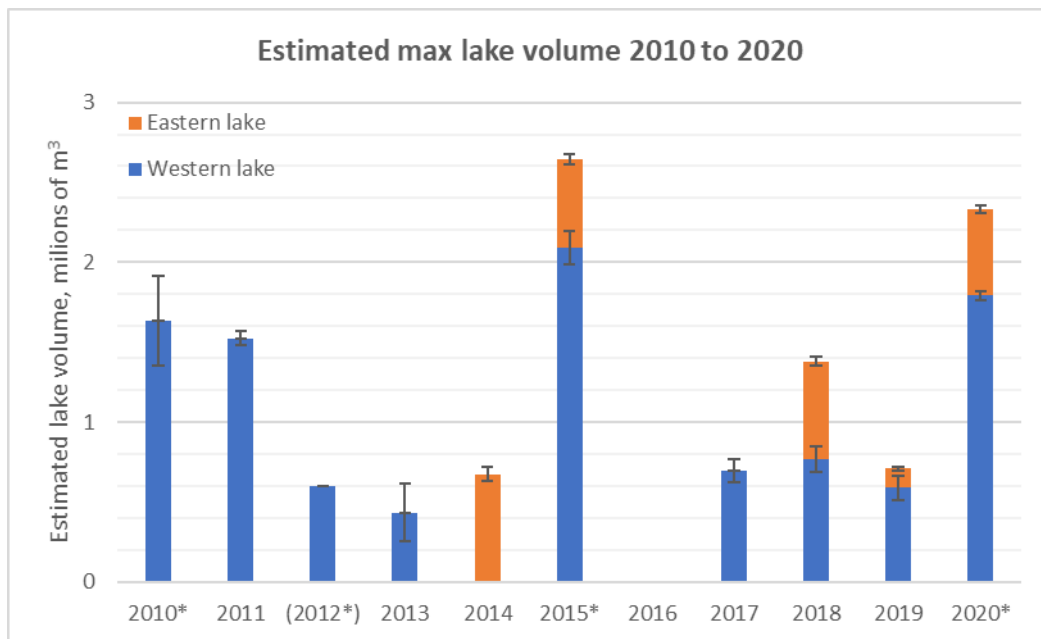


Figure 41: Estimated lake volume 2010-2020, based on the 2020 elevation model. Years with documented GLOF events are marked with an asterisk (*). The volume of 2012 (0.6 million m³) is taken from an estimate made by Kjølmoen (2016), which unfortunately did not include an error margin.

3.7 “New” GLOFs and drainage events in the period 2010-2020

It is evident that in the period 2010-2020 there have been several drainage events that have not been registered in NVE’s GLOF database. In Table 3 I have combined the data from NVE’s GLOF database with my own results. Please note that the estimated lake volume values in this table are the maximum known estimated volumes for both the Western and the Eastern lake combined. Considering both the size of the lakes and the uncertainty in the time between the date of the lakes’ maximum known extents and the date of the known drained states, I have also estimated a probability to how likely the drainage of the lakes was a GLOF event for each year. This shows that in addition to the GLOF events registered by NVE (2010, 2012, 2015 and 2020) there were GLOF events in 2019, 2018 and 2011 (high certainty), a probable GLOF event in, 2014 and possible GLOF events in 2017 and 2013. I will also argue that the documented GLOF event in 2012 should be labeled as “possible”, as this event was solely based on a single field observation in August, after the lake had drained, in combination with recorded water levels in the hydropower dam Fivlemyrane below Harbardsbreen.

Table 3: Estimated lake volume (Western and Eastern lake combined) with data from the NVE GLOF database (NVE, 2021b), and probability of possible GLOF events.

Year	Month/date (*=estimated)	Accuracy for estimated date [days]	PDD (for estimated date)	Max known Western lake extent [m ²]	Max known Eastern lake extent [m ²]	Estimated output volume (NVE) [10 ⁶ m ³]	Estimated potential combined lake volume [10 ⁶ m ³]	Comment	Probability of GLOF event
2020	06/24	-	189	157 000 ± 3 000	32 000 ± 4 000	-	2.3	Documented date and GLOF	Documented
2019	06/10*	± 4.5	115	57 000 ± 7 000	13 000 ± 1 000	-	0.7	Between 06/06 and 06/15	High certainty
2018	05/23*	± 2.5	100	71 000 ± 7 000	46 000 ± 2 000	-	1.4	Between 05/21 and 05/26	High certainty
2017	06/11*	± 13.5	100	65 000 ± 6 000	3 000 ± 1 000	-	0.7	Between 05/29 and 06/25	Possible
2016	-	-	-	-	-	-	-	The lakes did not form this year	-
2015	08/21	-	304	181 000 ± 9 000	42 000 ± 2 000	5.5	2.6	Documented date and GLOF	Documented
2014	06/20*	± 6.5	145	-	50 000 ± 3 000	-	0.7	Between 06/14 and 06/27. Only the Eastern lake formed this year	Probable
2013	06/26*	± 11.5	175	44 000 ± 15 000	-	-	0.4	Between 06/15 and 07/08	Possible
2012	Unknown	-	-	-	-	0.6	-	Possibly in early July, documented GLOF	Possible
2011	07/21*	± 7.5	364	134 000 ± 4 000	-	-	1.5	Between 07/14 and 07/29	High certainty
2010	08/04	-	399	143 000 ± 23 000	-	5.5	1.6	Documented date and GLOF	Documented

3.8 Harbardsbreen extent and area change

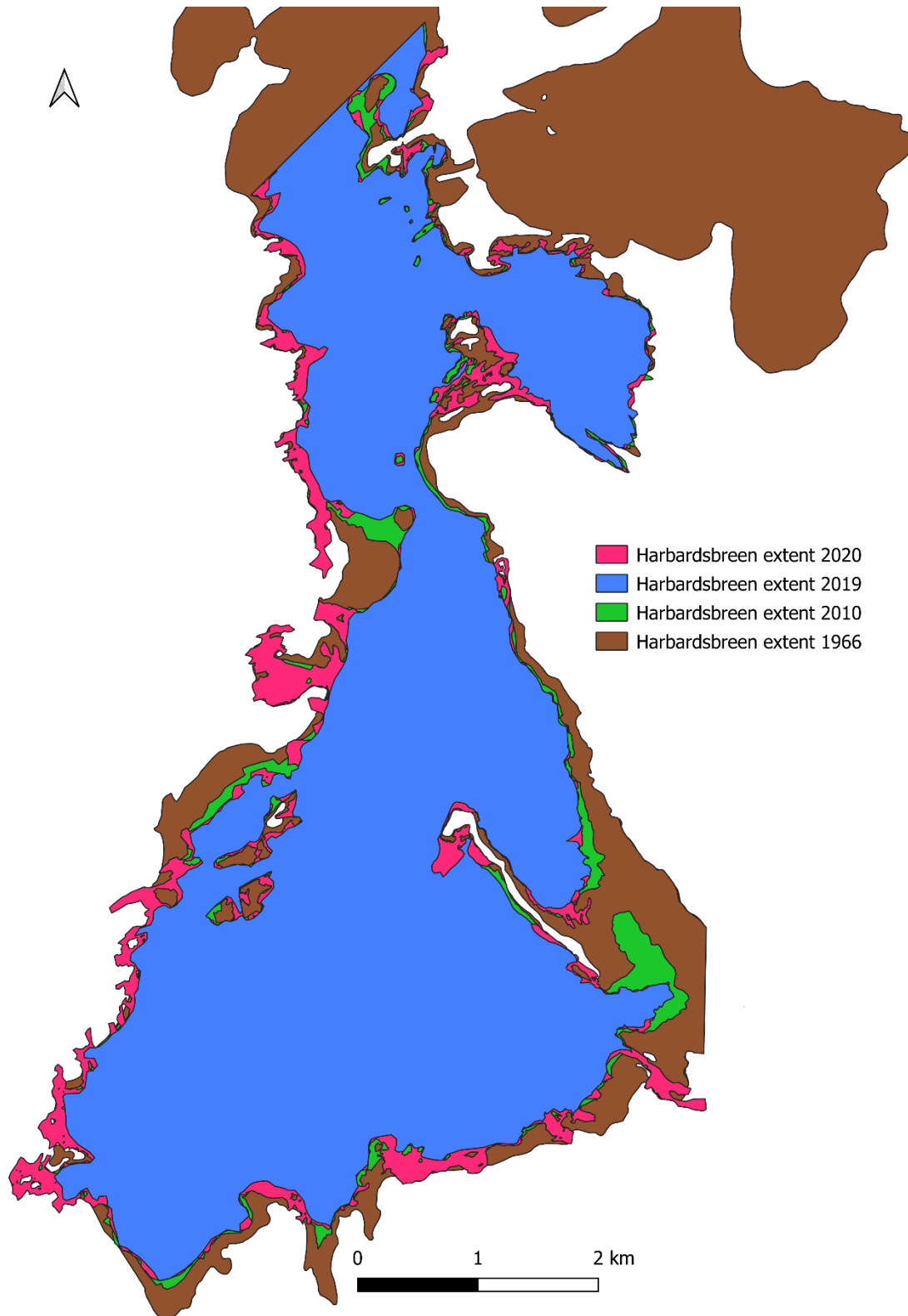


Figure 42: The glacier extent of Harbardsbreen in 1966, 2010, 2019 and 2020. Please note that the 2020 extent (red) is larger than the previous year, 2019 (blue). This is due to extensive and persistent snow cover in the end of the 2020 season.

Because Harbardsbreen was still snow covered at the end of the summer in 2020 the measured area this year is likely overestimated (Figure 42), hence there is no significant area change from 2010 to 2020. However, for reference I also measured the area in late summer 2019 (snow free ice margin), which shows a negative area change of more than 2 km² since 2010 (Figure 42 and Table 4). I have not included Austre Kollebreen or Fortundalsbreen bordering north and north-east of Harbardsbreen in the area measurements (visible in the 1966 extent in Figure 42).

Table 4: Measured total area of Harbardsbreen in 2010, 2019 and 2020.

Date.month.year	06.09.2010	26.08.2019	26.08.2020
Area	22.97 ± 0.15 km ²	20.81 ± 0.08 km ²	23.01 ± 0.14 km ²
Mapping source (resolution)	RapidEye (5m)	4-band PlanetScope (3m)	4-band PlanetScope (3m)

3.9 Elevation change

The elevation change of Harbardsbreen in the time period from 29.09.2010 to 18.08.2020 is shown in Figure 43. Most of the area of Harbardsbreen shows a negative elevation change. Due to frontal retreat the thinning is more than 25 vertical meters at the glacier front (to the south-east) and at the glacier margin by the lakes, while some smaller areas at higher altitudes have gained a few vertical meters. The few glacial areas which have shown a positive elevation change are in the lee sides of western winds, which will contribute to build up large amounts of snow throughout the winter. Outside the glacier perimeter one can see a scatter of positive elevation change, mostly in the 1-3 meters category. This can be explained by the fact that there was still a significant amount of snow on the glacier and in the mountains on August 18th when the LiDAR data of 2020 was collected. Control measurements of areas in stable terrain (bedrock) which were snow free in both 2010 and 2020 show a consistent precision in elevation accuracy, often less than 10 cm. This is well within the vertical error margin of 2 times ± 10 cm (Terratec, 2020). A more detailed closeup map of the area around the lakes is shown in Figure 44.

I found the average elevation change of Harbardsbreen to be -6.24 ± 0.13 m for the entire area of Harbardsbreen, and -6.39 ± 0.14 m for the area which was surveyed to find the mass balance for the period of 1996-2010 by Andreassen L. M. (2013).

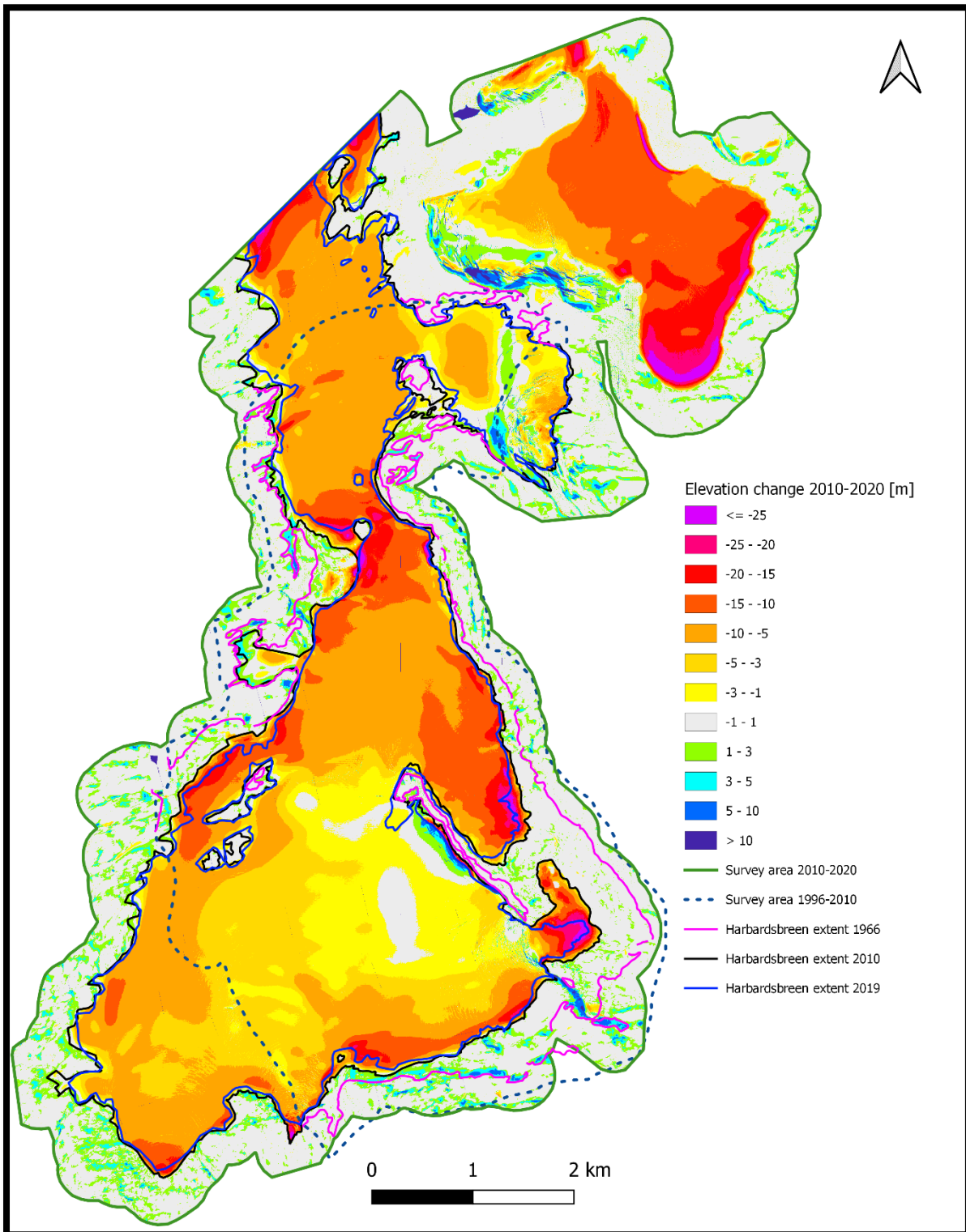


Figure 43: Elevation change in meters [m] of Harbardsbreen 29.09.2010-18.08.2020. Please note that for reference I have drawn the glacier extent from 2019 instead of 2020 because 2019 was snow free and in 2020 the glacier was still snow covered and the glacier border was very difficult to determine. Fortundalsbreen (upper right red area) is not considered in this study for any measurements. The glacier extent from 1966 is also shown for reference.

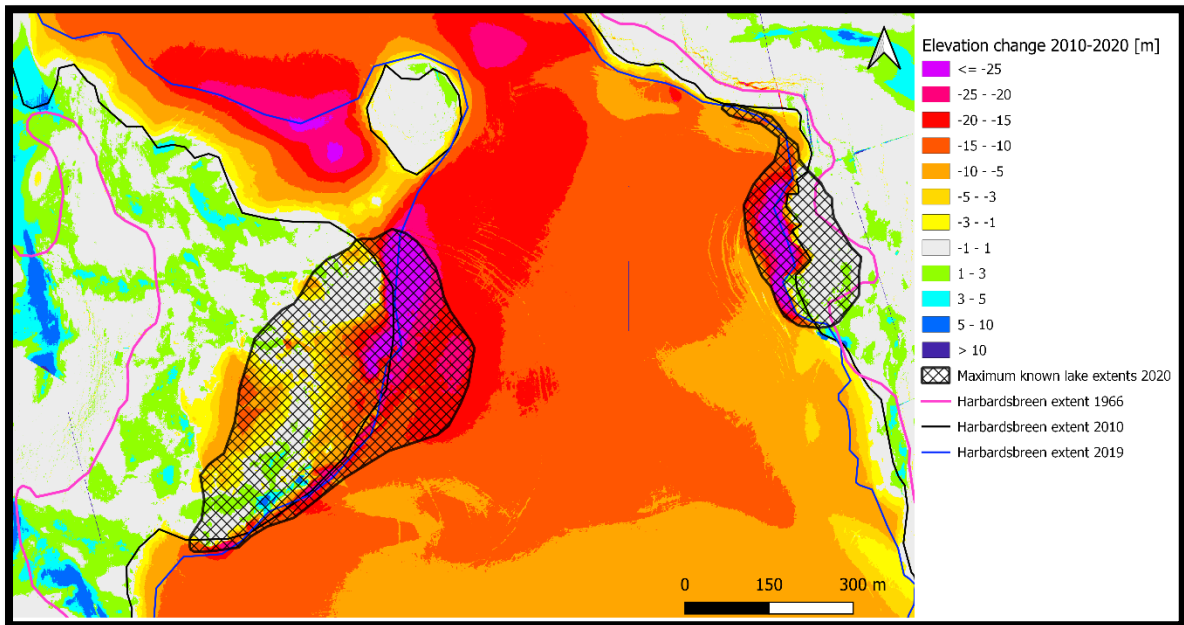


Figure 44: Elevation change of Harbardsbreen 29.09.2010-18.08.2020, for the area of interest around the lakes. Please note that a small area in the middle of the Western lake, outside the 2010 and 2019 glacier extent, has shown significant reduction in elevation in this time period. This is due to the fact that the lake was not completely drained at the time of the 2010 survey (September 29th).

3.10 Geodetic mass balance 2010-2020

Converting the average vertical elevation change to water equivalents using the ice density discussed in section 2.3 ($850 \text{ kg} \pm 60 \text{ kg/m}^3$) this represents an average mass balance of $-5.3 \pm 0.6 \text{ m.w.e.}$ for the entire Harbardsbreen, and $-5.4 \pm 0.6 \text{ m.w.e.}$ for the area which was surveyed for the 1996-2010 mass balance by Andreassen L. M. (2013) over the 2010-2020 period (Figure 45). This gives an average of $-0.53 \pm 0.06 \text{ m.w.e.}$ ($-0.54 \pm 0.06 \text{ m.w.e.}$) per year. Over the entire surveyed glacier surface this gives a mass loss of 122 ± 14 million cubic meters of water for the period 29.09.2010-18.08.2020.

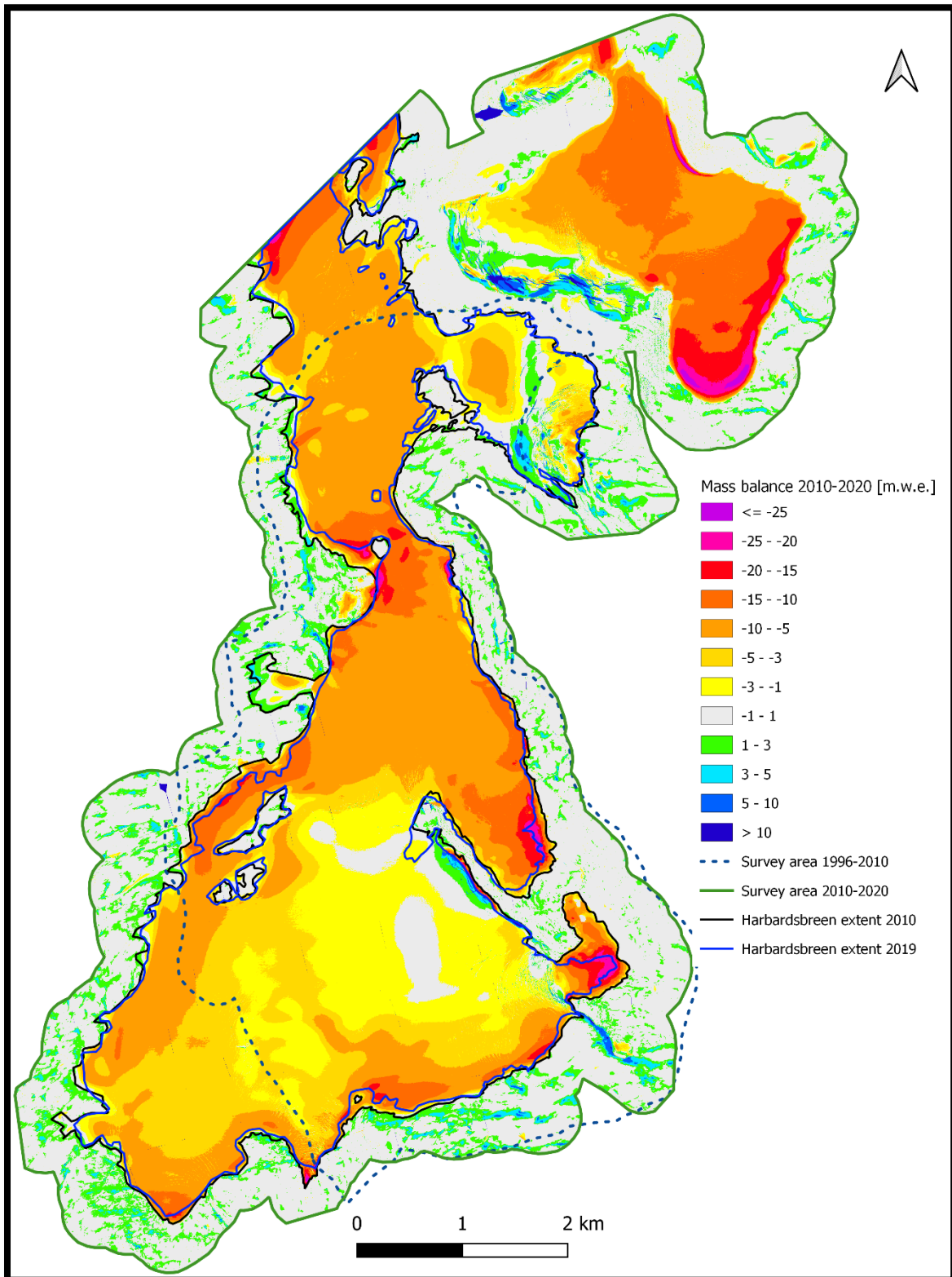


Figure 45: Geodetic mass balance measured in meters of water equivalents for the period 2010-2020. Total average mass balance is -5.3 ± 0.6 m.w.e. for the entire glacier surface, and -5.4 ± 0.6 m.w.e. for the area which was surveyed for the 1996-2010 period.

4 Discussion

4.1 Use of satellite photos

4.1.1 Availability and resolution of satellite images

The early satellite photos in the period 1972-1983 were difficult to interpret due to the poor image resolution of 60 by 60 meters per pixel of Landsat 1 to Landsat 4. Combining this with poor time resolution of normally only 1 to 3 photos of Harbardsbreen per month resulted in few cloud free images as most of the available images were covered in clouds. For the years 1972, 1977-1983 and 2012 there were no decent quality and cloud-free images available showing evidence of the presence of the lakes in the summer season. Thus, the maximum known lake extents are, particularly in years before 1984, not accurate. Since the start of the satellite data records both the spatial and temporal resolution of satellite photos has increased significantly, and since 2017 Planet Labs has delivered daily satellite imagery covering the whole world at a resolution of 3 by 3 meters. This will be very valuable for future studies which will use the same data sources as I have in this project.

4.1.2 Cloud cover

Most days are cloudy in Western Norway, particularly in mountain areas. This will of course vary from year to year and from season to season, but a good rule of thumb is to expect heavy cloud covers more often than not when using daily satellite imagery. This was also experienced by Andreassen et. al. (2021) in their extensive work using Sentinel-2 imagery for glacier monitoring in Norway and Svalbard.

Planet Labs has a built-in cloud cover filter on their download page, ranging from 0% to 100% cloud cover. However, I found this filter to be very inaccurate, with some photos having extensive cloud cover which were marked with very low percentage values, and vice versa. Also, because the area of interest only covers a small part of the entire scene there is always a chance that the area of interest will be cloud free if the cloud cover is scattered, as also found for Sentinel-images over Norway using ESA indicated cloud percentage (Andreassen, et al., 2021). Therefore, I will recommend for future studies to keep the cloud cover filter in the

default range of 0 to 100% to not miss possible good images of the field area of interest, and go through the imagery manually to find all the available high-quality imagery.

4.1.3 Preview of satellite imagery

The web-based service Planet Labs Explorer shows preview images of the available data which one can order for download. However, I found that the previewed images are in many cases not similar to what one gets in the downloaded file. This applies for the 4-band PlanetScope, RapidEye and Sentinel imagery. An example of this is shown in Figure 46 below using Sentinel-2 imagery. As the figure shows, the preview file is completely blown-out white apart from two gray spots, while the downloaded data file is both high in contrast and detail, and clearly shows the extent of the Western lake through a thin cloud cover. This is not fortunate, as one can risk missing days of both good and valuable satellite data. However, the Copernicus Open Access Hub is another option of previewing and downloading Sentinel-2 imagery, in which it is also easier to download Sentinel-2 imagery in bulk.

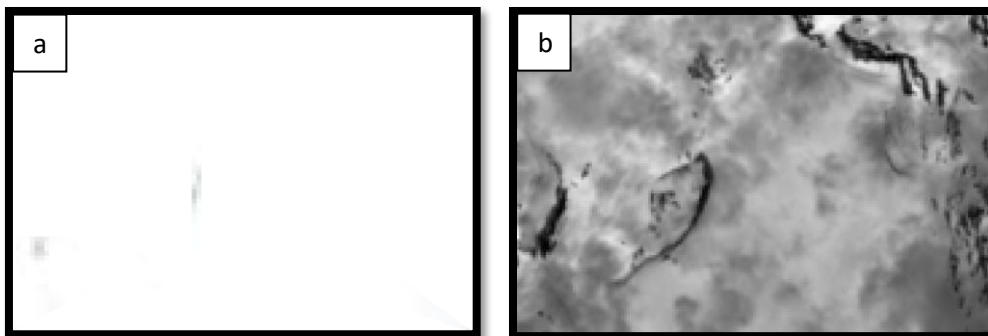


Figure 46: (a) In-browser web preview of Sentinel-2 Tile, 2017.05.29, (Scene ID: S2A_MSIL1C_20170529T105621_N0205_R094_T32VMP_20170529T105622). (b) The same dataset and the same area extent as in (a), downloaded and loaded into QGIS. Here the western lake is clearly visible, and there may be indications for the eastern lake too. (www.Planet.com/explorer)

4.1.4 Mapping of the lakes

Sometimes it was very difficult to find the lakes' extents, particularly when the lower resolution Sentinel-2 and Landsat were the only available sources of images and the lakes were partly ice covered and/or there was an extensive snow cover in the terrain. Figure 47 shows an example of Sentinel-2 imagery, showing the eastern lake as of May 26th 2019. I found Sentinel-

2 imagery to not be of high enough resolution for mapping smaller lake extents. Sentinel-2 imagery could be most helpful if the lake(s) were mostly ice free and thus had a high contrast to the glacier and the snow. However, as shown in Figure 47, Sentinel-2's spatial resolution of 10 by 10 meters per pixel is not ideal when measuring small lake extents in the scale of thousands of square meters which are partly to mostly ice covered.



Figure 47: Sentinel-2 imagery (resolution: 10 by 10 meters per pixel) of the Eastern lake as of 2019.05.26. The lake stretches from north to south in the middle of the image and is partly ice covered. Combined with snow cover in the terrain and on the glacier, sometimes it was virtually impossible to find a good estimate of the lakes' extents, as in this case.

4.1.5 Comparison of the different satellite data sources

A comparison of PlanetScope 3-band and 4-band, Sentinel-2 and Landsat 8 imagery is shown in Figure 48. Because 3-band PlanetScope imagery is designed to be all-purpose use satellite imagery, it often tends to be overexposed for snow and ice surfaces and thus leaves little to no details in white snow. The PlanetScope 4-band imagery on the other hand tends to be higher in contrast, as are Sentinel-2 and Landsat 8, however they have poorer spatial resolution.

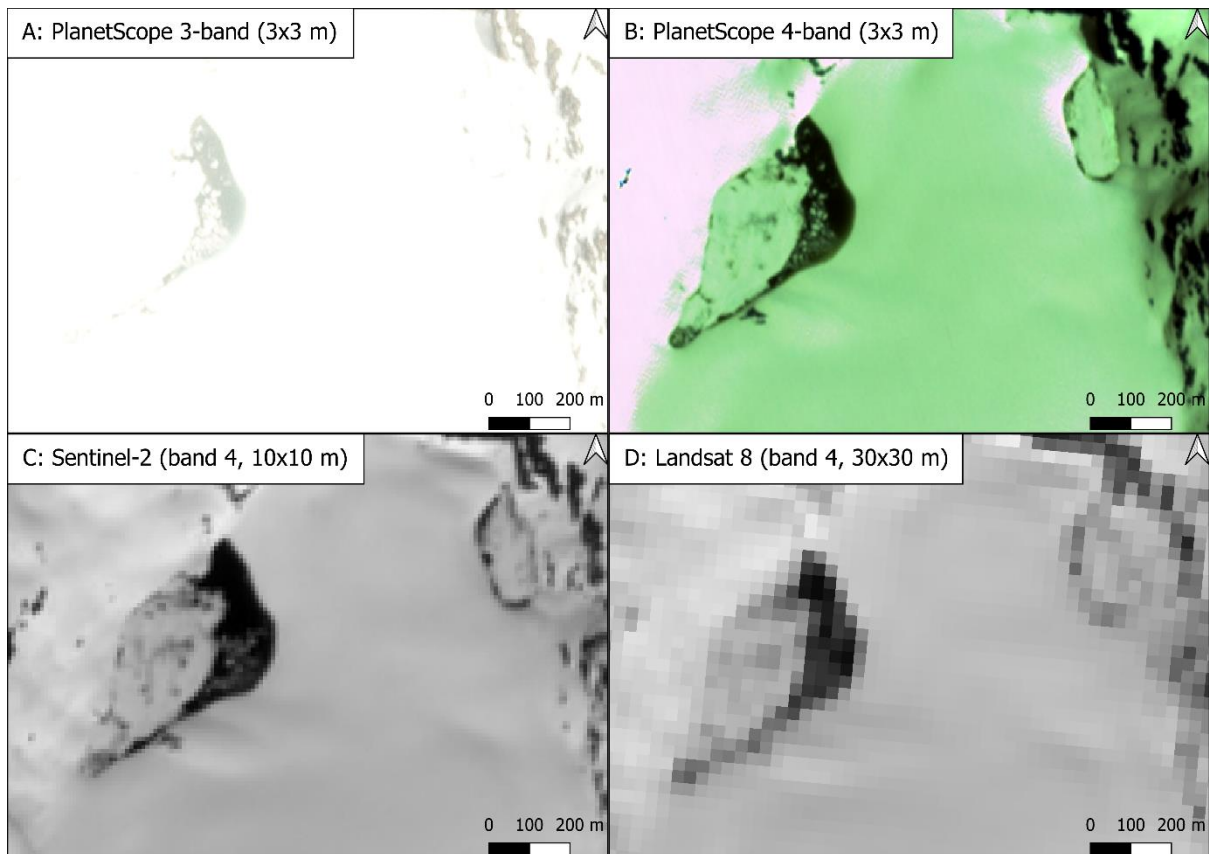


Figure 48: A comparison of 3-band and 4-band PlanetScope, Sentinel-2 (band 4) and Landsat 8 (band 4) imagery from June 18th and 19th 2020.

4.2 Temperature and precipitation

As Figure 17 shows, the melting season at Harbardsbreen has had a significant increase from an average of approximately 500 PDD in the 1980's to approximately 700 PDD in the 2000's and 2010's, an increase of approximately 40%. Comparing this to Figure 18, one can tell that the melting season has not become longer since the beginning of the records as it still averages at approximately 140 days. However, the average temperature per day with mean temperatures above 0°C has increased from just over 4°C to just above 5°C. This implies that the melting season is no longer than before, but it has become more intense with increasing average temperatures in the summer season.

In the period of 2010-2020 there are two years which show significant variation in PDD by date from the rest. Figure 15 shows that 2018 had both a very early and very abrupt start of the

smelting season, starting in early May. In 2015 on the other hand, the melting season did not start until mid to late June, and the summer was generally colder than in other years. Still, there is a registered GLOF event in 2015 (August 21st), and not in 2018. I will discuss this further in chapter 4.4.

On the other hand, the precipitation data (Figure 19 to Figure 21) shows no significant trend in change over the extent of the data records. There are large variations in annual precipitation from year to year, ranging from approximately 650 mm to more than 1450 mm, more than double. However, looking at the center-weighted 10-year average values, the average precipitation has been more or less stable throughout the period. I was expecting a more noticeable change in the average precipitation, as a warmer climate is often followed by an increase in precipitation. Still, the large annual variations seem to have a significant impact on the development of the glacial lakes.

4.3 Registered GLOF events in Norway

It is evident that there has been a significant increase in registered GLOF events in Norway, as presented in Figure 8 and Figure 9. This may to some degree be linked to climate change, however, this data is very likely to be skewed. In the early records the data may be underestimated due to a lack of observation services, whereas nowadays more locations are checked annually using satellite data as well as field observations. Up until more active monitoring of glacial activities was introduced, GLOF events were typically only documented if they caused direct harm to people, buildings or farmlands. Smaller flood events that were too small to cause any damages to inhabited areas would thus not be documented. In more recent years, however, there has been an increase in more active monitoring of various glacier locations, and for some locations even small GLOF event in the magnitude of just a few tens of thousands of cubic meters of water have been registered in NVE's database, e.g. at Supphellebreen (2005, 50 000 m³) and Nordre Folgefonna (2009, 12 000 m³) (NVE, 2021b). There seems to be an increase in the frequency of GLOF events in Norway in the last 30-year period of the records (1991-2020), but there are increasingly more accurate measurements in the latest years of the records, and even in the period of 1991-2020 the data may be skewed towards the last decade.

4.4 Defining GLOF events

It is evident that the lake(s) of Harbardsbreen have formed and drained nearly every year since 1972, which is the year of the earliest available Landsat satellite photos (Figure 13, p. 25). In the period of 2010-2020 I found the lake(s) to form every year except 2012 (no good imagery available in 2012, but NVE registered a GLOF event this year), and 2016. Also taking away the years with registered GLOF events, one is left with 2011, 2013, 2014, 2017, 2018 and 2019, all of which at least one of the lakes of Harbardsbreen grew to a significant size and later drained, some of which drained in a matter of just a few days.

Comparing this to NVE's GLOF database in Table 1, every registered event prior to 2010 (1996, 1997, 1998, 2000 and 2001) has only estimated dates, with an uncertainty ranging from just under 1 month to nearly 7 months, depending on the frequency of field observations. Also, the registered events prior to 2010 are not including estimated discharge volume.

I will therefore argue that every year which the lake(s) formed and drained in the period of 1996 to 2001 have been registered as a GLOF event by NVE in their GLOF database. In these years NVE carried out mass balance investigations and visited the glacier and observed the lake locations several times a year. In the years 2002-2009 I found the Western lake had formed every year with a maximum known extent of up to approximately the same as in 2015 and in 2020, and in some of the years the Eastern lake had formed too (Figure 13). In these years no routine field investigations were carried out and satellite imagery was not used for discovering GLOF events (Andreassen L. M., pers. comm., June 2021). NVE's GLOF database is mainly based on reported events, while satellite imagery has only been taken into use in recent years, e.g. Nagy & Andreassen (2019).

I find it both interesting and questionable that NVE has registered the drainage of the lake(s) of Harbardsbreen as GLOF events in their database solely based on one field observation when there was water in the lake(s), and another field observation when the lake(s) had drained, up to several months later. A GLOF event is, as introduced in chapter 1.3, defined as a rapid drainage event (flood) of a glacial lake. Solely based upon two field observations with up to several months between each observation there is no knowing if the drainage of the lake(s) was quick (scale of hours to days) or slow (scale of weeks to months) in the different years.

4.5 Lake development in 2010 to 2020 and GLOFs

As NVE's GLOF records show, in the past decade there has been registered GLOF events at Harbardsbreen in 2010, 2012, 2015 and in 2020. I have found evidence of high certainty of GLOF events in 2011, 2018 and 2019, a probable GLOF event in 2014 and possible GLOF events in 2013 and 2017 (Table 3, p. 50).

Comparing the detailed development of the lakes, temperature and precipitation (Figure 25 to Figure 35), it is clear that all the years with registered GLOF events, 2010, 2015 and 2020, have three things in common: (1) a maximum known lake area of the Western lake of more than 140 000 m², (2) the Western lake reached more than 100 000 m² before 120 cumulative PDD, and (3) there was more than 100 (up to 130) cumulative PDD only within the last two weeks before the start of the GLOF event, which gives an average at least 7.1°C (up to 9.3°C) mean temperature per day over 14 days before the GLOF event. Additionally, in 2010 there was a significant amount of precipitation as rain within the last two weeks before the GLOF event (total 80 mm over two weeks) which may have contributed to triggering the GLOF event. In 2015 and 2020 there were approximately 30 mm and 10 mm of precipitation the last two weeks prior to the GLOF event respectively. Only 10 mm of precipitation two weeks prior to the GLOF in 2020 is not likely to have had a significant effect on triggering the GLOF, whereas the 30 mm in 2015 may have had a contributing effect.

In the period 2010-2020, 2016 was the only year which neither the Western nor the Eastern lake formed. Studying the temperature development in Figure 31 (p. 40), one can see an early start of the melting season in the second week of May, however, this stops at approximately 30 PDD and is followed by a colder period (temperatures $\leq 0^{\circ}\text{C}$) which lasts about two weeks before the temperature starts rising again in the last week of May, this time more intensively. I believe this short warm period followed by a cold period is the reason why the lakes did not develop in 2016, as a similar pattern is not seen in any of the other years (2010-2020). The short warm period in the second week of May may have been enough to start the melting process and the formation of the subglacial drainage system, which may have endured the colder period of about two weeks which followed. This means that when the temperatures started to rise again in the last week of May, new meltwater would be freely drained under the glacier, which again would increase the flow capacity of the subglacial drainage system as more water drained and melted more ice in the meltwater tunnel. Combined with less than average precipitation as rain this summer (Figure 22, p. 31) which would have increased the

rate of snow and ice melt, this theory would explain why the lakes were not able to build to any detectable extents in the summer of 2016.

As presented in chapter 3.7, I found a high certainty of GLOF events in 2011, 2018 and in 2019. The event in 2011 shares the same characteristics as the registered events in 2010, 2015 and 2020: (1) a maximum known extent of the Western lake of 140 000 m² or more, (2) the Western lake reached a size of more than 100 000 m² before 120 PDD, and (3) there had been more than 100 cumulative PDD only within the last two weeks before the drainage of the lake.

In 2018 and 2019 however, the Western lake reached a maximum known extent of 71 000 m² and 56 000 m² respectively, and both years drained very early in the season (by May 26th and June 15th respectively). Studying Figure 33 one can clearly see a steep climb in the PDD values in 2018 at the start of the melting season. Figure 15 and Figure 16 also show that 2018 was the warmest year with the earliest start of the melting season in the period 2010-2020.

2019 however, was not particularly warm in the beginning of the melting season, as Figure 34 (p. 43) shows. It seems that the Western lake reached 55 000 m² very quickly (by May 24th), but then there was a colder period, and the lake did not grow significantly over the next two weeks (56 000 m² on June 6th). The lake drained right after the temperatures started to rise again, between June 6th and June 8th. This temperature increase combined with precipitation as rain after the colder period may have been the triggering cause of the GLOF event this year. I have labeled both 2018 and 2019 as high certainty of GLOF events.

In 2014 only the Eastern lake formed. I can only assume that the subglacial drainage system had time to develop for the Western lake before it reached a detectable size. The Eastern lake reached a maximum known extent of 50 000 m² on June 14th, before it had drained by June 27th. Precipitation as rain in the days before the maximum known extent may have been the triggering cause of the drainage event. I have labeled 2014 as a probable GLOF event.

In 2013 and 2017 I had very little information from satellite images to work with (Figure 28 and Figure 32). As Figure 22 (p. 31) shows, 2017 was the year with the most precipitation as rain in the melting season in the period 2010-2020, and the season of 2013 is also in the higher end compared to the other years. The amount of rain, and thus rainy and cloudy days, is reflected by the fact that I only got a single satellite photo of the Western lake in 2013 (maximum known extent: 44 000 m², June 15th), and two photos in 2017 (maximum known extent: 65 000 m², May 29th), as well as a photo showing the lake in its drained state from each

year, which was taken 3 and 4 weeks after respectively. Thus, I only labeled 2013 and 2017 as possible GLOF events, due to the lack of good satellite data.

4.6 Lake volume and discharge volume

Comparing the estimated lake volume to NVE's estimated flood volume (Table 3, p. 50), it is evident that there is a considerable difference. NVE's GLOF database shows an estimated flood volume of 5.5 million m³ in both 2010 and in 2015, whereas I found the estimated combined lake volume to be 1.6 and 2.6 million m³ respectively, which is 3.4 and 2.1 times lower than NVE's numbers. However, the estimated lake volumes are based upon the DEM made in 2020, and thus they may not be an accurate estimate as the glacier has thinned significantly around the lake margins in the period 2010-2020 (Figure 44, p. 54), which may underestimate the lake volume.

However, the difference in the estimated lake volume and the discharge volume may be explained by several factors. First, during a GLOF event the water from the glacial lake will form a meltwater tunnel beneath the glacier (Figure 2, p. 3). As the water flows through this tunnel, it will also melt a significant amount of the glacier ice due to friction, thus expanding the cross-sectional area of the tunnel which again will lead to a higher flow of water.

Second, there may already be a significant amount of water stored within (englacial) or beneath the glacier (subglacial). There may be englacial or subglacial lakes at Harbardsbreen which we do not know of yet, or the ice may just be porous and saturated with water. Neither of the cases are possible to detect using satellite images. However, in a recent study by Bigelow et. al. (2020) on a glacier lake at Kaskawulsh Glacier, Yukon, Canada, they found that 30-60% of the water stored in the catchment had been stored englacially, and 25-50% subglacially at peak level of the glacial lake. This may also be the case at Harbardsbreen, but further research would be needed to confirm this theory.

Third, the water in the lakes lifts the glacier and thus a significant part of the lake is partly stored subglacially prior to a GLOF event. This is not detectable on satellite photos, however, the radial crevasses on the glacier which circle the lakes (Figure 7, p. 9) are a clear sign that the glacier has been lifted by the water pressure, which supports this theory. Considering how far onto the glacier ice the crevasses reach, this means the lake ought to extend significantly beneath the ice in order to lift it enough to cause the formation of said crevasses.

Combined, these three factors can explain the difference in the estimated lake volume and NVE's estimated discharge volume.

4.7 Mass balance

Comparing my mass balance result for the period 2010-2020 to previous mass balance investigations in the periods 1966-1996 (Kjøllmoen B. , 1997) and 1996-2010 (Andreassen L. M., 2013) one can see a significant negative change in the mass balance since the first period (1966-1996) (Table 5). However, the period of 1996-2010 is more negative than what I found for the period 2010-2020. This corresponds to similar results on other glaciers for the same periods, as presented in Andreassen, Elvehøy, Kjøllmoen & Belart (2020), where they found the period 2001-2010 to be the most negative decade for glaciers in all regions in Norway except for the northernmost county, Troms og Finnmark. This study also suggests that the less negative decade of 2011-2020 could be explained by variations in large-scale atmospheric circulation, which causes more westerly winds and thus more winter precipitation.

Table 5 also shows the average annual PDD, as well as the average maximum known lake extent of both the Western and the Eastern lake for the different periods (for the 1966-1996 period the average lake extents is made with data from 1972-1996). Years with missing data have not been taken into account, however the years in which the lake(s) evidently did not form have been.

Table 5: Mass balance for the periods 1966-1996 (Kjøllmoen B., 1997), 1996-2010 (Andreassen L. M., 2013), and 2010-2020. For the period 2010-2020 I have included numbers from both the same survey area as for 1996-2010, as well as for the entire Harbardsbreen glacier area (parenthesis).

	1966-1996	1996-2010	2010-2020
Surveyed mass balance area	14.61 km ²	17.04 km ²	17.04 (23.01) km ²
Total average mass balance for the period	-8.5 ± 2.0 m.w.e.	-11.4 ± 0.7 m.w.e.	-5.4 ± 0.6 (-5.3 ± 0.6) m.w.e.
Average annual mass balance for the period	-0.28 ± 0.07 m.w.e. a ⁻¹	-0.82 ± 0.05 m.w.e. a ⁻¹	-0.54 ± 0.06 (-0.53 ± 0.06) m.w.e. a ⁻¹
Average annual PDD for the period	578	716	722
Average maximum known Western lake extent for the period	83 000 m ²	110 000 m ²	85 000 m ²
Average maximum known Eastern lake extent for the period	2 000 m ²	8 000 m ²	18 000 m ²

I will argue that there is a link between the glacier mass balance and the development of the lakes. The period with the most negative mass balance, 1996-2010, shows significantly larger maximum known Western lake extents than 1966-1996 (33% larger) and 2010-2020 (29% larger). The 2010-2020 period shows a less negative mass balance, even if the average annual PDD is insignificantly different from 1996-2010. The Eastern lake on the other hand, has appeared more frequently and reached larger known extents as the glacier has thinned since the beginning of the records, while the Western lake has shown slightly smaller extents in the period 2010-2020 compared to 1996-2010. If this trend continues, the Eastern lake may at some point in the future be the dominant lake at Harbardsbreen.

4.8 Proposed early warning of GLOF events at Harbardsbreen

As discussed, NVE has registered GLOF events at Harbardsbreen in 2010, 2012, 2015 and in 2020. In addition I have already argued and shown in chapter 3.7 that the drainage of the lakes in 2011, 2018 and 2019 could also be registered as GLOF events of high certainty, 2014 as a probable event, and 2013 and 2017 as possible GLOF events.

One of the goals of this study was to find a model which could say if there is a high chance of a GLOF event in the current season. It is evident that in the years of 2010, 2011, 2015 and 2020 the Western lake grew to a size of greater than 100 000 m² before 120 cumulative PDD, whereas all other years the Western lake never reached an area this large throughout the season. This could give reason to believe that if the Western lake reaches more than 100 000 m² within approximately 120 PDD, it could be of high certainty an early warning of a coming GLOF the current season.

However, it is evident that GLOF events also have occurred at smaller maximum known lake extents for both the Western and the Eastern lake. In the period from 2010-2020, the maximum known extents of the Western lake ranges from 44 000 m² (2013) to 181 000 m² (2015), and ranges from 13 000 m² to 50 000 m² for the Eastern lake. As the lakes have caused GLOF events in every year which the Western lake grew to a size larger than 100 000 m², I will also argue that the chance of a GLOF event increases by the size of the lake(s). It is also evident that the weather (temperature and precipitation) plays a key role in both the development of the lakes of Harbardsbreen and may be a trigger mechanism for a potential GLOF. Therefore, I will argue that the lake(s) have a potential of causing a GLOF event in any

year which the lake(s) grow(s) to a maximum extent in the scale of tens of thousands of square meters, with increasing chance by larger lake extents: If the lake(s) grow to an extent larger than 100 000 m² a GLOF event should be expected with high certainty.

4.9 Possibilities for future GLOF events at Harbardsbreen

There has been a remarked and accelerated shrinkage and retreat of glaciers since 2000 (Hugonett, et al., 2021). Many more glacier lakes have formed in recent years as the glaciers have retreated, and the growth of lakes and increased lake drainage may be linked to climate change (Andreassen L. M., pers. comm., June 2021).

As the elevation change maps of Harbardsbreen (Figure 43 and Figure 44) shows, there has been a significant negative change in elevation in the plateau area between the lakes from 2010 to 2020. As the glacier will melt and thin more in the future this will also lower the height of the glacier margin which dams the lakes. This will prevent the lakes from building up to the same elevations as they have done previously, and the location of the lakes may also move if the ice margin retreats. As the glacier ice thins there may be a higher chance that the water pressure of the lake will be able to lift the glacier ice more easily (and possibly earlier in the melting season) which may trigger GLOF events. However, as the glacier gets thinner, this also means the maximum potential volume of the lake will decrease as well. Consequently, future GLOF events may be more easily triggered at lower water levels and thus produce lower discharge volumes in flood events, as also concluded in a study of a GLOF event at Blåmannsisen by Engeset, Schuler & Jackson (2005).

However, a radar survey done in May 1999 (Kjøllmoen & Engeset, 2003) shows a deepening in the subglacial topography in the plateau area (Figure 49). The survey found that the glacier ice in the middle part of the plateau was up to 160 meters thick. They also suggested that there is a threshold in the bedrock topography, which could eventually cause a permanent lake to form if (or when) the glacier should melt completely. However, the elevation of this threshold is not certain, as this was estimated to be south and thus outside of the radar survey area. Still, this also means that if the glacier should melt enough to cause the lakes to have a lower elevation than what the threshold is, it is likely that a GLOF event cannot occur from these lakes at this point, but rather that the lakes will start to fill up the basin and thus increase

the glacier melt further. At this point, the lakes at Harbardsbreen may merge into one large lake if the plateau thins sufficiently.

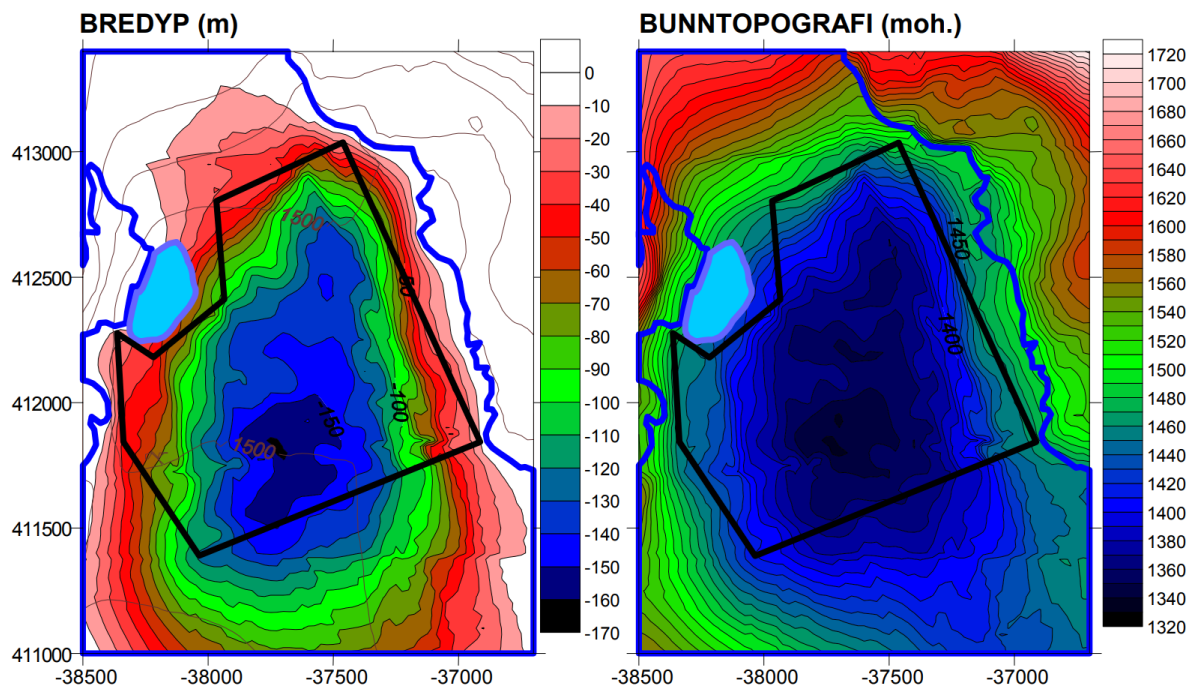


Figure 49: Results of radar survey in May 1999. The glacier margin is marked by the thick blue line, and the survey area by the thick black line. The left figure shows the thickness of the glacier ice measured in meters, and the right figure shows bedrock topography in meters above sea level. The estimations outside of the survey area are uncertain, particularly in the bottommost parts of the maps. The figure is taken from Kjølmoen & Engeset (2003).

4.10 Proposed future studies

It would be beneficial to know the exact elevation of the bedrock threshold discussed in chapter 4.9 (Figure 49). The potential danger of GLOF activities should be minimal once the glacier plateau melts thin enough so that the lakes will form at an elevation lower than the bedrock threshold. I propose to do a new radar survey at Harbardsbreen which includes this area, if it deems possible and feasible to do.

The lakes will, when the water level is high enough, lift the glacier. It would be interesting and beneficial to know how much water from the lake extends beneath the glacier. This is difficult to estimate, but one possibility could be to measure the elevation of the glacier around the lakes right before and right after a GLOF. This could be done by placing GPS trackers in a scattered pattern around the circumference of the lakes, which would continuously be measuring the elevation of the glacier surface, thus being able to detect elevation changes during a GLOF event.

5 Conclusions

5.1 Use of satellite data: Sentinel-2 and PlanetScope

I found the combination of using satellite imagery from Planet Labs (PlanetScope) and Sentinel-2 for mapping the glacial lakes of Harbardsbreen in the period 2010-2020 to be satisfying. Both sources have their advantages and their drawbacks: PlanetScope imagery has both higher spatial (3 by 3 meters per pixel) and temporal (daily images) resolution, but because it is designed for all-purpose monitoring of land it is often overexposed for use in glaciated and snow covered areas. On the other hand, the multispectral images from Sentinel-2 provide high contrast images even in snow and ice covered areas, and may be used for several purposes, like finding the normalized difference water index (NDWI). However, the resolution is only 10 by 10 meters per pixel, and because there are only two Sentinel-2 satellites (Sentinel-2A and Sentinel-2B) the temporal resolution is poorer as well compared to PlanetScope imagery, normally once every 1 to 3 days for the field area of Harbardsbreen. To conclude, neither Sentinel-2 nor PlanetScope imagery are perfect, but used together they can provide significantly more information on glaciers and glacial lake monitoring than if they are used on their own. I would highly recommend future studies of glaciers and/or glacial lake monitoring to use a combination of Sentinel-2 imagery and imagery provided by Planet Labs.

5.2 Mass balance and climate change

The average annual cumulative positive degree days (PDD) has increased by approximately 40% since the 1980's at Harbardsbreen. However, as the average number of days with temperatures above 0°C has not changed significantly, the average temperature per day in the melting season has increased by just over 1°C since the start of the temperature records in 1957. This temperature increase is reflected in the mass balance of Harbardsbreen.

Harbardsbreen has melted significantly in the period 29.09.2010-18.08.2020, with an average annual mass balance of -5.3 ± 0.6 m.w.e. (-0.53 ± 0.06 m.w.e. a^{-1}) over the entire surveyed glacier area (23.01 ± 0.14 km² (26.08.2020)). This gives an estimated 122 ± 14 million m³ of water which has melted at Harbardsbreen in this period. The development of the lakes is reflected in the mass balance, with the most negative period being 1996-2010 (-0.82 ± 0.05 m.w.e. a^{-1}), in which the Western lake shows a 29% larger average maximum known

extent than for the period 2010-2020 (-0.53 ± 0.05 m.w.e. a^{-1}), and 34% larger extents than for years before 1996 (1966-1996 mass balance: -0.28 ± 0.07 m.w.e. a^{-1}). In the period of 2010-2020 the maximum known lake extent of the Western lake in particular has been more unpredictable than for the previous two periods. On the other hand, the Eastern lake has formed both larger extents and more frequently in the last period compared to the other two.

5.3 Long term changes of the lakes at Harbardsbreen

I have found that the Western lake at Harbardsbreen has formed nearly every year since 1972 which have had sufficient satellite data, with the exception of 1999 and 2016. The annual maximum known lake extents show that the Western lake has consistently grown to a size of up to approximately 100 000 m^2 before the year 2000, while in the period 2003-2010 the Western lake has reached an extent of approximately 150 000 m^2 or more for all years except 2009. However, for the period 2011-2020, the maximum known extent of the Western lake has been unpredictable compared to the previous decades, ranging from less than 50 000 m^2 to more than 180 000 m^2 . On the other hand, the Eastern lake first appeared once in 1988, and has since 2000 formed regularly, and more frequently the last decade. This may be a response to the thinning of the glacier due to warmer temperatures and more intensive melting seasons.

5.4 GLOF events in 2010-2020

NVE's GLOF database shows that since 2010 there has been registered GLOF events at Harbardsbreen in 2010, 2012, 2015 and in 2020. In addition to this, I have found evidence with high certainty of GLOF events in 2011, 2018 and 2019, a probable GLOF event in 2014 and possible GLOF events in 2013 and 2017. In the period 2010-2020, 2016 was the only year in which neither the Western nor the Eastern lake formed at Harbardsbreen. The reason for this is likely related to a colder period lasting two weeks which came right after the melting season of 2016 had started, combined with little precipitation as rain. For no years in the period I found any of the lakes to persist through the winter and into the next summer, the lakes would always drain some time during the current summer season or fall.

5.5 Proposed early warning of GLOF events

All the GLOF events in 2010, 2011, 2015 and 2020 share the same characteristics in the development of the Western lake and weather data (temperature and precipitation): (1) The Western lake grew to a maximum known extent of more than 140 000 m², (2) The Western lake reached more than 100 000 m² before 120 cumulative PDD, and (3) there was more than 100 (up to 130) cumulative PDD within the last two weeks before the GLOF event which gives an average at least 7.1°C (up to 9.3°C) mean temperature per day over the last 14 days before the GLOF event. In the years 2010, 2011 and 2015 precipitation as rain may also have been a triggering factor for causing a GLOF event.

However, I also found a high certainty of GLOF events in 2018 and 2019, in which the Western lake reached a maximum size of 71 000 m² and 56 000 m² respectively, and probable and possible GLOF events have been found for smaller lake extents (2013, 2014 and 2017). Therefore, I have proposed that if the lakes of Harbardsbreen form and grow to an extent in the scale of 10⁴ m² or more, this would be an early warning of a probable coming GLOF event in the current summer season, and highly certain if the lakes grow to an extent in the scale of 10⁵ m², of which the risk and probability of a GLOF event increases by the lake extent.

6 Data availability

The lake polygons of Harbardsbreen created in this master thesis will be made available through NVE's Copernicus glacier service website:

<https://www.nve.no/hydrology/glaciers/copernicus-glacier-service/glacier-lakes/>

I will prepare the polygons as a shapefile with a metadata description following NVE's current data attribute fields for glacier lake outlines. The attribute fields in the shapefile will be filled with date of acquisition, type of sensor, short method description, name of mapper, etc.

7 References

- Andreassen, L. M. (2013). *Endringer av Harbardsbreen 1996-2010*. NVE.
- Andreassen, L. M., & De Marco, J. (2018). *NVE report 44/2018: Brekartlegging med drone*. NVE.
- Andreassen, L. M., Elvehøy, H., Kjøllmoen, B., & Belart, J. M. (2020). Glacier change in Norway since the 1960's - an overview of mass balance, area, length and surface elevation changes. *Journal of Glaciology*, 66(256), 313-328.
- Andreassen, L. M., Elvehøy, H., Kjøllmoen, B., & Engeset, R. V. (2016). Reanalysis of long-term series of glaciological and geodetic mass balance for 10 Norwegian glaciers. *The Cryosphere*, 10, 535-552.
- Andreassen, L. M., Moholdt, G., Kääb, A., Messerli, A., Nagy, T., & Winsvold, S. H. (2021). *NVE report nr 3/2021: Monitoring glaciers in mainland Norway and Svalbard using Sentinel*. NVE.
- Andreassen, L. M., Winsvold, S. H., Paul, F., & Hausberg, J. E. (2012). *NVE report 38/2012: Inventory of Norwegian glaciers*. NVE.
- Benn, D. I., & Evans, D. J. (2010). *Glaciers & Glaciation* (2 ed.). Hodder Education.
- Bigelow, D. G., Flowers, G. E., Schoof, C. G., Mingo, L. D., Young, E. M., & Connal, B. G. (2020). The role of englacial hydrology in the filling and drainage of an ice-dammed lake, Kaskawulsh Glacier, Yukon, Canada. *Journal of Geophysical Research: Earth Surface*, 125.
- Carrivick, J. L., & Tweed, F. S. (2016). A global assessment of the societal impacts of glacier outburst floods. *Global and Planetary Change*, 144, 1-16.
- Clarke L., K. J.-V.-C. (2014). Assessing transformation pathways. In: *Climate change 2014: Mitigation of climate change. Contribution of working group III to the fifth assessment report of the Intergovernmental Panel on Climate Change*. Cambridge University Press, Cambridge, United Kingdom and New York, NY, USA.: [Edenhofer, O., R. Pichs-Madruga, Y. Sokona, E. Farahani, S. Kadner, K. Seyboth, A. Adler, I. Baum, S.

- Brunner, P. Eickemeier, B. Kriemann, J. Savolainen, S. Schlömer, C. von Stechow, T. Zwickel and J.C. Minx (eds.)].
- Cuffey, K., & Paterson, W. S. (2010). *The Physics of Glaciers* (4th ed.). Oxford, UK: Elsevier.
- Dubey, S., & Goyal, M. K. (2020). Glacial lake outburst flood hazard, downstream impact, and risk over the Indian Himalayas. *Water Resources Research*, 56(4).
- Engeset, R. V., Schuler, T. V., & Jackson, M. (2005). Analysis of the first jökulhlaup at Blåmannsisen, northern Norway, and implications for future events. *Annals of Glaciology*, 42, 35-41.
- Harrison, S., Kargel, J. S., Huggel, C., Reynolds, J., Shugar, D. H., Betts, R. A., . . . Vilímek, V. (2018). Climate change and the global pattern of moraine-dammed glacial lake outburst floods. *The Cryosphere*, 12, 1195-1209.
- Hugonett, R., McNabb, R., Berthier, E., Menounos, B., Nuth, C., Girod, L., . . . Kääb, A. (2021). Accelerated global glacier mass loss in the early twenty-first century. *Nature*, 592, 726-731.
- Huss, M. (2013). Density assumptions for converting geodetic glacier volume change to mass balance. *The Cryosphere*, 7, 877-887.
- IPCC. (2019). *IPCC special report on the ocean and cryosphere in a changing climate*. [Pörtner, H.-O., Roberts, D. C, Masson-Delmotte, V., Zhai, P., Tignor, M., Poloczanska, E., Mintenbeck, K., Alegría, A., Nicolai, M., Okem, A., Petzold, J., Rama, B., Weyer, N. M. (eds.)].
- Jackson, M., & Ragulina, G. (2014). *NVE report 83/2014: Inventory of glacier-related hazardous events in Norway*. NVE.
- Kjøllmoen, B. (1997). *NVE report 06/1997: Volumendringer på Harbardsbreen 1966-96*. NVE.
- Kjøllmoen, B. (2011). *NVE report 3/2011:Glaciological investigations in Norway in 2010*. NVE.

- Kjøllmoen, B. (2016). *NVE report 88/2016: Glaciological investigations in Norway 2011-2015*. NVE.
- Kjøllmoen, B., & Engeset, R. (2003). *Glasiologiske undersøkelser på Harbardsbreen 1996-2001*. NVE.
- Kjøllmoen, B., Andreassen, L. M., Elvehøy, H., & Jackson, M. (2020). *NVE report 34/2020: Glaciological investigations in Norway 2019*. NVE.
- Liestøl, O. (1956). Glacier dammed lakes in Norway. *Norsk geografisk tidsskrift*, 15 (3/4), 121-149.
- Lussana, C., Tveito, O. E., Dobler, A., & Tunheim, K. (2019). seNorge_2018, daily precipitation, and temperature datasets over Norway. *Earth System Science Data*, 11, 1531-1551.
- McFeeters, S. K. (1996). The use of the Normalized Difference Water Index (NDWI) in the delineation of open water features. *International Journal of Remote Sensing*, 17(7), 1425-1432.
- Meteorologisk Institutt. (2021, January 20). *Klima fra 1900 til i dag: Vestlandet siden 1900*. Retrieved March 22, 2021, from <https://www.met.no/vaer-og-klima/klima-siste-150-ar/regionale-kurver/vestlandet-siden-1900>
- Nagy, T., & Andreassen, L. M. (2019). *NVE report 40/2019: Glacier lake mapping with Sentinel-2 imagery in Norway*. NVE.
- Nesje, A., Bakke, J., Dahl, S. O., Lie, Ø., & Matthews, J. A. (2008). Norwegian mountain glaciers in the past, present and future. *Global and Planetary Change*, 60(1-2), 10-27.
- NVE. (2010, August). *Harbardsbreen, Sogn*. Retrieved December 14, 2020, from www.nve.no: <https://www.nve.no/hydrologi/bre/jokulhlaup-glof/harbardsbreen-sogn/>
- NVE. (2015, June). *Jøkulhlaup (GLOF)*. Retrieved December 14, 2020, from www.nve.no: <https://www.nve.no/hydrologi/bre/jokulhlaup-glof>
- NVE. (2021a). *Bredata*. Retrieved May 27, 2021, from [NVE](http://www.nve.no): <https://www.nve.no/hydrologi/bre/bredata/>

- NVE. (2021b). *Glacier lake outburst floods*. Retrieved March 8, 2021, from NVE: <http://glacier.nve.no/Glacier/viewer/GLOF/enno/>
- Ruddiman, W. F. (2014). *Earth's Climate, Past and Future* (3rd ed.). New York: W.H. Freeman and Company.
- Shukla, A., Garg, P. K., & Srivastava, S. (2018). Evolution of glacial and high-altitude lakes in the Sikkim, Eastern Himalaya over the past four decades (1975-2017). *Frontiers in Environmental Science*, 6(81).
- Terratec. (2020). *Laseskanning for nasjonal detaljert høydemodell, NDH Jostedalsbreen 2pkt 2020*. Terratec.
- Thorsnæs, G. (2020, December 12). *Store Norske Leksikon*. Retrieved May 21, 2021, from Norges største breer: https://snl.no/Norges_største_breer
- Zemp, M., Thibert, E., Huss, M., Stumm, D., Rolstad Denby, C., Nuth, C., . . . Andreassen, L. M. (2013). Reanalyzing glacier mass balance measurement series. *The Cryosphere*, 7, 1227-1245.

